

THE *EINSTEIN* SLEW SURVEY

MARTIN ELVIS, DAVID PLUMMER, JONATHAN SCHACHTER, AND G. FABBIANO
 Harvard-Smithsonian Center for Astrophysics, 60 Garden Street, Cambridge, MA 02138

Received 1991 May 31; accepted 1991 August 15

ABSTRACT

A catalog of 819 sources detected in the *Einstein* IPC Slew Survey of the X-ray sky is presented; 313 of the sources were not previously known as X-ray sources. Typical count rates are $0.1 \text{ IPC count s}^{-1}$, roughly equivalent to a flux of $3 \times 10^{-12} \text{ ergs cm}^{-2} \text{ s}^{-1}$. The sources have positional uncertainties of $1.2'$ (90% confidence) radius, based on a subset of 452 sources identified with previously known pointlike X-ray sources (i.e. extent less than $3'$).

Identifications based on a number of existing catalogs of X-ray and optical objects are proposed for 637 of the sources, 78% of the survey, (within a $3'$ error radius) including 133 identifications of new X-ray sources. A public identification data base for the Slew Survey sources will be maintained at CfA, and contributions to this data base are invited.

Subject headings: BL Lacertae objects: general — catalogs — quasars: general — X-rays: general — X-rays: stars — surveys

1. INTRODUCTION

Sky surveys have always played a major role in astronomy. In the present era in astronomy, we are rapidly accumulating new sky surveys across the whole spectrum. In particular, the advent of imaging telescopes has made X-ray surveys possible that are comparable in sensitivity to those at other wavelengths. The *Einstein Observatory* (*HEAO 2*; Giacconi et al. 1979a) was the first imaging X-ray astronomy satellite, and many papers have reported on surveys of restricted regions of the sky made using pointed observations taken with the Imaging Proportional Counter (IPC, Gorenstein, Harnden, & Fabricant 1981) on board *Einstein*. (The “Medium Survey,” e.g. Gioia et al. 1990; the “Deep Survey,” e.g. Primini et al. 1991; Table 1). As a result we are in the peculiar position in the soft X-ray band covered by *Einstein* ($\sim 0.2\text{--}3.5 \text{ keV}$), of knowing more about the faint sources than about the bright sources. The limited sky coverage of the Medium and Deep Surveys results in their having effective *upper* limits to their sensitivity as well as lower limits since bright sources are rare on the sky (Fig. 1; Table 1). This limitation complicates $\log N\text{-}\log S$ and source evolution studies (Fig. 1) since for bright source counts we have to refer to the hard X-ray surveys, usually to the Piccinotti et al. (1982) *HEAO A-2* survey which covered the $2\text{--}10 \text{ keV}$ energy band. For example, Schmidt (1990) has emphasized how the Piccinotti et al. and the Medium Survey source counts are in contradiction for AGNs and clusters of galaxies (although evolution may explain these problems; Gioia et al. 1990). What is needed is a $\log N\text{-}\log S$ with the same instrument over the whole X-ray flux range. A survey of the bright sources in the soft X-ray range is thus important, and only a survey covering most of the sky can find the relatively rare bright sources. A survey using the same instrument as used for the *Einstein* Medium and Deep Surveys would greatly simplify interpretation. Samples of bright sources selected uniformly by their X-ray properties are also valuable for follow-up detailed work with other instruments, e.g., *ROSAT*, *ASTRO-D*.

We have constructed a survey of the sky with the *Einstein* IPC using the “Slew” data taken when the satellite was moving (“slewing”) from one target to the next. By co-adding all these slews, we have achieved a useful sensitivity over a large solid angle, some 50% of the sky. The main properties of the *Einstein* IPC Slew Survey are given in Table 2. Because it was not clear that this survey could be constructed successfully, it was not attempted earlier. The resources needed to process the data were large, making the effort too large for the uncertain payoff. Computer processing power and on-line storage capacity have grown by orders of magnitude in the last few years so that it is now possible for projects of this size to be carried out experimentally by a small team relatively quickly, and thus at low risk. This paper describes the *Einstein* Slew Survey and presents the resulting catalog of X-ray sources.

The complete information content of the Slew Survey is more than the source catalog. A CD-ROM issued by SAO (Plummer et al. 1991) contains the full data on the individual photons in the Slew Survey and the aspect solution file for each slew. This enables a user to derive fluxes and upper limits for any position on the sky covered by the Slew Survey. The CD-ROM also contains more information on the source detections (see “lists/unix/srcs.lis,” “lists/vms/srcs.lis,” etc.). The CD-ROM is available from SAO (send requests by e-mail to the *Einstein* Data Products Office, edpo@cfa.harvard.edu), or via the *Einstein* On-Line Information System, *einline* (Harris et al. 1991).

2. DATA SELECTION

For the survey we selected all the data taken while the *Einstein* satellite was slewing with the IPC at the focus (“SLEW” mode data—hence the survey name). Only the IPC data is valuable for this survey. Table 3 compares a “figure of merit” for this type of work for the four focal plane instruments on *Einstein*. The combination of wide field of view, high quantum efficiency, and large fraction of time in the focal plane make

TABLE 1
Einstein SURVEYS

Name	Area ^a	$f_{\text{lim}}^{\text{b}}$ (upper ^c)	$f_{\text{lim}}^{\text{b}}$ (lower)	Number of Sources	References
Deep	2.3	$\sim 7 \times 10^{-14}$	$\sim 4 \times 10^{-14}$	25	Primini et al. 1991
Medium	780	$\sim 5 \times 10^{-12}$	$\sim 2 \times 10^{-13}$	835	Gioia et al. 1990
Slew	35,060 ^d	$\sim 1 \times 10^{-9}$	$\sim 3 \times 10^{-12}$	819	This paper

^a Square degrees (deg^2).

^b Units: $\text{ergs cm}^{-2} \text{s}^{-1}$.

^c Defined as the flux below which 90% of the sources lie.

^d Defined by the minimum exposure (1.0 s) at which a source was detected.

the IPC over 100 times more valuable than the next most useful instrument, the HRI. Only slews for which IPC targets lay at each end were used (i.e., no instrument changes during the slew). Also only slews in which data dropouts were small (<1 major frame; 40.96 s) were included. This gave 2799 useful slews with a total instrument on-time of 10^6 s of data, and 2.6×10^6 photons.

All photon events were accepted: unlike the processing of the pointed data, no Sun/Earth angle or pulse height event (PHA) screening was made. Screening proved unnecessary for most of the survey since its purpose is to reduce the background, which is negligible for the short exposures in the Slew Survey. In processing we omitted photons from regions near the IPC “ribs” (features produced by the window support structure of the IPC; Harnden et al. 1984), and near to the edges of the detector. Edge photons are not processed in the standard, pointed, data either.

Figure 2 shows the exposure map for the Slew Survey. The concentration of exposure near the ecliptic poles is clear. This concentration occurs for all Earth-orbiting satellites with fixed

solar panels since one axis must point toward the Sun and the satellite lies in the ecliptic plane. The spacecraft is then only free to rotate along arcs of ecliptic longitude. There is lower than average exposure in parts of the Galactic plane, because the IPC was turned off if it was expected to slew across the brightest few sources, and these are concentrated in the Galactic plane. This was a protection against detector gas breakdown that could be induced by too many counts being detected in a small region. The Slew Survey thus has zero exposure on the Crab Nebula. This policy was not always successfully followed and we do have exposure on GX 5-1, which was fortunate for our purposes since it allowed a “proof-of-concept” at an early stage (Fig. 3).

Figure 4 is an exposure histogram showing the fraction of the sky covered to a given exposure depth. From this, and the log N -log S of the Medium Survey (Gioia et al. 1990), one can predict that the Slew Survey will contain of order 1000 sources, which in fact is a quite accurate prediction.

3. ASPECT SOLUTION

The key to producing a Slew Survey is to solve for the pointing position of the satellite with time as it slews across the sky (the “aspect” or “aspect solution”). To determine the *Einstein* aspect during slews it was necessary to use the on-board gyro-

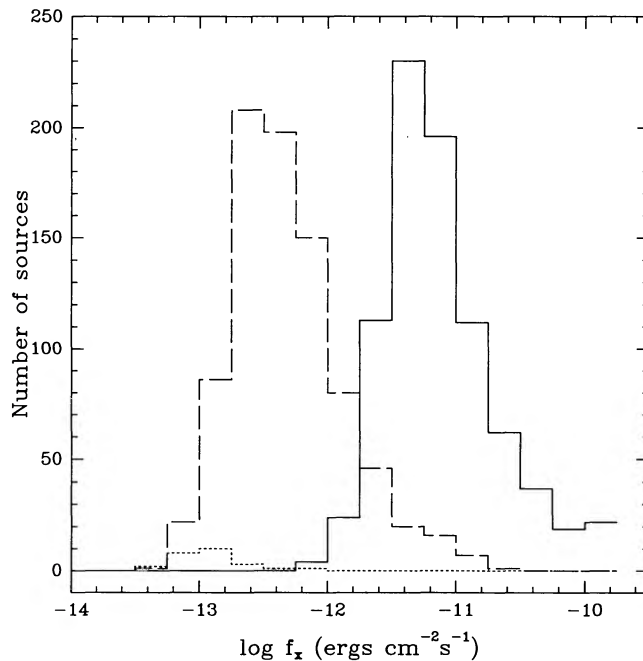


FIG. 1.—Distribution of source fluxes from the Slew Survey (solid line) compared with those of the extended Medium Survey (dashed line; Gioia et al. 1990) and the Deep Survey (dotted line; Primini et al. 1991)

TABLE 2
Einstein IPC SLEW SURVEY PROPERTIES

Property	Value
Observing time	0.99×10^6 s
Effective exposure ^a	0.47×10^6 s
Total number of photons	2.6×10^6
Mean background	~ 0.7 photons per source box ^b
Minimum number of photons per source (for mean background)	$5 (P_{\text{rand}} \sim 1 \times 10^{-4})$
Mean exposure	12 s
Mean limiting count rate	0.45 counts s^{-1}
Mean limiting flux ^c	$14 \times 10^{-12} \text{ ergs cm}^{-2} \text{s}^{-1}$
Number of sources	1075
Identifications ^d	Stars: $m_V < 7$ AGN: $m_V < 17$

^a Including corrections for vignetting and excluding the “ribs” regions.

^b $6' \times 6'$ box.

^c 0.2–4.0 keV, for a conversion factor of 3.26×10^{-11} ergs per count appropriate for a power-law energy index of 0.5 and a Galactic N_{H} of 2.0×10^{20} atoms cm^{-2} as used in the *Einstein* Medium Survey (Gioia et al. 1984)

^d Based on Medium Survey nomogram (Maccacaro et al. 1988).

TABLE 3
RELATIVE VALUE OF *Einstein* INSTRUMENTS FOR SLEW SURVEYING

Instrument	(FOV × % time × QE) ^a	Figure of Merit
IPC	$1800 \times \sim 0.5 \times 0.7$	630
HRI	$216 \times \sim 0.2 \times 0.1$	4.3
SSS	$9 \times \sim 0.15 \times 0.9$	1.2
FPCS	$\leq 90 \times \sim 0.15 \times 0.01$	0.14

^a FOV = field of view in square arcminutes; % time = fraction of time in focal plane; QE = quantum efficiency.

scope rate data ("gyro data"). The on-board star trackers, which are the primary means of providing the aspect solution for the pointed observations, could not be used since the satellite moved some 5'-6' during a single readout interval (1 minor frame = 0.32 s, the standard minimum read-out interval for a NASA mission), while the star trackers could only follow stars at rates of $<2' \text{ s}^{-1}$ (Koch et al. 1978).

At any time during the mission, three of the six gyros in the gyro assembly were operating. Each gyro yields a spin rate every minor frame, and the gyros are oriented so that any set of three will give sufficient information to determine rotations about the three spacecraft axes. The existing calibration of the gyro rates to rotation rates was designed only to be accurate enough to bring the spacecraft to a direction where the star trackers, with their $\sim 2^\circ$ field of view, could acquire a field. Accurate pointing depended on the star trackers.

To use the gyros alone for deriving a Slew aspect required that the existing calibration be checked and modified to give

solutions accurate at the arcminute level anywhere during a slew. Two things made this possible: (1) the level of accuracy required is of order 1'—similar to the IPC point spread function—which is some 30 times less demanding than for pointed observations; and (2) enough well-positioned X-ray sources are known which are bright enough to be detected in a single slew. These sources give us an internal check on the quality of our aspect solution on several hundred individual slews, thus allowing a reliable Slew aspect solution to be developed.

Figure 5 shows the initial offsets between the slew-derived position and the accurate positions for known X-ray sources in the *HEAO 1* A-3 (Remillard et al. 1991) and pointed IPC catalogs (2E; Harris et al. 1991) detected in individual slews. The coordinates are oriented along and perpendicular to the slew direction. Several features can be seen: There is a concentration of points near the origin, implying that a good fraction of the time the gyro system does give good aspect during slews; this concentration is however offset along the slew direction by $\sim 3'-5'$; there is a "tail" of poorly positioned sources along the slew direction; and there is a "halo" of poorly positioned sources extending to large distances from the central cluster near the origin.

The offset of the central cluster is due to an ambiguity in the documentation of the timing information. We determined empirically that the aspect data and photon data sent in a single data packet (minor frame) refer to different times: the photon data to the current minor frame, and the aspect data to the preceding minor frame. This is negligible in pointed mode but in Slew mode leads to the observed offset.

The "tail" of poor aspect slews we found to be due to the

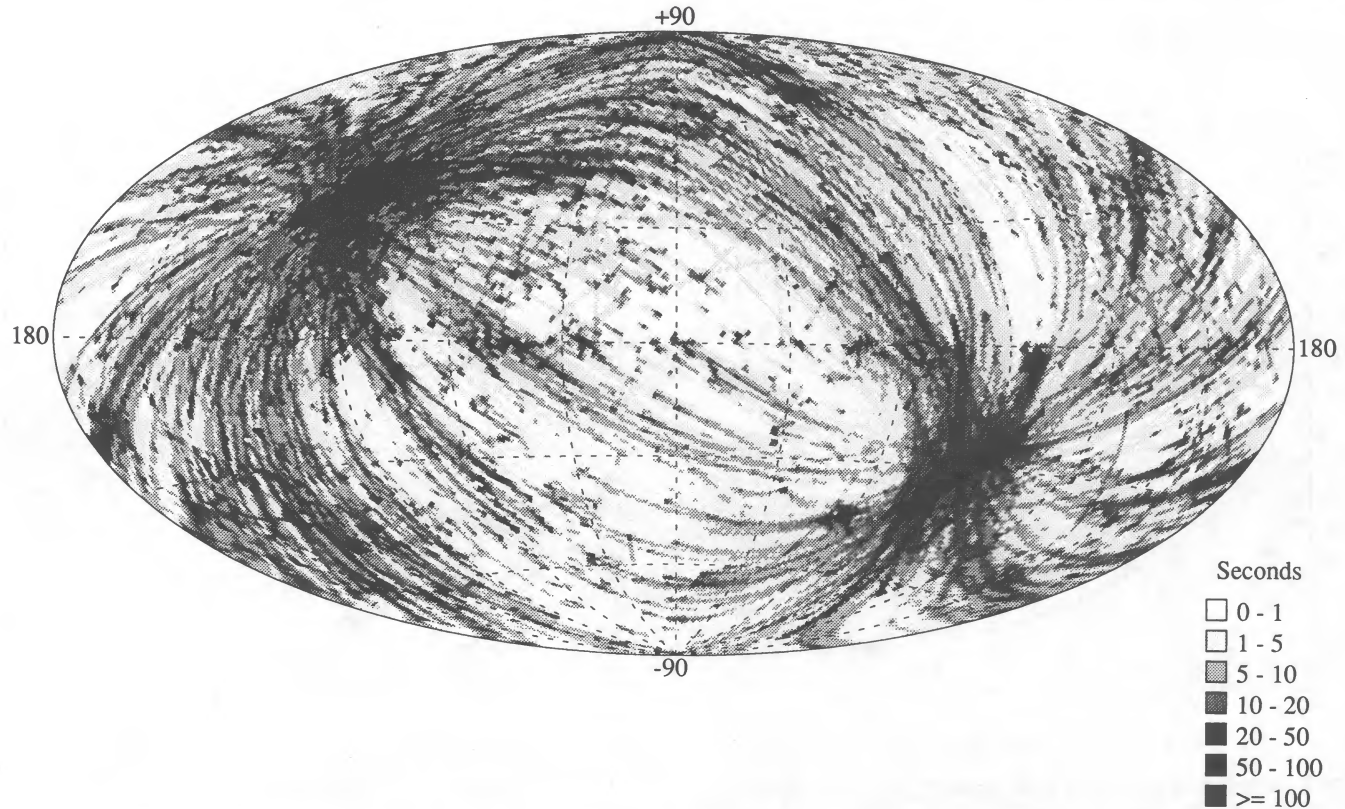


FIG. 2.—Exposure map for the Slew Survey in Galactic coordinates. Slew paths are readily seen going in great circles between the ecliptic poles.

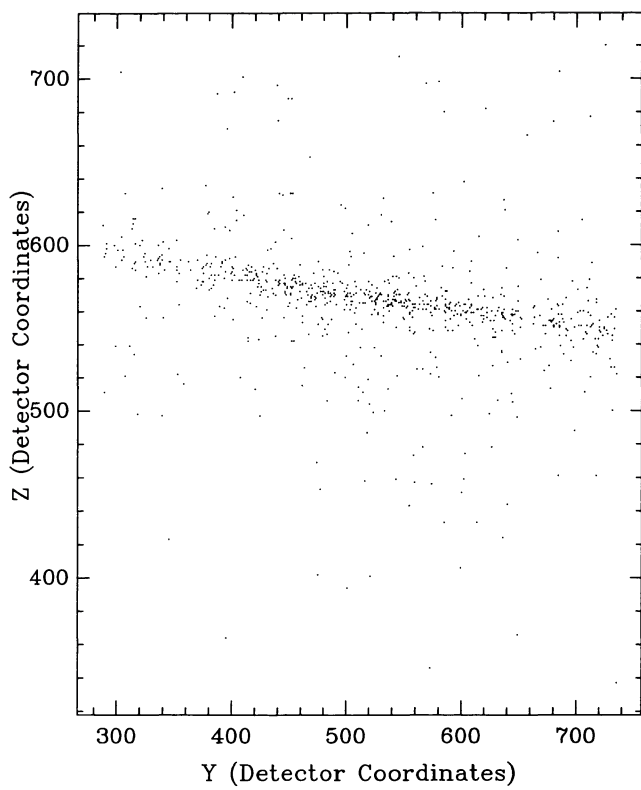


FIG. 3a

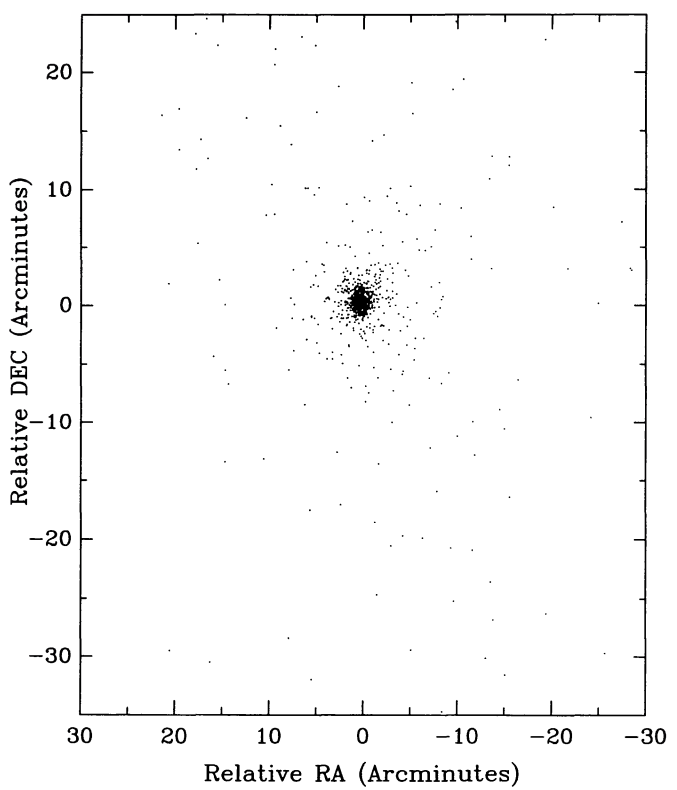


FIG. 3b

FIG. 3.—GX 5-1 (1ES 1758-250) seen before (a) and after (b) Slew aspect was applied. Applying the Slew aspect correction, which takes into account the motion of the satellite, produces a well-defined image (b). The background over the whole $1^\circ \times 1^\circ$ field shown is 65 counts for an exposure of 14 s.

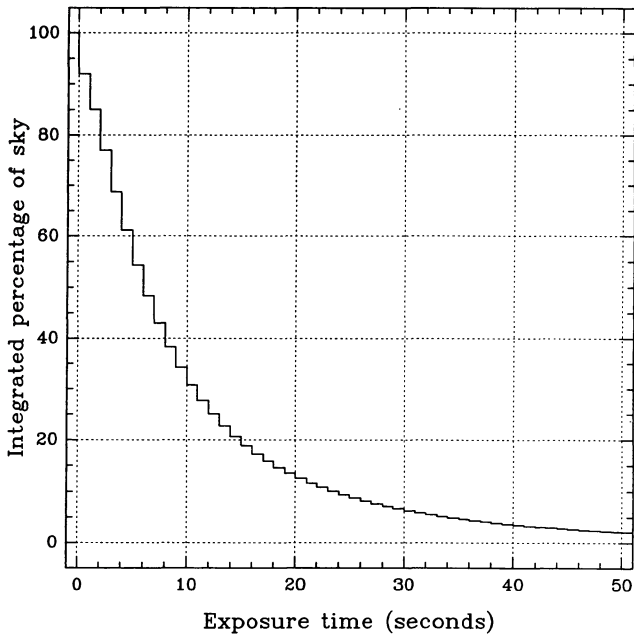


FIG. 4.—Fraction of the sky to a given exposure in the Slew Survey

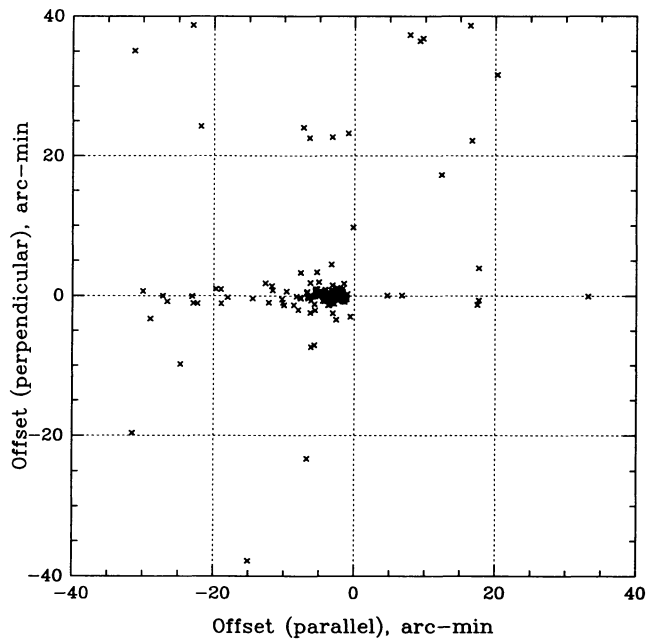


FIG. 5.—Initial offsets in arcminutes between Slew-derived and accurate X-ray source positions for 172 known X-ray sources (Remillard et al. 1991; 2E Catalog) detected in individual slews.

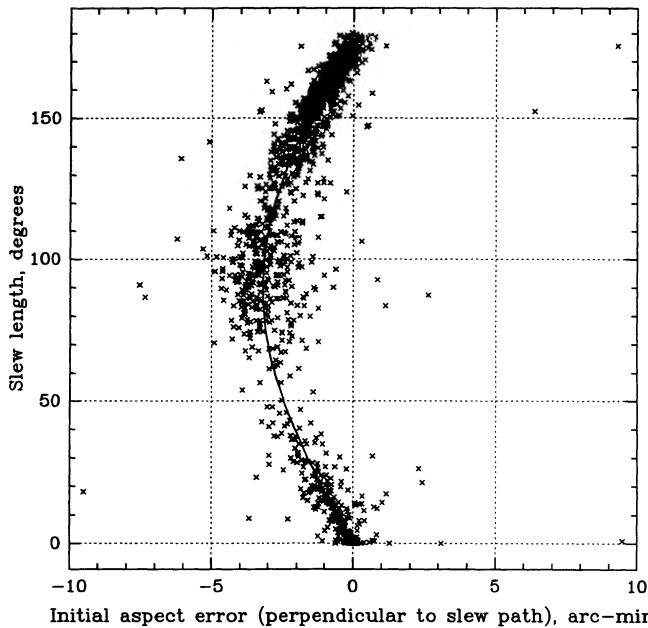


FIG. 6a

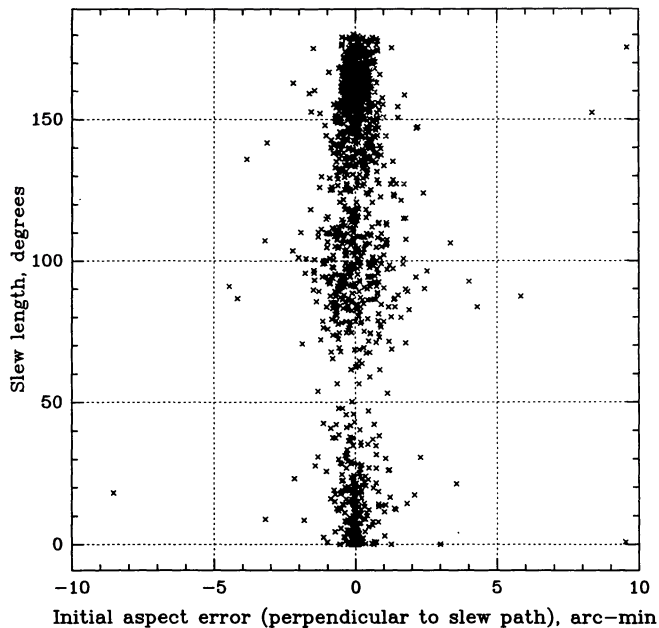


FIG. 6b

FIG. 6.—(a) Offset in arcminutes (perpendicular to slew direction) between the Slew-calculated position at the end of the slew and the accurate position from the pointed, star tracker, solution vs. slew length in degrees. The plot is for the data before the application of the correction made by rotating the assumed plane of the gyro assembly and is for gyro combination B. The solid curve shows the size of the correction. (b) Offsets as in (a) after gyro orientation corrections.

quality of the pointed aspect at the start of the slew. The ‘MAP-MODE’ star tracker aspect (where the trackers send back the positions of all stars in the field) is not sufficiently reliable (e.g., Harris, Stern, & Biretta 1990), and it is essential to go back into the pointed observation until “LOCKED” star tracker aspect is found. (In LOCKED aspect the tracker records only the position of the chosen guide star.) Errors of a few arcseconds in the starting position extrapolate to large errors when the spacecraft slews through tens of degrees.

The cause of much of the spread seen in Figure 5 is seen in Figure 6a. This shows the offset perpendicular to the slew direction as a function of position along the slew path. The clear “bow” shape arises naturally from a displacement of the gyro assembly from its assumed orientation with respect to the spacecraft axes. This offset can be illustrated by imagining a vector rotating 180° within a given plane. This represents the actual rotation of the satellite. Now consider a second vector parallel to the first vector at its original position. Rotate the second vector within a second plane tilted slightly from the first plane such that they intersect along the line of the vectors’ original direction. The second vector represents the rotation of the satellite as reported by the displaced gyros. The two vectors will be coincident at the start and end of the 180° rotation but will be offset in between, reaching a maximum at 90°. The offset at 90° exactly equals the relative offset of the two planes, and therefore the offset of the gyro assembly. By rotating the gyro assembly axes according to the maximum observed offset, the “bow” distortions in the derived positions can be virtually eliminated (Fig. 6b). A separate set of corrections is needed for each set of gyros which indicates that the rotations are not of the gyro assembly as a whole but of the individual gyros mounted in the assembly. Errors in the assumed gyro orienta-

tions of a few arcminutes are entirely negligible for pointed observations. The rotations for each set of gyros were fixed and are given in Table 4.

In addition the conversion from gyro spin rate to angular rotation is only calibrated to a level sufficient for pointed operation. In the Slew Survey this conversion is critical and leads to errors when extrapolating the gyro solution over large slew angles. We calculate the initial offset between the known, star tracker-derived, pointing position and the gyro-extrapolated position at the end of the each slew. Each offset is measured as a small difference, δ , in R.A., decl., and Roll angle. Since we measure three δ ’s and can adjust the scale factors for three gyros, there is sufficient information to force this offset to be zero for each slew. The corrections needed are of order 3’. We used the following procedure: using the initial offsets we guess an appropriate trial scale factor for each gyro in turn. This leads to a change in the three δ ’s for each of the three gyros. The resulting 3×3 matrix forms a set of simultaneous equations

TABLE 4
OFFSETS FOR EACH SET OF GYROS

Gyro Combination ^a	Gyros in Use	ΔX	ΔY
A	1, 2, 3	0.0	0.0
B	2, 3, 5	3.2	0.0
C	2, 3, 4	4.25	1.25
D	2, 4, 6	6.0	0.0
E	3, 5, 6	6.0	1.75
G	3, 4, 6	4.75	1.75

^a Gyro combination F did not contribute usable slews to the survey.

which can be solved to give scale factors for each gyro that will exactly set the δ 's to zero. This procedure produces a sufficiently accurate aspect solution, as determined, post facto by the identification process (see § 6). The scale factors, however, are mostly not systematic. This suggests that there is a residual aspect error that could, if corrected, improve the Slew Survey aspect. The solution may lie in treating the orientation of each gyro separately instead of "rotating" the whole gyro assembly.

Finally, slews having scale factor corrections larger than 2% were found to introduce greater errors in position. In very short slews, for example, the aspect became so bad that sources were distorted into smears that were not detected at all. We simply excluded any slews for which we derived scale factor corrections larger than 2% (8.6% of the total), leaving the total of 2799 useful slews.

The offsets of the Slew positions from the accurate positions of known X-ray sources in the *HEAO 1 A-3* catalog (Remillard et al. 1991) and the Bright Star Catalog (Hoffleit & Jaschek 1982) for the final set of corrected aspect slews gave the offset diagram seen in Figure 7a. The true reliability of the Slew Survey aspect solution is better than is immediately apparent from Figure 7a since false identifications produce a significant "background" at radii $> 3'$. Figure 7b shows the distribution of offsets from a false set of Slew Survey sources obtained by shifting all the Slew Survey sources by 1° in R.A. Figure 7c shows a plot of the average background due to false identifications plotted against the radial histogram of Figure 7a. Subtracting this background rate implies a 90% confidence radius of order an arcminute for the Slew Survey aspect. Figure 7d shows an integrated histogram with the background subtracted which allows the derivation of confidence radii of the reader's choice. We derive a 90% confidence radius of $1.2'$ and a 95% radius of $2'$ from Figure 7d.

4. SOURCE DETECTION

The short exposures of the Slew Survey over most of the sky lead to an expectation value of 0.1 photons in a standard $2.4'$ square IPC detection cell. Since we expect ~ 1000 sources over the sky, approximately 99.996% of the 2.58×10^7 detection cells would be empty of sources. The "sliding box" detection algorithm used for the pointed data (Harnden et al. 1984) is thus highly inefficient for the slew survey.

4.1. Percolation Algorithm

Instead, we have developed a "percolation" algorithm that tests each photon for the presence of unusual numbers of near neighbors. Since there are only $\sim 3 \times 10^6$ photons in the survey this takes a factor of ~ 50 fewer operations than the sliding box method. The percolation algorithm is exactly analogous to the method described by Huchra & Geller (1984) for the selection of groups of galaxies from the CfA Redshift Survey (bright galaxies, like Slew Survey photons, are sparsely distributed on the sky) except that the Slew Survey contains only the two dimensions of R.A. and decl., and has no equivalent of the redshift dimension. The Slew Survey percolation algorithm loops through every photon in the field and searches for other photons within the percolation length. If another photon is found, it is added to the group and subsequently searched for neighbors. The process continues until no more photons lie

within a percolation length. Figure 8 describes the process in a flowchart. These groups constitute our candidate sources for the Slew Survey. This algorithm has the advantage of not being biased against extended sources as is a sliding box (by subtracting a source-enhanced background). It does, of course, have a surface brightness limit when the mean distance between source photons exceeds the percolation length. A percolation length of $2'$ (\sim double the FWHM of the IPC point spread function) produced good results except in regions of high exposure where the background began to become important (see below). All groups detected by the percolation algorithm with fewer than three photons were automatically rejected.

4.2. Exposure Map

It was then necessary to determine which photon groupings constituted significant sources. This significance is highly dependent on the local background and the distribution of exposure time around a source. Figure 9 illustrates some of the difficulties. The contours are isoexposure levels. Each field covers $30' \times 30'$, and the exposure map has a resolution of $1'$. Detailed structure on the few arcminute scale is evident. Because of the random nature of the slew paths, there is no predictable structure to the exposure maps. Figure 9 also shows the individual photons in the regions. Each frame is centered on a Slew Survey source which illustrates that the size of the point-spread function is comparable with the exposure map structure. It is clear that the detailed exposure distribution in the surrounding region must be calculated in order to compare the background from this region with the number of counts detected in the "source" region defined by the percolation detect algorithm.

The exposure maps were generated from the aspect solution and the timing gap records ("tgr" files) for each slew ("HUT"). A template of the relative exposure within the 1° IPC field of view was made including corrections for vignetting and ribs at the full $8''$ resolution of the detector. The vignetting is a radial function which reaches 46% at the midpoint of the side of the IPC; the regions affected by the ribs (which are $4'$ wide and roughly $20'$ from the center, parallel to the sides; see Harnden et al. 1984 for details) are set to zero exposure. This map was then moved across the sky at the rate determined by the aspect solution and effective exposure time assigned to bins 1 arcmin^2 on the sky accordingly. For convenience, the sky was divided into a set of $6.5'$ square bins on 6° centers. No exposure was accumulated during times when the detector was off, or data was not received for other reasons (e.g., telemetry dropout).

4.3. Source Probabilities

The Poisson probability of a collection of "source" photons arising by chance inside a source region centered on the percolation centroid can be calculated given a local background. Source counts were derived by taking all counts within a $6'$ on a side box centered on the centroid given by the percolation algorithm. Background was estimated from two "square annuli" of inner side $6'$, outer side $12'$, and inner side $12'$, outer side $30'$ (background regions 1 and 2). The mean exposure times in the source and the background regions were derived by averaging the $1'$ bins of the exposure map. In the case where there were no background counts, we calculated the probabili-

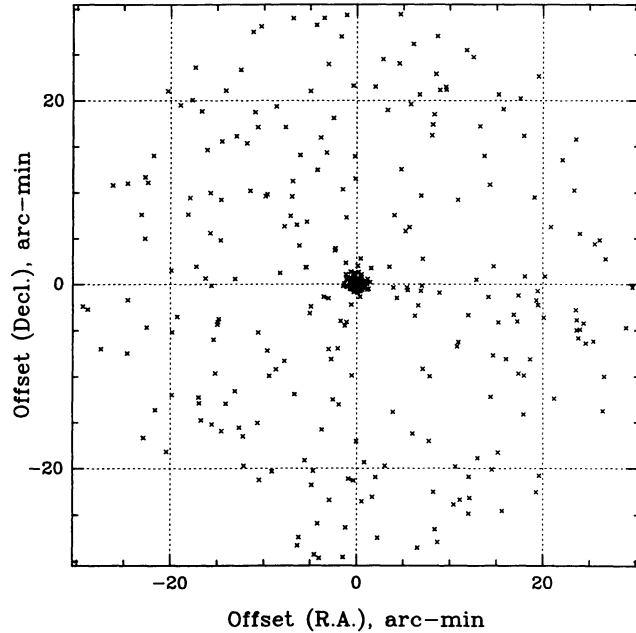


FIG. 7a

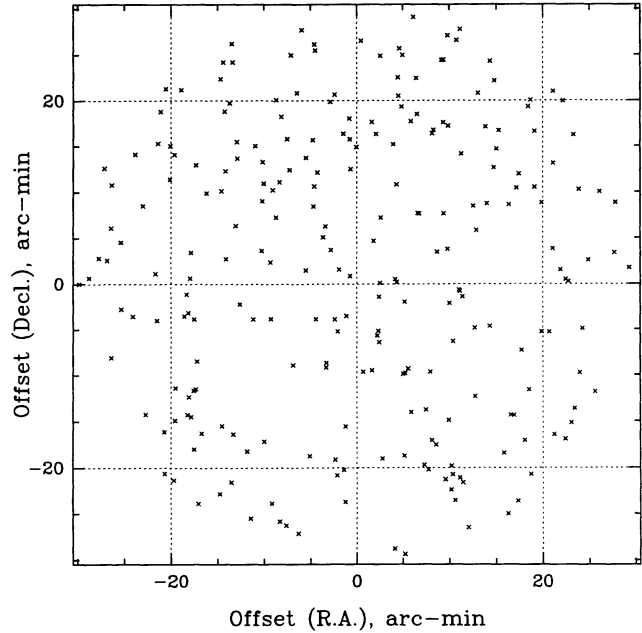


FIG. 7b

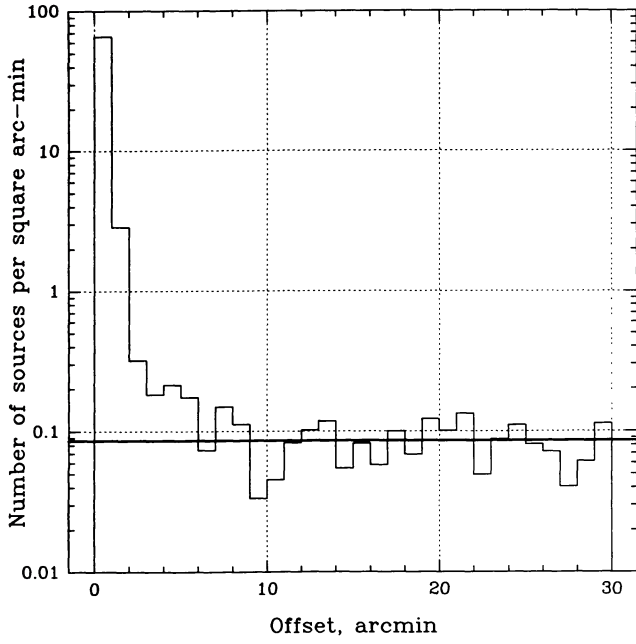


FIG. 7c

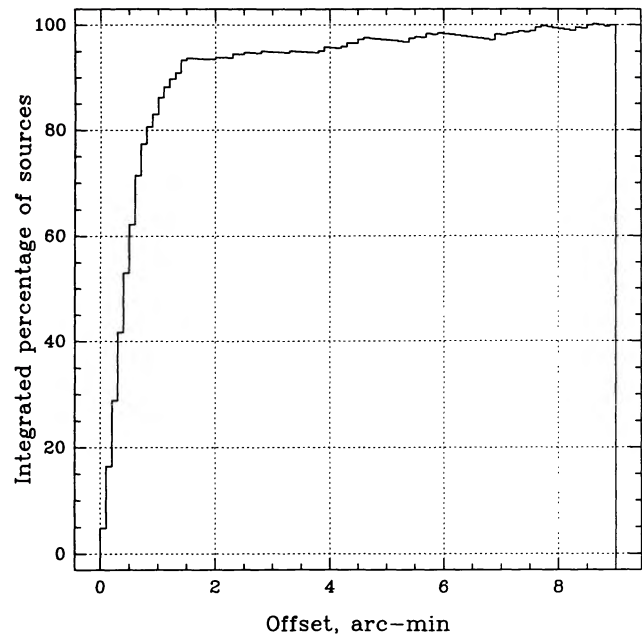


FIG. 7d

FIG. 7.—(a) Offsets of Slew source positions from Bright Star Catalog identifications, in R.A. and decl., after all aspect corrections are applied. (b) Offsets as in (a) but for an artificial set of Slew Survey sources created by shifting the real Slew Survey source by 1° in R.A.. This shows the background rate of identifications due to accidental matches of position. (c) Radial version of (a) with a heavy line marking the false identification background rate from (b). (d) Integrated histogram of (a) with the background from (b) subtracted.

ties by assuming one background count. Otherwise, we used background region 2 for background subtraction. The probability, P_{rand} , was determined for each candidate source. (On the CD-ROM, P_{rand} is called Prob2; Prob1, the same probability using the background region 1, was also calculated and is listed on the CD-ROM.) The values of P_{rand} order the candidate sources according to their likely reality (small probabilities being more likely real). P_{rand} does not by itself tell us which

sources to accept. For this we must define a threshold value of P_{rand} .

4.4. Estimating the False Source Rate

4.4.1. Relation between Probability Thresholds and Photon Number

The false source rate is a function of the threshold probability and the number of counts in a source. We can estimate the

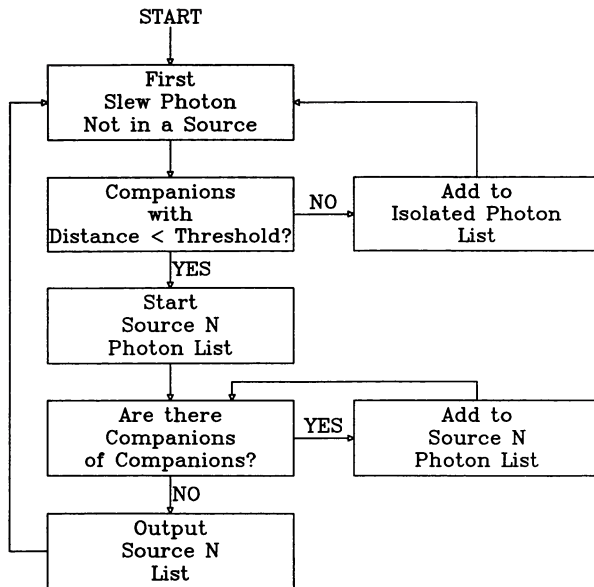


FIG. 8.—Percolation algorithm flowchart

fraction of false sources from global properties of the Slew Survey. For example, Figure 10 shows a histogram of the number of single photon candidates (sources most likely to be false) as a function of P_{rand} . The histogram peaks at a probability of 0.5 where the number of “source” photons equals the number of background photons, which is the most likely case. (Above a probability of 0.5 our sample will necessarily always be incomplete because the percolation algorithm cannot include candidates with zero counts in the source box.) If the probability

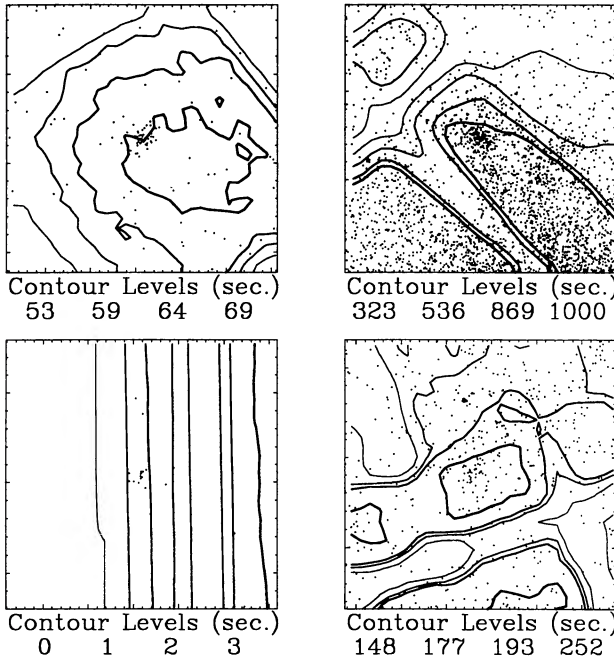


FIG. 9.—Four typical regions of the Slew Survey exposure map. Each region is 30' on a side, the size of background region 2, and is centered on a Slew source. The Slew Survey names are, clockwise from the upper left, 1ES 1340-611, 1ES 2031-411, 1ES 1142+198, and 1ES 1746-370.

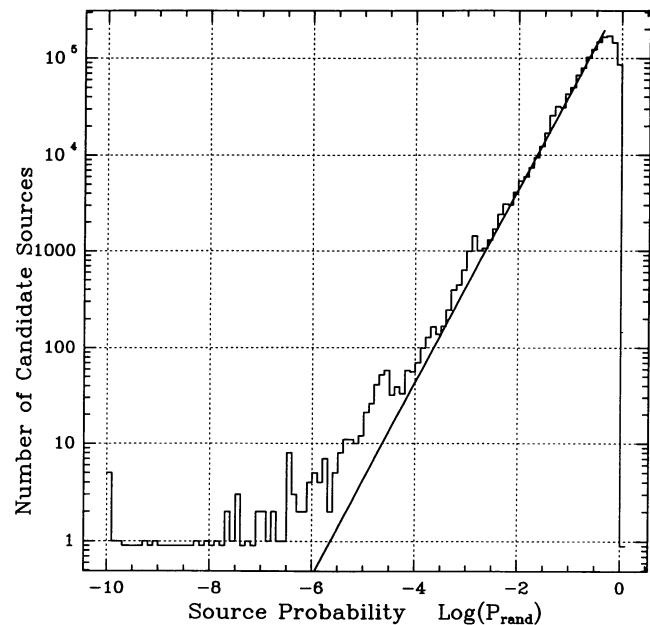


FIG. 10.—Number of candidate sources with 1 photon detected by the percolation algorithm vs. Poisson probability, P_{rand} . The solid line shows the number expected assuming there are no real sources in the data. This is a reasonable approximation for three decades of P_{rand} .

calculation is appropriate to the data, then we should find that the number of candidate sources drops linearly with the probability. We show a straight line of slope 1 in Figure 10 which was normalized by setting the area under the line equal to the area under the histogram up to a probability of 0.5. This normalization assures that the line intersects the histogram at $P_{\text{rand}} \sim 0.5$. Since the line fits the data well for about four decades in probability, we conclude that the Poisson probability is a good description of the data. This is a conservative approach because we are assuming that the percentage of “true” sources within the total sample is essentially zero, whereas some single-photon “sources” will indeed be real sources.

We generated diagrams similar to Figure 10 for cases of two to 10 source counts, since in our experience this range of counts have appreciable (10%–20%) contamination by false sources. The *fraction of false sources accepted* for a given threshold probability (P_{th}) is the normalized area lying below the straight line and with $P_{\text{rand}} \leq P_{\text{th}}$. Similarly, the *fraction of real sources rejected* is the area above the straight line and with $P_{\text{rand}} > P_{\text{th}}$. Figure 11a shows the two fractions for $\log(P_{\text{rand}}) = -3.95$, and Figure 11b shows them for $\log(P_{\text{rand}}) = -5$. For ≥ 3 photons, the curves change only slightly if $\log(P_{\text{rand}})$ is reduced to -6 . We find that for a given P_{rand} value, the false source rate is a strong function of the number of photons for ≤ 8 photons. Therefore, it is misleading to quote merely an average false source rate (integrated over all numbers of source counts), given the large number of few-count sources. We take the more conservative approach of demanding a maximum false source rate for each number of counts individually.

We chose a false source rate of 2% for the Slew Survey, to guarantee high reliability of the source list. To determine the corresponding threshold probability as a function of the number of counts, we determined, for each value of probability (in 0.25 $\log P_{\text{rand}}$ steps) in the range $-6 < \log(P_{\text{rand}}) < -3.95$, the

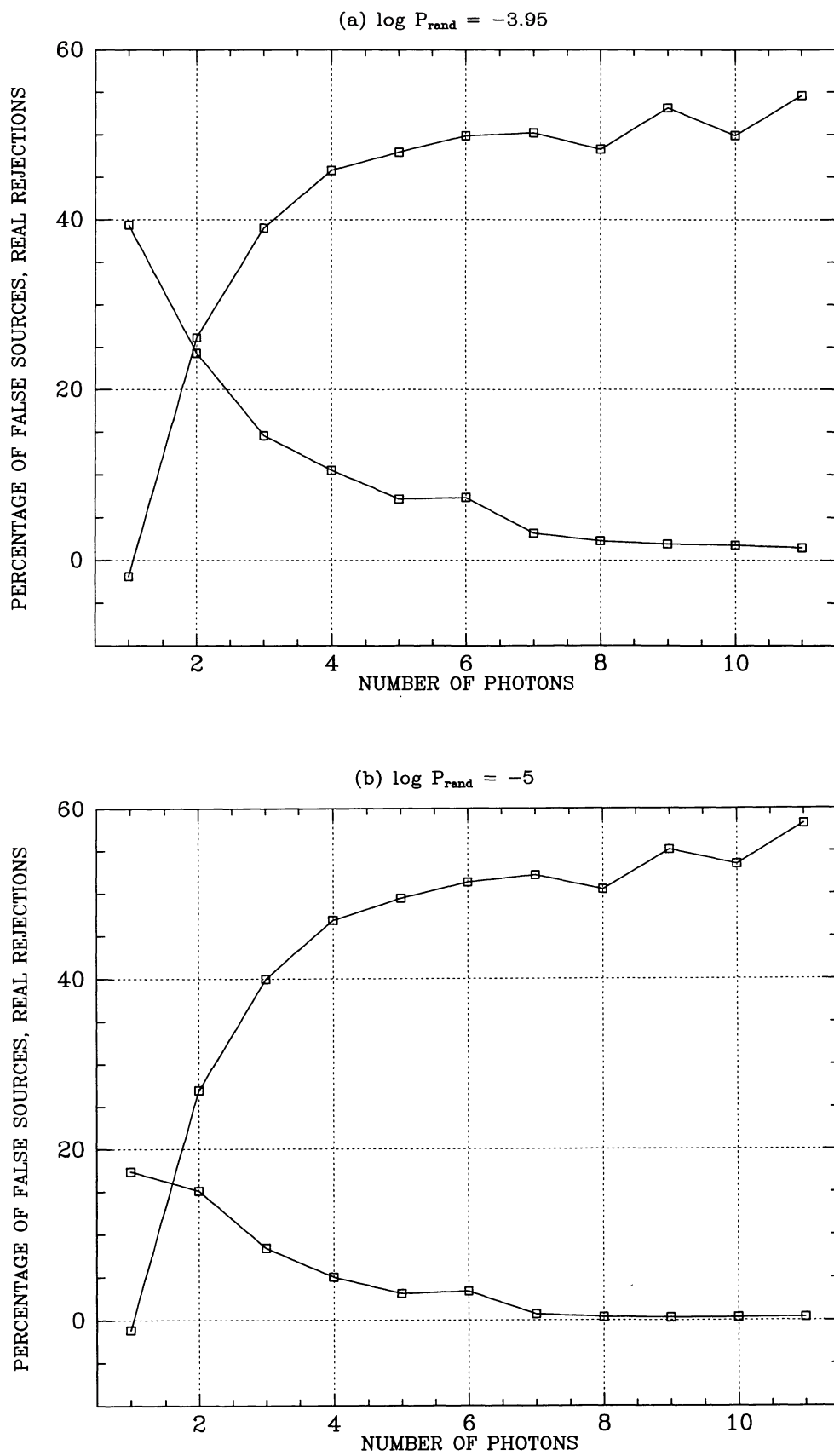


FIG. 11.—The percentage of false Slew Survey sources accepted (*lower curve*) and percentage of real sources rejected (*upper curve*) are shown as a function of the number of counts for two different probability thresholds. We show the cases of $\log (P_{\text{rand}}) = -3.95$ (a) and $\log (P_{\text{rand}}) = -5$ (b).

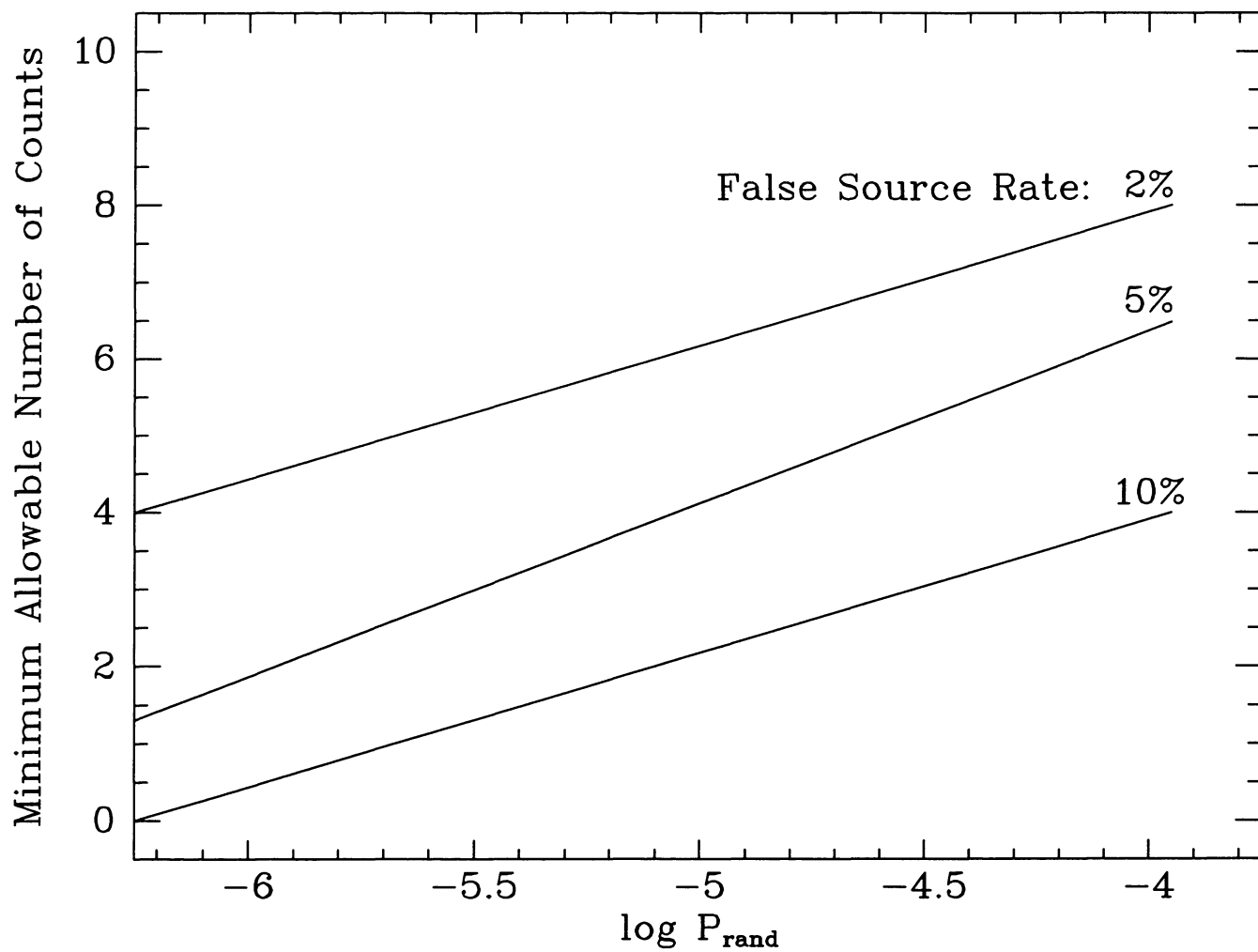


FIG. 12.—The dependence of the minimum allowable number of counts on $\log(P_{\text{rand}})$ is shown for three different false source rates: 2%, 5%, and 10%. A false source rate of 2% and $\log(P_{\text{rand}}) \leq -3.95$ were adopted for the Slew Survey catalog.

minimum allowable number of counts. The minimum number, for example at $\log(P_{\text{rand}}) = -5$, is six counts for 2% false sources. For higher false source rates, lower photon thresholds apply: four for 5%, and two for 10%. In other words, for $\leq 2\%$ false sources and $\log(P_{\text{rand}}) > -5$, all detected sources with five counts or fewer must be rejected. In a plot of $\log(P_{\text{rand}})$ versus number of counts, a given false source rate is well approximated by a straight line interpolated from the integer values. We show the 2%, 5%, and 10% lines in Figure 12; other values of false source rate can be estimated from the figure.

4.4.2. A Global Probability Threshold

We also performed an independent test to establish a global threshold probability for real sources. We made identifications of all the candidates with ≥ 3 photons against two catalogs of known X-ray sources that have positions known to better than 1'—the *Einstein* IPC Catalog (2E; Harris et al. 1991) and the *HEAO* A-3 Catalog (Remillard et al. 1991). Figure 13 shows the offset of the Slew position from the known position in arcminutes for sources matched in this way against the probability of the source being a chance congregation of photons, P_{rand} . Extended sources (clusters of galaxies, supernova rem-

nants, and all other IPC sources with “extent parameter” $> 3'$) were excluded from this comparison.

It is clear from Figure 13 that for small probabilities ($P_{\text{rand}} < 10^{-6}$) almost all the sources must be real since they are clustered at offsets of order the aspect accuracy derived from individual slews. Similarly at large probabilities ($P_{\text{rand}} > 10^{-3}$), there are a great number of false sources since they are distributed nearly uniformly in offset. Based on this diagram, we imposed an additional $\log(P_{\text{rand}}) = -3.95$ threshold, regardless of the number of photons in the source. Our threshold P_{rand} for accepting a candidate source as real is clearly at a level where the fraction of identified sources lying within 2' of the optical position begins to decrease rapidly (Fig. 14).

The criteria of 2% false sources and $\log(P_{\text{rand}}) \leq -3.95$ yields a list of 819 prospective sources with 16 false sources expected to be included.¹ If the statistics were Gaussian, the probability

¹ The source list on the CD-ROM was created with the condition $\log(P_{\text{rand}}) \leq -3.95$, but without the 2% false source cut. As a result, many more sources (1067) were reported to be real. Only those sources with $\log(P_{\text{rand}}) \leq -3.95$ and lying above the 2% curve in Fig. 12 are accepted for our analysis here, giving a final number of 819.

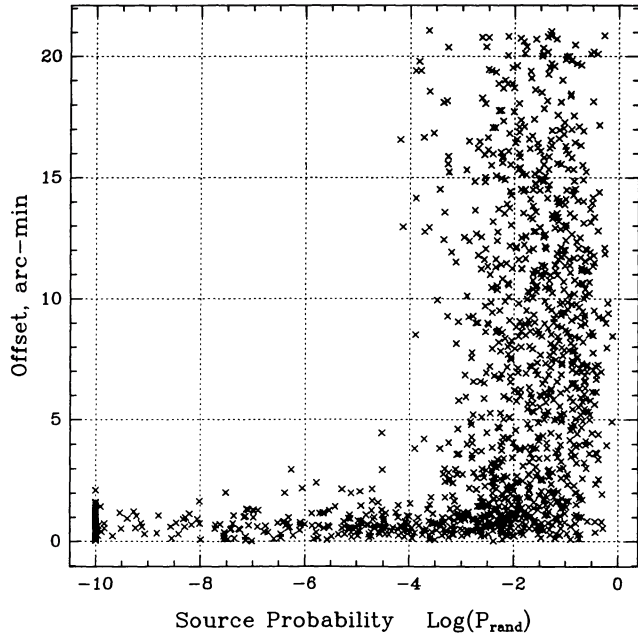


FIG. 13.—Offset in arcminutes between the Slew source positions and the accurate positions of known X-ray sources (for objects in Remillard et al. 1991 and nonextended objects in the 2E catalog) vs. probability of a source arising by chance.

constraint would correspond to a 3.3σ threshold. However, as demonstrated in the foregoing analysis, the highly asymmetric nature of the Poisson distribution for such small numbers of counts makes the detections more significant than common experience with 3σ results would suggest.

The estimate of threshold P_{rand} is based solely on known

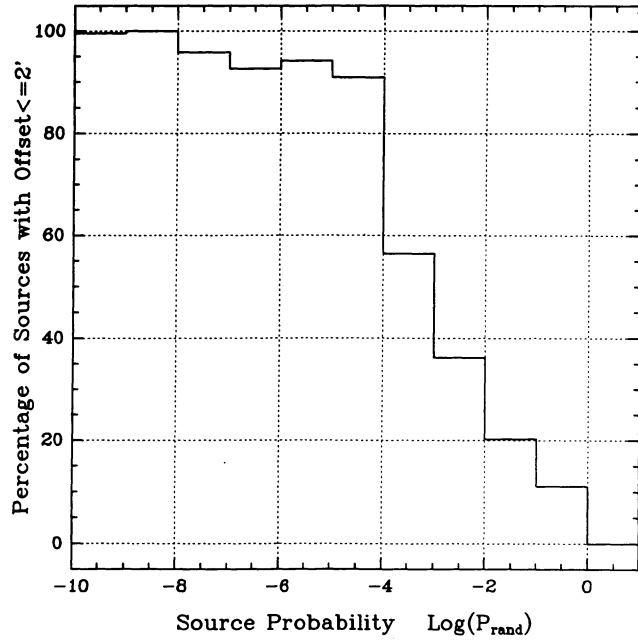


FIG. 14.—Fraction of Slew sources lying within 2' of the position of a known X-ray source (for objects in Remillard et al. 1991 and nonextended objects in the 2E catalog) vs. probability of a source arising by chance.

sources (i.e., large numbers of counts) and is therefore conservative. Sources on the 2% curve in Figure 12 and with $\log P_{\text{rand}} > -3.95$ may in fact be real. Some of these sources may be extractable by searching the original Slew Survey data at a predefined set of positions such as those of an optical catalog. This is possible given the software and data on the CD-ROM (Plummer et al. 1991). The source list (see § 6) gives the values of P_{rand} for each source so that readers may set more stringent thresholds if they wish.

As a final check, two of us (M. E. and J. S.) visually inspected each of the proposed sources for cases of dubious detections. A total of 10 sources were eliminated in this manner. Of these eight were rejected because photons from the outer fringes of a bright source caused a spurious second detection; two were rejected because the exposure gradients across the region were extreme and an isolated region of high exposure led to a “source.” A reliability index (1, 2, 3; 3 best) was compiled based on the visual inspection (see § 6).

In Figure 14, the fraction of objects within 2' of the correct position is plotted against the probability of a source arising by chance. Note that the figure contains an excess of sources near to zero offset even at $P_{\text{rand}} > 10^{-3}$, which is consistent with Figure 12. This again implies that other real sources exist in the data. Searches of the Slew Survey data base at given positions, defined a priori by, e.g., an optical catalog may give significant detections even if no source appears in this catalog. (Since the number of trials is small, a lower significance threshold can be used.)

4.5. High Background and Extended Sources

As noted above, in regions of high exposure the percolation algorithm did not produce sensible results because the mean distance between background photons became similar to the

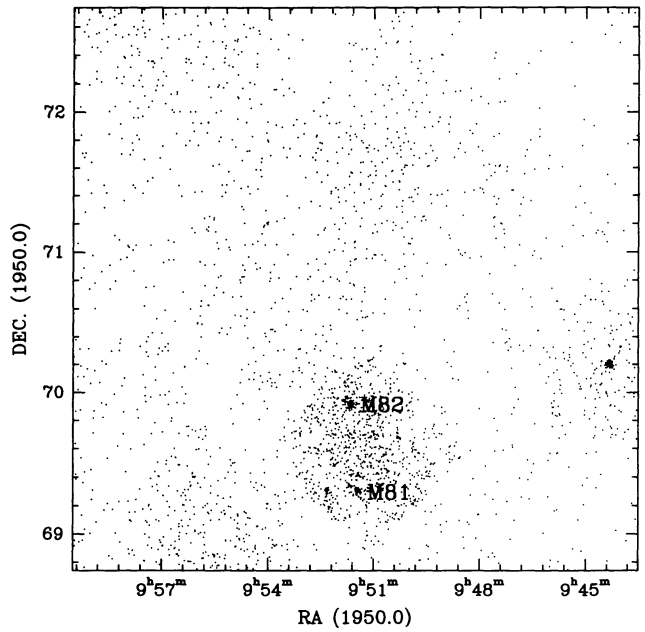


FIG. 15.—The M81/M82 region showing how the high density of background photons confuses the percolation algorithm with the standard percolation radius of 2'.

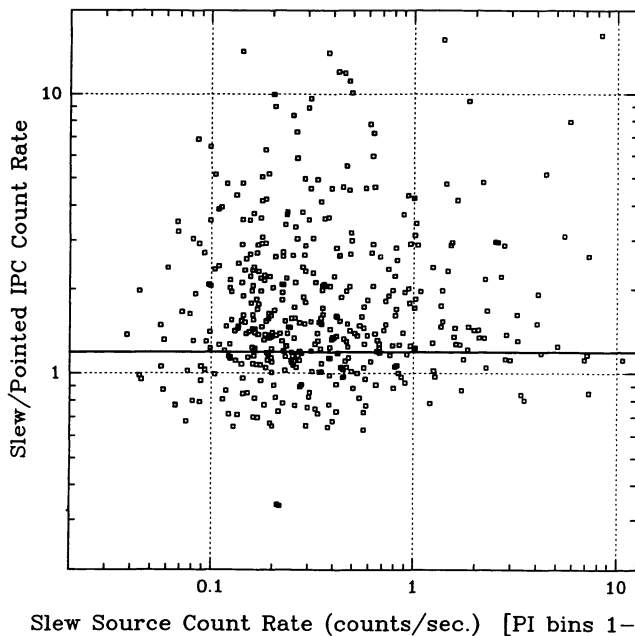


FIG. 16a

FIG. 16.—(a) Slew Survey count rate vs. ratio of Slew/Pointed IPC count rate (“2E”). (b) Slew Survey count rate restricted to PI 2-10 vs. ratio of Slew/Pointed IPC count rate (“2E”).

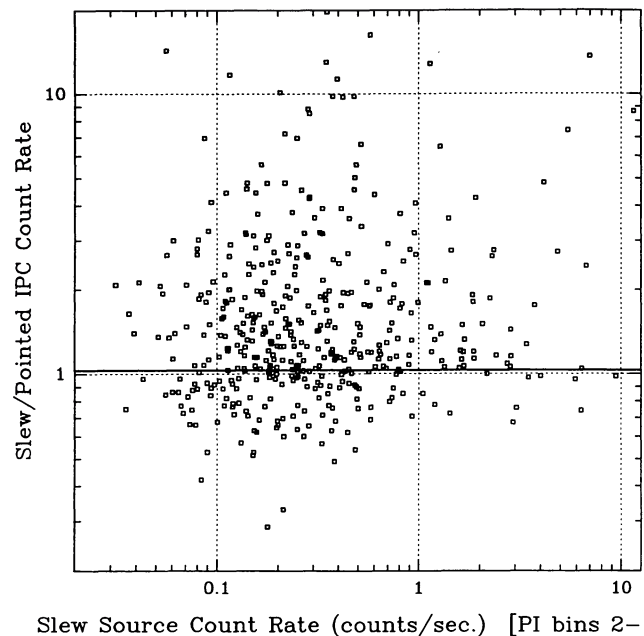


FIG. 16b

percolation length. Thus large areas of background were included with sources, leading to large extended “sources.” This tends to merge sources together and leads to their systematic undercounting in these regions. We dealt with this problem by selecting all sources with a maximum photon distance from the percolation centroid of $>9'$. We then reran the percolation algorithm with a smaller percolation length, which normally resolved the problem. Figure 15 shows how the galaxies M81 and M82 were initially included in a single source, but were resolved by using a shorter percolation length.

We found that when $\text{Prob1}/\text{Prob2}$ (defined in § 4.3) is large ($>10^3$), the source is extended, or that there are multiple sources within $15'$. A visual inspection of all cases with $\text{Prob1}/\text{Prob2} > 10^3$ was made (M. E. and J. S.). For all such sources an “Image Code” was assigned which notes extended sources larger than $\sim 15'$ (E), regions with multiple sources within $15'$ (M), and sources which are a part of a larger extended source (P). Sources with acceptable $\text{Prob1}/\text{Prob2}$ are assigned the code “A.”

Some sources are truly extended on this scale. Each extended source was inspected visually, which we found to be an effective, but unfortunately subjective, means of discriminating real sources from confusion with background. This procedure added 33 sources and improved the positions of 78. A more automatic means of changing the percolation length with the exposure to match the mean free path between background photons needs to be developed. Some few sources have extent of order degrees (e.g., the Cygnus Loop, Puppis A). Although these are not included in our source catalog, the data are on the CD-ROM. These sources will be treated fully in a later paper (Schachter et al. 1991; see also § 7).

5. SOURCE PROPERTIES

Having produced a list of reliable sources, we need to determine their properties. The IPC gives information on positions, count rates, structure, and pulse height (energy).

The reliability of the positions was established using known X-ray sources, as described above (§ 3; Fig. 7c).

Count rates were derived from the $6'$ diameter box used for the probability calculation with background from background region 2 (see § 4.3).

For extended sources (e.g., clusters of galaxies, supernova remnants, and those labeled “E” in the source table), the count rates will clearly not be accurate. For most of these, a better count rate can be derived using the counts and exposure in the $6'-12'$ “square annulus” surrounding the central detection cell (background region 1). This information is available on the CD-ROM version of the Slew Survey (see “lists/unix/readme.txt,” “lists/vms/readme.txt.,” etc.).

The count rates were checked for accuracy by comparing the Slew Survey rates with those derived from the pointed IPC data for sources in common. In Figure 16a we plot the Slew Survey count rates as listed in this catalog versus the pointed IPC count rates from the 2E catalog (Harris et al. 1991). There is a strong correlation with a slight offset (a factor 1.19) toward higher count rates in the Slew Survey. This is due primarily to our use of all 15 PI bins in the Slew Survey, compared with the standard two to 10 used in pointed data. (The restricted range for pointed data is used to minimize background, which is unnecessary in the Slew Survey.) When we restrict the Slew Survey source count rates to the same PI bins, the offset is reduced to a factor 1.03, as shown in Figure 16b. The source of

TABLE 5
IDENTIFIED SOURCES TO DATE

Class	Number of New X-Ray Sources	Total Number of Identifications	% Survey Detected	% Survey Predicted (MS)
AGNs	9	124	19	30
BL Lacs	0	31	5	10
Clusters	11	78	12	20
CVs	0	22	3	6
Stars:	92	242	38	20
Known Active	2	46
Binaries	4	19
Wind candidates (OBA)	11	32
Coronal candidates ($\geq F$)	68	127
Unknown, peculiar	7	18
X-ray binaries and pulsars	0	39	6	6
Other:	21	101	16	8
Galaxies	17	37
SN Remnants	0	28
White dwarfs	1	6
2E sources	0	23
SIMBAD sources	3	6
EXOSAT sources	0	2

this residual offset is still under investigation. The errors on these count rates are nontrivial to determine since both the background and the source counts are not in the Gaussian limit and so do not add in quadrature. The problem of calculating these uncertainties in the Poisson case has recently been investigated by Kraft, Burrows, & Nousek (1991), and we have used their methods with software routines which they kindly supplied to us. (Note that the uncertainties on the CD-ROM assumed Gaussian statistics. Updated values can be obtained using *einline*; Harris et al. 1991).

Several measures of source extent were attempted. Large sources, $>9'$ diameter, are readily selected using the maximum distance of a source photon from the percolation centroid. Smaller extended sources are clearly seen on the maps but are not so easily characterized. We are continuing a search for an objective means of classifying the size of sources.

The mean pulse height bin for each source was calculated from the photons in the $6'$ box. The “pulse height–invariant” (PI) bins were used since they have a first order correction to remove the effects of the variable gain of the IPC (Harnden et al. 1984). (This variation changes the mapping of photon energy to pulse height bin.) That an extreme ultraviolet source from the Wide Field Camera on *ROSAT* (1ES 1631+781) has a mean PI bin of 2 (on a scale from 1, low energy, to 15, high energy) shows that the PI data carry useful information.

6. SOURCE LIST

The Slew Survey source catalog contains 819 sources. Table 5 gives a summary of the identifications made.

6.1. Table of Objects

Table 6 is the Slew Survey source catalog. The identifications suggested in Table 6 are discussed in the next section (§ 7). Table 6 has the following entries.

Column (1).—Source name. “1ES” stands for first *Einstein*

Slew Survey source. Coordinate names are based on the B1950.0 position constructed from hours, minutes \pm degrees, tenths of degrees, truncated according to the IAU convention.

Columns (2) and (3).—Position. These are given in B1950.0 coordinates, based on the percolation algorithm centroid. Where noted, positions have been refined by changing the percolation length as discussed in § 4.5. Errors on position are primarily systematic, arising from the aspect solution. A 90% error radius of $1.2'$ and a 95% radius of $2.0'$ are estimated from Figure 7d.

Column (4).—Count rate. Mean count rate in all PI bins (1–15). This is on average a factor 1.19 larger than the standard IPC “broad-band” count rate (based on PI channels 2–10) used in the 2E catalog (see § 5). Counts are taken from a box $6'$ on a side centered on the percolation algorithm centroid. Background counts scaled for exposure and area from a box $30'$ on a side (background region 2) have been subtracted. Errors represent a 1σ confidence interval. When total source plus background in the source box had ≤ 100 counts, the error bars are based on a Poisson probability distribution as computed in Kraft et al. (1991), which gives asymmetric error bars. For sources with a larger number of photons, a Gaussian approximation was used.

Column (5).—Number of photons (NP) in the box which is $6'$ on a side and number of slews (NS) that contribute photons to the object. Other slews may have passed over the source positions but yielded no photons.

Column (6).—Probability, P_{rand} . Probability of finding the number of photons listed in column (5) relative to background region 2. Small numbers indicate a higher chance that the source is real. Values of $P_{\text{rand}} < 1 \times 10^{-10}$ are listed as equal to 1×10^{-10} . To generate the list of accepted sources, we used thresholds as in § 4.5.

Column (7).—Exposure. Total Slew Survey exposure time averaged over the box which is $6'$ on a side used in column (3).

TABLE 6
THE FIRST *Einstein* SLEW SURVEY CATALOG

Slew Design	RA 1950	DEC 1950	IPC Rate (cts s ⁻¹)	NP/NS	P _{rand}	Exp. (s)	PI	Q1	EOS # EMSS	Δ2E (<i>i</i>)	A3 EXO	Δ1H (<i>i</i>)	Cat.	Class: Type/z	Name	ΔC (<i>i</i>)
1ES0003+158	00 03 23	+15 52 55	0.09 ^{+0.03} _{-0.03}	20/3	7.03E-05	145.0	6	3A	12	0.6	HB	AGN:0.112	PHL 658	0.5
1ES0003+199	00 03 48	+19 55 15	1.63 ^{+0.35} _{-0.31}	26/3	1.00E-10	15.4	4	3A	x1H0003+200	0.8	HB	AGN:0.025	MRK 395	0.7
1ES0004+287	00 04 04	+28 44 18	0.29 ^{+0.07} _{-0.06}	26/4	1.00E-10	77.2	5	3A	m15	0.4	WLY	S:KOV	WLY 5	0.8
1ES0005+159	00 05 17	+15 59 01	0.12 ^{+0.05} _{-0.04}	13/5	4.26E-05	79.8	11	3A
1ES0008+107	00 08 00	+10 42 03	0.57 ^{+0.08} _{-0.07}	63/4	1.00E-10	102.9	6	3A	29	0.5	x1H0014+111	0.8	HB	AGN:0.089	III ZW 2	0.8
1ES0008-025	00 08 46	-02 35 02	0.29 ^{+0.14} _{-0.11}	7/3	2.17E-05	21.1	6	3A
1ES0013+195	00 13 37	+19 35 38	0.28 ^{+0.13} _{-0.11}	7/5	1.04E-05	22.6	6	3A	SBD	S:M4	G 32-6*	0.0
1ES0021-723	00 21 39	-72 21 40	0.09 ^{+0.03} _{-0.03}	19/5	7.46E-06	143.6	5	3A	82	0.9	SBD	P	47 TUC	1.3
1ES0022+638	00 22 26	+63 52 03	9.91 ^{+0.65} _{-0.66}	236/9	1.00E-10	23.5	7	3A	83	2.3	x1H0022+638	1.6	A3	SNR	TYCHO	1.7
1ES0033+595	00 33 04	+59 33 23	0.59 ^{+0.22} _{-0.18}	10/5	1.00E-10	16.2	7	3A
1ES0037+405	00 37 30	+40 33 19	0.06 ^{+0.02} _{-0.02}	29/4	1.92E-05	301.7	6	3A	113	0.2	2E	...	5C3 76	0.2
1ES0037+293	00 37 43	+29 18 26	0.23 ^{+0.10} _{-0.08}	10/3	5.14E-06	36.6	10	3A	m118	2.2	MS	CG:0.069	A77	2.2
1ES0039-095	00 39 19	-09 34 43	0.96 ^{+0.12} _{-0.11}	83/8	1.00E-10	79.6	7	3A	136	0.4	2E	CG:0.052	A85	0.7
1ES0039+400	00 39 36	+40 03 04	0.09 ^{+0.02} _{-0.02}	48/6	1.00E-10	370.5	7	3E	141	1.0	VV	AGN:0.102	IV ZW 29	0.7
1ES0039+409	00 39 58	+40 59 48	0.41 ^{+0.05} _{-0.05}	90/6	1.00E-10	197.5	5	3E	147	0.2	x1H0039+408	0.4	UGC	GAL:-0.001	M 31	0.4
1ES0041-182	00 41 09	-18 15 26	0.88 ^{+0.15} _{-0.14}	40/4	1.00E-10	43.4	4	3A	163	0.8	WLY	S:KOII	WLY 31	1.0
1ES0041+402	00 41 57	+40 16 51	0.08 ^{+0.03} _{-0.03}	19/5	6.12E-05	160.3	6	3A
1ES0043+113	00 43 00	+41 23 27	0.07 ^{+0.02} _{-0.01}	49/2	1.47E-09	464.5	5	3A	169	0.3	SBD	...	P SKHB 307	0.2
1ES0044-211	00 44 31	-21 06 21	0.14 ^{+0.05} _{-0.04}	26/3	3.87E-06	119.2	7	3A	179	2.8	2E	GAL	2E	2.5
1ES0044+239	00 44 40	+23 59 27	0.65 ^{+0.09} _{-0.09}	63/6	1.00E-10	90.8	5	3A	181	0.3	SAO	AC:KII	ζ AND	0.4
1ES0045-255	00 45 07	-25 33 58	0.16 ^{+0.03} _{-0.03}	37/4	1.00E-10	191.9	5	3A	184	0.3	RNG	GAL:0.01	NGC 253	0.6
1ES0045+211	00 45 41	+31 09 34	0.12 ^{+0.06} _{-0.05}	8/3	4.86E-05	55.7	9	3A
1ES0048+291	00 48 50	+29 07 15	0.20 ^{+0.09} _{-0.07}	10/1	8.34E-05	39.6	7	3A	m198	0.8	x1H0043+294	0.9	VV	AGN:0.036	VV	0.9
1ES0050+124	00 50 58	+12 25 09	0.39 ^{+0.09} _{-0.08}	27/3	1.00E-10	64.2	5	3A	209	0.2	SAO	AC:GII	I ZW 1	0.2
1ES0051-749	00 51 26	-74 55 33	0.30 ^{+0.06} _{-0.06}	36/5	1.00E-10	101.1	6	3A	214	0.2	SAO	AC:GIIb	CV TUC	0.1
1ES0052+251	00 52 09	+25 09 35	0.27 ^{+0.08} _{-0.07}	16/5	3.06E-10	52.5	5	3A	217	0.5	x1H0048+250	0.6	VV	AGN:0.154	PG	0.5
1ES0053+604	00 53 42	+60 27 09	2.05 ^{+0.33} _{-0.30}	45/8	1.00E-10	21.4	6	3A	x1H0053+604	0.4	A3	XRB:Be	γ CAS	0.4
1ES0054+231	00 54 32	+23 09 18	0.20 ^{+0.06} _{-0.05}	25/2	2.83E-08	93.5	4	3A	232	0.2	SAO	AC:GIIIb	SAO 074388	0.3
1ES0054+145	00 54 38	+14 30 45	0.15 ^{+0.05} _{-0.05}	15/4	2.93E-06	78.5	6	3A	233	1.3	x	...	VV	AGN:0.171	PHL 909	1.7
1ES0055+227	00 55 17	+22 45 02	0.17 ^{+0.07} _{-0.06}	12/3	1.08E-04	53.7	4	3A
1ES0057+315	00 57 06	+31 33 45	0.91 ^{+0.12} _{-0.11}	69/8	1.00E-10	72.2	5	3A	244	0.7	x1H0106+324	0.7	VV	AGN:0.015	MRK 352	0.7
1ES0100+405	01 00 56	+40 35 02	0.22 ^{+0.07} _{-0.06}	17/3	4.77E-09	64.0	5	3A	254	0.9	SBD	S	G 132-50A*	1.3
1ES0101+410	01 01 48	+41 02 52	0.23 ^{+0.10} _{-0.08}	10/2	2.16E-05	35.6	7	3A	260	1.0	GCV	S:PEC(UG)	RX AND	1.0

TABLE 6—Continued

Slew Design.	RA 1950	DEC 1950	IPC Rate (cts s ⁻¹)	NP/NS	P _{rand}	Exp. (s)	PI	QI	EOS # EMSS	Δ2E (<i>t</i>)	A3 EXO	Δ1H (<i>t</i>)	Cat. Type/ <i>z</i>	Name	ΔC (<i>t</i>)	
1ES0102-722	01 02 25	-72 17 50	0.82 ^{+0.09} _{-0.09}	106/9	1.00E-10	117.7	6	3A	261	0.4	x	...	2E	SNR	SMC	1.7
1ES0103-726	01 03 32	-72 38 01	0.18 ^{+0.05} _{-0.05}	25/9	1.03E-07	101.7	5	3A	267	1.3	x	...	GCV	S	SZ TUC	2.2
1ES0107-580	01 07 55	-58 02 07	0.55 ^{+0.33} _{-0.24}	4/1	3.39E-07	7.2	6	3A
1ES0108+174	01 08 25	+17 24 40	0.06 ^{+0.02} _{-0.02}	23/5	6.18E-05	230.5	7	3A	311	1.5	ABL	CG:0.066	A154	1.8
1ES0114-027	01 14 06	-02 46 03	1.85 ^{+0.17} _{-0.17}	128/3	1.00E-10	67.7	4	3A	339	0.6	BSC	AC:G5IIIe	AY CET	0.5
1ES0114+065	01 14 18	+06 33 35	0.25 ^{+0.08} _{-0.07}	15/2	5.01E-09	51.5	5	3A	340	0.6	x	...	SAO	S:G5	UV PSC	0.7
1ES0115+634	01 15 17	+63 28 26	1.52 ^{+0.29} _{-0.26}	33/5	1.00E-10	20.9	9	3A	345	0.6	1H0115+635	0.4	A3	XRB-Be	V635 CAS	0.4
1ES0115-737	01 15 45	-73 42 18	0.18 ^{+0.04} _{-0.04}	39/7	1.00E-10	160.0	7	3A	350	0.4	x1H0115-737	0.1	A3	XRB	SMC X-1	0.1
1ES0115-272	01 15 50	-27 14 37	0.26 ^{+0.10} _{-0.08}	11/3	4.64E-07	36.8	8	3A	349	0.8	ABL	CG	A2895	2.3
1ES0119-286	01 19 31	-28 36 22	0.61 ^{+0.21} _{-0.18}	11/4	1.00E-10	17.0	4	3A	x1H0122-281.B	0.3	HB	AGN:0.117	GD 1339	0.3
1ES0120+004	01 20 16	+00 26 50	0.34 ^{+0.15} _{-0.12}	8/5	2.23E-06	21.1	5	3A	SAO	S:G0	HD 8358*	0.5
1ES0120+340	01 20 20	+34 05 43	1.01 ^{+0.18} _{-0.16}	40/2	1.00E-10	37.7	7	3A	369	1.0	2E
1ES0121-590	01 21 53	-59 03 48	2.29 ^{+0.18} _{-0.18}	171/3	1.00E-10	72.9	5	3A	378	0.2	x1H0122-590	0.3	HB	AGN:0.045	FAIR 9	0.3
1ES0122+084A	01 22 29	+08 29 52	0.17 ^{+0.06} _{-0.05}	15/8	6.28E-06	68.6	7	2A	SBD	CG:0.045	A193*	2.9
1ES0122+084B	01 22 33	+08 26 23	0.21 ^{+0.07} _{-0.06}	14/7	9.35E-07	55.0	7	3A	ABL	CG:0.045	A193*	0.8
1ES0122+190	01 22 52	+19 04 33	0.12 ^{+0.06} _{-0.05}	10/6	5.01E-05	63.8	8	3A
1ES0124+189	01 24 50	+18 35 36	0.20 ^{+0.07} _{-0.06}	12/2	8.01E-07	50.7	4	3A	390	0.5	VV	AGN:0.017	MRK 359	0.4
1ES0131+203	01 31 02	+30 23 53	0.42 ^{+0.06} _{-0.06}	72/7	1.00E-10	150.1	7	3A	409	0.5	x1H0129+303	0.9	RNG	GAL:0.001	NGC 598	0.4
1ES0133+207	01 33 42	+20 43 05	0.14 ^{+0.04} _{-0.04}	23/6	3.98E-07	121.4	6	3A	437	0.8	x	...	HB	AGN:0.425	3C47	1.0
1ES0136-182	01 36 30	-18 12 37	0.18 ^{+0.03} _{-0.03}	64/9	1.00E-10	282.3	4	3A	455	0.7	SBD	S:M5.5V/e	LHS 9	1.2
1ES0138+391	01 38 57	+39 08 58	0.12 ^{+0.05} _{-0.04}	16/7	2.53E-05	93.5	7	2A	1H0140+393	1.0	VV	AGN:0.080	B2 0138+39B	0.9
1ES0139-189	01 39 05	-18 54 14	0.42 ^{+0.18} _{-0.14}	8/4	1.78E-07	17.6	4	3A
1ES0139-581	01 39 39	-68 07 54	1.38 ^{+0.19} _{-0.18}	63/9	1.00E-10	43.1	3	3A	469	0.4	x1H0136-581	0.6	A3	CV	BL HYI	0.6
1ES0142+614	01 42 51	+61 29 52	3.36 ^{+0.36} _{-0.31}	41/7	1.00E-10	12.0	7	3A	x1H0132+607	0.3	A3	XRB	X0142+614	0.4
1ES0143-253	01 43 17	-25 18 04	0.30 ^{+0.12} _{-0.10}	9/6	6.80E-08	27.3	4	3A	BSC	S:F1V	ε SCL	0.2
1ES0149+229	01 49 27	+22 37 36	0.22 ^{+0.10} _{-0.08}	8/5	2.23E-06	32.6	11	3A	ABL	CG:0.016	A262	2.5
1ES0149+258	01 49 42	+35 53 33	0.29 ^{+0.07} _{-0.06}	33/3	1.00E-10	90.0	7	3E	493	2.1	WLY	S:G5IV+	WLY 81AB	0.2
1ES0150+293	01 50 12	+29 19 29	0.33 ^{+0.08} _{-0.06}	39/5	1.00E-10	106.3	4	3A	495	0.7	BSC	S:A3IV	SAO 4554	0.9
1ES0158-365	01 58 00	-36 33 06	0.19 ^{+0.09} _{-0.07}	9/7	5.44E-05	38.2	6	3A	MS
1ES0158+003	01 58 32	+00 19 29	0.51 ^{+0.10} _{-0.09}	34/5	1.00E-10	59.6	5	3A	m513	0.5	2E	...	MS	0.5

TABLE 6—Continued

Slew Design.	RA 1950	DEC 1950	IPC Rate (cts s ⁻¹)	NP/NS	P_{rand}	Exp. (s)	PI	QI	EOS # EMSS	$\Delta 2E$ (γ)	A3 EXO	$\Delta 1H$ (ℓ)	Cat.	Class.: Type/z	Name	ΔC (ℓ)
1ES0203+158	02 03 36	+15 51 15	0.12 ^{+0.05} _{-0.04}	17/3	3.43E-05	95.0	6	3A	TT ARI	0.3
1ES0204+150	02 04 11	+15 03 29	0.53 ^{+0.06} _{-0.06}	105/7	1.00E-10	180.3	7	3A	m522	0.3	x1H0157+142	0.3	A3	CV	MRK 586	1.0
1ES0205+024	02 05 14	+02 29 43	0.20 ^{+0.07} _{-0.06}	15/3	4.83E-07	61.3	6	3A	526	1.0	HB	AGN:0.155	GPX 002	0.7
1ES0206+522	02 06 19	+52 12 18	0.61 ^{+0.20} _{-0.17}	12/6	1.00E-10	18.6	6	3A	534	0.3	1H0203+513	0.6	VV	AGN:0.049	AC:G5III+F5V	0.6
1ES0209+300	02 09 29	+30 04 50	0.46 ^{+0.10} _{-0.09}	30/3	1.00E-10	60.7	5	3A	544	0.7	BSC	...	ζ TRI	0.6
1ES0212-010	02 12 00	-01 00 09	1.02 ^{+0.12} _{-0.12}	78/4	1.00E-10	73.9	6	3A	548	0.3	x1H0215-007	0.2	VV	AGN:0.027	MRK 590	0.2
1ES0212+735	02 12 54	+73 33 32	0.17 ^{+0.07} _{-0.06}	10/2	8.90E-07	50.0	7	3A	549	2.2	HB	AGN:2.367	\$5 0212+735	2.2
1ES0215-021	02 15 02	-02 08 16	0.27 ^{+0.13} _{-0.10}	7/2	1.97E-05	22.8	10	3A
1ES0219+428	02 19 30	+42 48 27	0.29 ^{+0.03} _{-0.03}	156/11	1.00E-10	453.8	6	3A	558	0.2	X	...	VV	BL:0.444	3C 66A	0.1
1ES0221+323	02 21 55	+32 20 21	0.23 ^{+0.11} _{-0.09}	8/4	9.39E-05	28.7	10	3A
1ES0224+307	02 24 32	+30 45 04	0.45 ^{+0.08} _{-0.07}	43/3	1.00E-10	88.2	5	3A	569	0.2	X	...	SBD	S	BD+30 397AB	1.1
1ES0225+310	02 25 18	+31 05 29	0.35 ^{+0.07} _{-0.06}	38/4	1.00E-10	96.5	8	3A	573	0.1	x1H0218+304	0.7	VV	AGN:0.016	MRK 1040	0.4
1ES0226-615	02 26 54	-61 32 41	0.58 ^{+0.23} _{-0.19}	9/5	3.07E-08	14.4	4	3A	SAO	S:F8	SAO 248569	1.1
1ES0229+200	02 29 58	+20 04 18	0.51 ^{+0.16} _{-0.14}	14/5	1.00E-10	25.9	7	3A
1ES0232-090	02 32 10	-09 00 53	0.36 ^{+0.11} _{-0.10}	44/5	1.00E-10	62.6	6	3A	590	0.6	x1H0227-094	0.5	VV	AGN:0.043	NGC 986	0.5
1ES0232-440	02 32 25	-44 01 08	0.47 ^{+0.50} _{-0.42}	11/4	1.00E-10	7.3	5	3A	592	1.1	x1H0226-448	0.8	SBD	AC:M0Vp	HD 16157	0.7
1ES0235+016	02 35 45	+01 40 50	0.64 ^{+0.30} _{-0.24}	7/4	1.03E-05	9.9	6	3A	617	1.0	VV	AGN:0.024	NGC 1019	1.3
1ES0235+164	02 35 54	+16 24 15	0.04 ^{+0.01} _{-0.01}	35/6	7.97E-06	450.4	7	3E	618	0.2	HB	BL:0.940	OD 160	0.4
1ES0236+610	02 36 46	+61 00 07	0.26 ^{+0.10} _{-0.09}	12/4	7.25E-06	37.1	7	3A	627	1.1	X	...	GCV	S:B1EB:	LS I +61 303	1.0
1ES0236-002	02 36 51	-00 14 19	0.18 ^{+0.07} _{-0.06}	11/5	3.02E-07	51.8	6	3A	628	0.8	2E
1ES0237-531	02 37 05	-53 10 24	0.64 ^{+0.24} _{-0.20}	10/4	2.40E-09	14.5	4	3A	X	...	SBD	S:F8IV/V+	HD 16699*	0.4
1ES0238-009	02 38 43	-00 54 23	0.26 ^{+0.12} _{-0.10}	9/3	1.39E-05	29.0	3	3A	X	...	SAO	S:F7IV	SAO 130055	0.6
1ES0238+057	02 38 52	+05 45 46	0.21 ^{+0.10} _{-0.08}	8/6	5.01E-05	31.3	5	3A	SBD	S:M	BD+05 378	1.4
1ES0238+069	02 38 55	+06 58 40	0.17 ^{+0.04} _{-0.04}	29/5	1.00E-10	134.7	8	3A	645	0.3	VV	AGN:0.028	MRK 596	0.3
1ES0240-002	02 40 08	-00 13 50	0.53 ^{+0.06} _{-0.06}	85/4	1.00E-10	148.8	5	3A	649	0.5	x1H0244+001	0.4	VV	AGN:0.003	NGC 1068	0.4
1ES0241+622	02 41 02	+62 15 37	0.19 ^{+0.07} _{-0.06}	13/2	2.65E-06	53.9	8	3A	653	0.1	x1H0240+621	0.2	VV	AGN:0.044	4U 0241+61	0.2
1ES0241-381	02 41 26	-38 06 21	2.22 ^{+1.17} _{-0.91}	5/2	1.57E-07	2.2	2	2A	1H0247-370	2.0	SBD	AC:G6V+	SAO 193879	2.0
1ES0242-675	02 42 29	-67 33 30	0.36 ^{+0.16} _{-0.13}	8/4	1.48E-05	19.4	7	3A
1ES0244+694	02 44 21	+69 26 27	0.62 ^{+0.23} _{-0.20}	10/3	8.78E-09	14.9	5	3A	663	0.9	SAO	S:A3V	SAO 012445	0.7
1ES0244+191	02 44 38	+19 09 57	0.29 ^{+0.10} _{-0.09}	13/3	7.30E-08	39.0	6	3A	664	0.1	SAO	S:G0	SAO 093105	0.1
1ES0245+309	02 45 42	+30 54 16	0.96 ^{+0.19} _{-0.17}	32/5	1.00E-10	31.6	5	3A	669	0.4	WLY	S:G9	VY ARI	0.3
1ES0247-253	02 47 16	-25 20 03	0.18 ^{+0.08} _{-0.07}	7/1	1.04E-05	35.5	8	3A
1ES0249-251	02 49 09	-25 08 09	0.18 ^{+0.06} _{-0.05}	14/4	7.24E-08	67.0	6	3A	673	1.0	ABL	CG:0.116	A389	1.3

TABLE 6—Continued

Slew Desig.	RA 1950	DEC 1950	IPC Rate (cts s ⁻¹)	NP/NS	P _{rand}	Exp. (s)	PI	QI	EOS #	Δ2E (γ)	A ₃ EXO	Δ1H (ℓ)	Cat.	Class: Type/z	Name	ΔC (ℓ)
1ES0250-129	02 50 06	-12 58 07	0.17+0.07 -0.06	13/2	1.06E-05	57.9	4	3A	674	0.9	BSC	S:K2V	HD 17825	0.0
1ES0250-618	02 50 41	-61 50 01	0.35+0.14 -0.12	9/5	2.98E-07	23.1	4	3A	1H0256-617	0.6	SBD	AC:K1Vp	SAO 248669	0.6
1ES0255+139	02 55 06	+13 56 13	0.16+0.08 -0.06	8/2	9.40E-05	40.9	8	2A	ABL	CG:0.072	A399*	...
1ES0255+128	02 55 08	+12 50 34	0.26+0.04 -0.04	75/3	1.00E-10	235.2	7	3A	682	0.3	ABL	CG:0.076	A401	1.8
1ES0256+133	02 56 06	+13 21 56	0.26+0.07 -0.06	28/3	1.00E-10	85.2	8	3E	687	1.6	1H0253+138	1.9	UGC	GAL	U02468	1.5
1ES0257+442	02 57 22	+44 15 24	0.74+0.37 -0.29	6/4	8.04E-06	7.5	6	3A	UGC
1ES0303+067	03 03 35	+06 44 59	0.30+0.14 -0.12	7/4	1.79E-05	20.8	10	3A
1ES0304+497	03 04 56	+40 45 05	2.67+0.69 -0.60	18/3	1.00E-10	6.6	5	3A	724	0.8	X	...	BSC	S:BBV	β PER	0.9
1ES0305-284	03 05 50	-28 24 24	0.33+0.15 -0.12	9/3	2.62E-05	22.8	7	3A	SBD	S:K7V	CD-28 1030*	0.2
1ES0309-291	03 09 58	-29 11 02	1.02+0.24 -0.22	22/6	1.00E-10	20.5	4	3A	WLY	S:F8IV+	WLY 127AB	0.2
1ES0310-568	03 10 04	-56 49 43	0.23+0.10 -0.08	9/9	2.29E-05	32.7	7	2A
1ES0310-640	03 10 10	-64 05 01	0.23+0.09 -0.07	11/9	3.88E-07	41.0	6	2A
1ES0311-227	03 11 59	-22 46 44	1.27+0.13 -0.13	108/7	1.00E-10	82.1	5	3A	740	0.3	x1H0311-227	0.2	A3	CV	EFR ER	0.2
1ES0313-770	03 13 00	-77 03 18	0.14+0.05 -0.04	17/2	4.47E-06	89.2	6	3A	746	0.3	HB	AGN 0.223	PKS	0.4
1ES0316-444	03 16 11	-44 24 39	0.97+0.45 -0.38	7/4	1.16E-06	6.7	7	3A	x1H0316-445	0.4	ABL	CG:0.070	A3112	0.4
1ES0316+413	03 16 31	+41 19 48	7.25+0.16 -0.16	2420/6	1.00E-10	316.4	7	3A	761	0.2	x1H0316+413.AB	0.3	A3	CG:0.018	A426*	0.3
1ES0316+031	03 16 44	+03 11 20	0.25+0.10 -0.09	11/4	1.20E-05	36.1	4	3A	752	0.8	X	...	WLY	S:G5V	WLY 137	0.0
1ES0323+285	03 23 32	+28 32 16	3.50+0.22 -0.23	252/4	1.00E-10	70.7	6	3A	770	0.2	x1H0334+291	0.3	SBD	AC:G5IV+K0	UX ARI	0.3
1ES0323+022	03 23 39	+02 14 37	0.80+0.24 -0.21	15/6	1.00E-10	17.6	7	3A	771	0.3	x1H0323+022	0.2	VV	BL 0.147	H 0323+022	0.3
1ES0324+095	03 24 26	+09 33 42	0.54+0.21 -0.16	9/4	9.51E-09	15.7	7	3A	BSC	S:B8Vn	HD 21364	0.3
1ES0325+042	03 25 17	+04 13 13	0.29+0.12 -0.10	10/5	2.85E-06	29.4	6	3A
1ES0327-242	03 27 11	-24 16 15	0.19+0.06 -0.05	22/3	8.24E-08	87.5	3	3A	m783	0.7	SAO	S:K5	SAO 168581	0.4
1ES0328+054	03 28 14	+05 27 48	0.46+0.17 -0.14	12/5	8.52E-08	23.0	6	3A
1ES0330-621	03 30 08	-62 07 17	0.42+0.20 -0.16	8/5	3.76E-05	16.2	7	3A
1ES0334+004	03 34 14	+00 25 24	4.02+0.11 -0.11	1349/9	1.00E-10	331.8	4	3A	804	0.3	x1H0327+000	0.2	SBD	AC:G9V	V711 TAU	0.3
1ES0339-214	03 39 52	-21 24 12	0.75+0.12 -0.11	46/4	1.00E-10	57.9	6	3A	m826	0.1	MS	AGN 0.015	MS	0.2
1ES0341-538	03 41 40	-53 49 14	0.37+0.16 -0.13	9/4	1.92E-05	20.6	7	3A	845	1.9	1H0341-537	1.3	ABL	CG:0.059	A3158	1.3
1ES0347-121	03 47 02	-12 08 33	1.47+0.27 -0.25	34/7	1.00E-10	22.4	5	3A
1ES0347+170	03 47 33	+17 05 31	0.47+0.09 -0.08	38/3	1.00E-10	75.9	5	3A	894	0.3	X	...	MCS	WD:DA2	ζ PER	0.3
1ES0352+308	03 52 14	+30 53 54	2.07+0.37 -0.34	36/5	1.00E-10	16.9	8	3A	906	0.5	x1H0352+308	0.2	A3	XRB-Be
1ES0352-686	03 52 52	-68 40 15	0.49+0.12 -0.11	22/14	1.00E-10	40.9	6	3A
1ES0353-741	03 53 23	-74 10 07	0.20+0.07 -0.06	17/3	5.17E-06	64.3	7	3A	m908	0.6	1H0350-735	1.7	A3	CG:0.127	MS	1.7
1ES0355-612	03 55 19	-61 12 55	0.33+0.10 -0.09	18/12	2.85E-09	45.9	6	3A

TABLE 6—Continued

Slew Design.	RA 1950	DEC 1950	IPC Rate (cts s ⁻¹)	NP/NS	<i>P</i> _{rand}	Exp. (s)	PI	QI	EOS # EMSS (<i>i</i>)	Δ2E (<i>i</i>)	A3 EXO	Δ1H (<i>i</i>)	Cat.	Class.: Type/z	Name	ΔC (<i>i</i>)	
IES0357-400	03 57 56	-40 01 50	0.30 ^{+0.12} _{-0.10}	10/6	6.64E-06	28.1	6	3A	SBD	S:K0	HD 25300	1.2	
IES0403-373	04 03 13	-37 19 12	0.42 ^{+0.15} _{-0.13}	12/6	3.97E-08	25.1	6	3A	SBD	GAL:0.055	ESO 359-19	0.2	
IES0405-123	04 05 25	-12 20 06	0.36 ^{+0.09} _{-0.08}	24/1	1.00E-10	58.3	7	3A	938	0.9	1H0413-116	0.8	VV	AGN:0.574	MS	0.8	
IES0407-080	04 07 17	-08 01 52	1.98 ^{+0.32} _{-0.29}	46/2	1.00E-10	22.5	5	3A	943	0.5	1H0409-078	0.5	A3	AC	SAO 130984	0.6	
IES0408-587	04 08 20	-58 47 54	0.37 ^{+0.17} _{-0.14}	7/6	2.48E-06	17.4	9	2A	
IES0410+103	04 10 37	+10 19 34	0.79 ^{+0.17} _{-0.15}	29/7	1.00E-10	34.5	6	3A	949	1.1	x1H0409+102	2.3	ABL	CG:0.090	A478	1.5	
IES0411+261	04 11 30	+26 09 35	0.14 ^{+0.07} _{-0.06}	8/2	9.65E-05	46.4	5	3A	952	0.7	SAO	S:G5	SAO 076514	1.6
IES0412-382	04 12 09	-38 12 03	0.64 ^{+0.30} _{-0.24}	7/3	1.17E-06	10.1	6	3A	EXC	GAL:0.050	ESO(B) 303R	1.5
IES0412+060	04 12 48	+06 04 15	0.16 ^{+0.03} _{-0.03}	41/5	1.00E-10	206.9	4	3A	956	0.2	BSC	S:G0IV	HD26933	0.5	
IES0413-625	04 13 36	-62 34 55	0.15 ^{+0.05} _{-0.05}	17/7	2.27E-06	83.6	5	3A	m958	1.2	BSC	S:G8II-III	HD27256	1.6	
IES0414+009	04 14 19	+00 57 36	1.61 ^{+0.66} _{-0.54}	8/2	7.74E-10	4.8	6	3A	959	0.8	x1H0414+009	0.6	HB	BL:0.287	1H	0.6	
IES0414+365	04 14 49	+36 35 19	0.30 ^{+0.16} _{-0.12}	5/4	5.86E-07	16.0	9	3A	
IES0414+379	04 14 58	+37 54 33	0.41 ^{+0.12} _{-0.10}	18/4	1.00E-10	38.6	7	3A	963	0.7	1H0414+380	0.6	VV	AGN:0.048	3C 111.0	0.6	
IES0415+231	04 15 06	+23 09 27	0.35 ^{+0.12} _{-0.12}	8/4	7.50E-07	21.1	6	3A	SBD	S:K0	HD 284303	1.2	
IES0415+283	04 15 24	+28 19 50	0.26 ^{+0.09} _{-0.08}	13/5	4.34E-07	42.5	6	3A	GCV	S:K3E-K7E	V410 TAU	0.3	
IES0418+281	04 18 51	+28 10 32	0.26 ^{+0.11} _{-0.09}	9/3	1.52E-05	29.5	6	3A	987	0.8	1H0419+280.A	0.7	SBD	AC:G2II	SAO 076567	0.6	
IES0418-550	04 18 52	-55 03 02	0.34 ^{+0.07} _{-0.06}	39/6	1.00E-10	101.2	6	3A	988	0.5	x1H0414-551	0.4	VV	AGN:0.005	NGC 1566	0.4	
IES0419+148	04 19 36	+14 48 40	0.07 ^{+0.03} _{-0.02}	22/12	1.33E-05	197.1	6	3M	SBD	S:F8	HD 285758	2.2	
IES0419+149	04 19 57	+14 56 42	0.09 ^{+0.03} _{-0.02}	31/12	4.15E-08	240.4	5	3M	1000	0.7	SAO	S:G0	SAO 093836	0.7	
IES0421+146	04 21 22	+14 38 46	0.17 ^{+0.03} _{-0.03}	47/16	1.00E-10	221.0	5	3A	1020	0.2	SAO	S:G0	SAO 093910	0.3	
IES0423+154	04 23 29	+15 28 54	0.25 ^{+0.05} _{-0.04}	42/13	1.00E-10	143.8	5	3A	1034	0.5	BSC	S:F0V	HD28052	0.5	
IES0423+146	04 23 51	+14 36 12	0.11 ^{+0.04} _{-0.03}	17/10	1.58E-05	112.8	10	1A	SAO	S:G7III	SAO 093935	0.9	
IES0424+177	04 24 18	+17 44 42	0.16 ^{+0.07} _{-0.06}	11/5	2.64E-05	54.6	6	3A	1043	0.4	2E	
IES0424+099	04 24 48	+09 54 13	0.14 ^{+0.05} _{-0.04}	15/9	5.61E-06	80.3	8	2A	
IES0425-573	04 25 03	-57 18 41	0.67 ^{+0.20} _{-0.17}	17/6	1.00E-10	22.7	5	3A	1H0419-577	0.1	A3	AGN	1H	0.1	
IES0426-131	04 26 43	-13 07 07	0.12 ^{+0.03} _{-0.03}	11/3	4.96E-05	72.1	6	3A	BSC	S:B:Vne	DU ERI	2.6	
IES0429-537	04 29 33	-53 43 18	0.69 ^{+0.22} _{-0.19}	14/8	1.10E-10	18.5	4	3A	1H0435-531	0.4	VV	AGN:0.040	FAIR 303	0.3	
IES0429+130	04 29 36	+13 00 09	0.20 ^{+0.09} _{-0.07}	9/5	1.16E-05	38.0	4	3A	SBD	CG:0.055	ESO 118-30	2.7	
IES0430+052	04 30 32	+05 14 57	0.68 ^{+0.03} _{-0.03}	834/32	1.00E-10	1153.3	7	3A	1087	0.1	x1H0426+051	0.1	VV	AGN:0.033	3C 120	0.1	
IES0430+179	04 30 38	+17 54 34	0.12 ^{+0.04} _{-0.03}	23/4	3.48E-07	134.1	6	3A	m1089	0.2	1H0427+177	0.3	BSC	S:B9:Vn	HD28867	0.3	
IES0430-615	04 30 47	-61 31 22	0.38 ^{+0.06} _{-0.05}	75/7	1.00E-10	162.6	6	3E	1090	1.8	SBD	CG:0.055	ESO 118-30	2.7	
IES0431-133	04 31 21	-13 22 00	1.00 ^{+0.06} _{-0.06}	315/7	1.00E-10	292.3	6	3A	1092	0.5	x1H0430-133	0.7	ABL	CG:0.032	A496	1.2	
IES0433+270	04 33 42	+27 02 15	0.73 ^{+0.10} _{-0.09}	69/3	1.00E-10	90.5	4	3A	1103	0.4	SAO	S:K2	SAO 076672	0.2	

TABLE 6—Continued

Slew Design.	RA 1950	DEC 1950	IPC Rate (cts s ⁻¹)	NP/NS	<i>P_{r and}</i>	Exp. (s)	PI	QI	EOS # EMSS	Δ2E (<i>i</i>)	A3 EXO	Δ1H (<i>i</i>)	Cat.	Class: Type/z	Name	ΔC (<i>i</i>)
1ES0435-472	04 35 54	-47 17 14	0.50+0.23 -0.18	8/5	5.27E-06	14.1	4	3A
1ES0437-046	04 37 02	-04 41 30	0.50+0.16 -0.14	14/6	1.95E-10	25.3	8	3A	GCV	S	BF ERI
1ES0437+444	04 37 21	+44 25 55	2.76+0.93 -0.79	11/1	1.00E-10	3.9	10	3A	GCV	S	OU PER
1ES0439-085	04 39 30	-08 32 20	0.21+0.10 -0.08	8/4	6.02E-05	32.1	5	3A
1ES0439-682	04 39 56	-68 14 44	0.20+0.08 -0.07	13/11	1.39E-05	50.8	2	3A
1ES0441-107	04 41 22	-10 46 31	0.12+0.04 -0.04	20/4	9.93E-07	117.6	8	3A	1142	0.7	SAO	S:A5	RZ ERI
1ES0444-704	04 44 32	-70 24 51	0.20+0.07 -0.06	11/5	3.26E-08	48.5	3	3A	HD	S:K7	HD270712
1ES0446+449	04 46 12	+44 56 08	0.15+0.05 -0.04	30/4	2.06E-06	128.1	8	3E
1ES0447+068	04 47 10	+06 51 40	0.77+0.33 -0.27	8/1	2.14E-07	9.6	4	3A	SAO	S:F6V	SAO 112106
1ES0452-559	04 52 25	-55 55 54	0.27+0.08 -0.07	17/3	1.00E-10	55.1	5	3A	1177	1.2	x1H0451-560	1.0	A3	AC	1H	1.0
1ES0453-685	04 53 50	-68 33 40	0.16+0.07 -0.06	12/8	7.09E-05	54.9	6	3A	1184	0.6	SBD	SNR	0453-68.5
1ES0454-220	04 54 00	-22 03 30	0.17+0.07 -0.06	14/2	5.87E-06	62.1	8	3A	1185	0.3	HB	AGN:0.534	PKS
1ES0457+017	04 57 00	+01 42 29	0.39+0.08 -0.06	50/2	1.00E-10	117.1	5	3A	1191	0.1	x	WLY	S:MEV	WLY 182
1ES0459+034	04 59 31	+03 27 38	0.45+0.11 -0.10	24/2	1.00E-10	48.0	7	3A	m1208	0.3	1H0510+031	0.1	VV	AGN:0.016	GHIGO	0.1
1ES0459-753	04 59 47	-75 21 49	0.44+0.16 -0.13	12/6	2.34E-08	24.0	8	3A	x1H0502-755	0.8	SBD	AC:K1IIIp	HD32918	0.9
1ES0501+589	05 01 50	+58 57 06	0.35+0.11 -0.13	16/3	1.00E-10	41.0	6	3A	1213	0.3	1H0501+592	0.2	A3	AC	BM CAM	0.2
1ES0504-575	05 04 40	-57 32 10	0.77+0.26 -0.22	12/7	1.00E-10	14.7	4	3A	WLY	S:FSV	WLY 189
1ES0505-054	05 05 01	-05 28 03	0.35+0.07 -0.07	33/5	1.00E-10	82.4	8	3A	m1220	0.1	MS	AC	MS	DEM 17
1ES0505-679	05 05 48	-67 56 28	0.71+0.16 -0.14	28/9	1.00E-10	35.6	5	3A	1222	0.3	2E	SNR	...
1ES0505-546	05 05 58	-54 38 09	0.47+0.20 -0.16	8/6	6.29E-08	16.0	6	3A
1ES0506-680	05 06 11	-68 05 36	0.28+0.11 -0.09	15/7	2.18E-05	39.6	7	3M	1223	0.7	2E	SNR	N23 (LMC)
1ES0510-119	05 10 00	-11 56 02	0.31+0.11 -0.09	13/8	2.57E-08	36.5	6	3A	SAO	S:B8V	SAO 159223
1ES0510-162	05 10 42	-16 16 16	0.07+0.03 -0.02	24/3	8.62E-05	207.0	6	3A	1236	0.6	x	SAO	S:AP	μ LEP
1ES0513-002	05 13 38	-00 12 51	0.58+0.16 -0.14	18/1	1.00E-10	28.5	7	3A	1240	0.6	x	VV	AGN:0.033	AKN 120
1ES0518-453	05 18 24	-45 49 42	0.47+0.08 -0.07	44/5	1.00E-10	85.6	6	3A	1252	0.2	x1H0507-459	1.0	VV	AGN:0.034	PIC A	1.0
1ES0519-690	05 19 55	-69 05 09	0.68+0.07 -0.07	111/18	1.00E-10	151.7	6	3A	1257	0.1	2E	SNR	LMC	0.2
1ES0521-720	05 21 17	-72 00 27	7.27+0.24 -0.24	919/18	1.00E-10	125.1	7	3A	1264	0.1	x1H0521-720	0.1	A3	XRB	LMC X-2	0.1
1ES0523-543	05 23 53	-54 19 13	0.36+0.16 -0.13	8/4	1.04E-05	19.5	8	3A
1ES0524-711	05 24 50	-71 11 13	0.12+0.04 -0.03	27/11	1.94E-06	144.8	6	3A	1276	1.2	SBD	S:Be	BI 156
1ES0525-660	05 25 22	-66 02 01	0.34+0.08 -0.07	33/18	1.00E-10	79.1	5	3M	1277	0.4	x	...	2E	SNR	N49B (LMC)	0.3

TABLE 6—Continued

Slew Desig.	RA 1950	DEC 1950	IPC Rate (cts s ⁻¹)	NP/NS	P _{rand}	Exp. (s)	PI	QI	EOS #	Δ2E (γ)	A3 EXO	Δ1H (γ)	Cat.	Class: Type/z	Name	ΔC (γ)
1ES0526-661	05 26 03	-66 07 35	0.85+0.11 -0.10	78/30	1.00E-10	85.9	6	3A	1279	0.8	x	...	2E	SNR	N49 (LMC)	0.8
1ES0527+111	05 27 10	+11 11 38	0.93+0.24 -0.21	29/2	1.69E-10	23.9	4	2A	x
1ES0527-328	05 27 37	-32 51 21	0.14+0.04 -0.05	17/1	7.81E-06	86.5	9	3A	1286	0.4	x1H0527-328	0.6	A3	CV	TV COL	0.6
1ES0528-654	05 28 32	-65 29 15	2.17+0.18 -0.18	180/30	1.00E-10	66.7	5	3A	1290	0.6	x	...	SAO	S:K1IIUp	SAO 249286	0.5
1ES0529-003	05 29 26	-00 19 55	0.59+0.07 -0.07	84/4	1.00E-10	131.4	4	3A	1293	0.3	BSC	S:B0III+09	6 ORI	0.3
1ES0529+097	05 29 30	+09 47 32	0.28+0.08 -0.07	18/1	1.00E-10	85.1	5	3A	1294	0.3	GCV	S:M4VE	V 998ORI	0.2
1ES0531+100	05 31 48	+10 05 18	0.18+0.05 -0.05	22/2	2.87E-08	95.4	5	3A	1315	0.1	SBD	S	HD 245059	0.3
1ES0532+215	05 32 12	+21 34 35	3.94+1.38 -1.17	14/1	7.97E-08	3.0	7	2M	x1H0534-667	0.2	A3	XRB	LMC X-4	...
1ES0532-664	05 32 49	-66 24 19	0.44+0.08 -0.07	41/16	1.00E-10	83.5	6	3A	1368	0.2	SAO	S:OE5	ORI STARS	0.2
1ES0532-054	05 32 50	-05 25 07	1.24+0.06 -0.06	455/7	1.00E-10	388.6	7	3A	1366	0.1	x	...	BSC	S:O9III	HD 37043	0.5
1ES0532-059	05 32 57	-05 56 16	0.44+0.03 -0.03	106/8	1.00E-10	212.1	4	3A	1377	0.7	x
1ES0533+215	05 33 04	+21 31 54	1.91+0.41 -0.41	25/1	1.00E-10	11.6	7	2M	x1H0534-667	0.2	A3	XRB	LMC X-4	0.2
1ES0534-580	05 34 02	-58 03 53	0.47+0.08 -0.07	44/5	1.00E-10	86.9	4	3A	1425	0.5	x1H0538-577	0.4	A3	CV	TW PIC	0.4
1ES0534-077	05 34 16	-07 42 00	0.24+0.06 -0.05	9/6	3.92E-07	34.4	7	3A	SBD	...	KMS 66	1.9
1ES0534-699	05 34 27	-69 57 16	0.06+0.02 -0.02	55/16	2.01E-05	437.0	5	3A	1436	0.9	2E	SNR	DEM 238	0.7
1ES0535-660	05 35 40	-66 03 59	2.83+0.18 -0.18	321/30	1.00E-10	111.6	6	3A	1461	0.2	x	...	2E	SNR	N63A (LMC)	0.1
1ES0536-580	05 36 36	-58 02 39	0.13+0.06 -0.05	11/4	6.25E-05	66.7	9	3A
1ES0538-691A	05 38 05	-69 11 48	0.12+0.02 -0.02	128/27	1.00E-10	518.9	7	3A	1499	0.6	x	...	2E	SNR	N157B (LMC)	0.6
1ES0538-019	05 38 14	-01 58 54	0.73+0.31 -0.25	8/2	6.83E-08	10.3	5	3A	1500	1.0	SBD	S:O9Iab:	HD 3742*	0.9
1ES0538-641	05 38 40	-64 06 42	16.97+0.56 -0.56	945/26	1.00E-10	55.3	7	3A	1H0538-641	0.2	A3	XRB	LMC X-3	0.1
1ES0538+037	05 38 46	+03 45 20	0.20+0.07 -0.06	14/1	2.28E-06	5547	5	3A	1507	0.6	SAO	S:G5	SAO 113040	0.9
1ES0538-691B	05 38 52	-69 06 32	0.08+0.02 -0.02	97/22	3.86E-06	467.4	6	1M	1513	1.4	x	...	2E	SNR	2E	1.4
1ES0540-697	05 40 06	-69 46 09	10.71+0.10 -0.10	11654/44	1.00E-10	1077.1	7	3A	1522	0.2	x1H0540-697	0.1	A3	XRB	LMC X-1	0.1
1ES0540-693	05 40 37	-69 21 35	0.48+0.03 -0.03	555/42	1.00E-10	947.5	7	3A	1525	0.2	x	...	2E	P	2E	0.4
1ES0543-655	05 43 02	-55 34 09	0.40+0.18 -0.15	8/5	1.87E-05	17.2	5	3A	RNG	GAL:0.016	NGC 2087	3.0
1ES0543-683	05 43 39	-68 23 17	0.22+0.08 -0.08	23/7	6.01E-10	82.4	5	3A	1550	1.0	x	...	2E	S	2E	0.9
1ES0548-322	05 48 50	-32 16 54	2.22+0.18 -0.18	194/3	1.00E-10	85.7	5	3A	1574	0.2	x1H0548-322	0.3	HB	BL:0.069	PKS	0.1
1ES0552-641	05 52 04	-64 06 06	0.17+0.07 -0.06	13/9	5.06E-05	56.1	7	3A
1ES0556-642	05 56 30	-64 15 18	0.17+0.07 -0.06	12/11	1.21E-05	56.5	5	3A
1ES0547-697	05 47 35	-69 42 44	0.04+0.01 -0.01	114/18	3.81E-07	1048.2	6	3A	1570	0.8	2E	SNR	N135 (LMC)	0.5
1ES0548-336	05 48 50	-33 38 50	0.40+0.15 -0.13	10/4	1.76E-08	23.1	4	3A
1ES0546-642	05 46 30	-64 15 18	0.34+0.15 -0.12	8/4	4.66E-06	20.8	6	2A
1ES0558-504	05 58 33	-50 27 29	2.00+0.46 -0.41	22/6	1.00E-10	10.9	4	3A	x1H0557-503	0.6	HB	AGN:0.137	PKS	0.6

TABLE 6—Continued

Slew Desig.	RA 1950	DEC 1950	IPC Rate (cts s ⁻¹)	NP/NS	P _{rand}	Exp. (s)	PI	QI	EOS # EMSS	Δ2E (<i>t</i>)	A3 EXO	Δ1H (<i>t</i>)	Cat.	Class.: Type/z	Name	ΔC (<i>t</i>)		
1ES0559-399	05 59 51	-39 56 35	0.07+0.03 -0.02	32/4	8.98E-05	247.8	6	3A	EXC	GAL	GAL 0559-3959	2.7	
1ES0602-482	06 02 48	-48 17 36	0.60+0.28 -0.23	8/4	2.33E-05	11.4	5	3M	SAO	SAO 217708	0.5		
1ES0603-484	06 03 27	-48 27 25	0.84+0.32 -0.27	10/4	5.37E-08	10.8	3	3M	SAO	S:G5	
1ES0613+227	06 13 52	+22 46 40	0.98+0.33 -0.29	15/3	1.08E-07	12.7	7	3E	HD	S:K2	HD254475	1.4	
1ES0614+227	06 14 20	+22 45 29	1.11+0.44 -0.37	12/2	1.02E-05	8.6	7	3E	
1ES0614-584	06 14 57	-58 24 41	0.41+0.10 -0.09	24/9	1.00E-10	51.9	4	3A	
1ES0615-655	06 15 27	-65 32 01	0.22+0.10 -0.08	9/7	9.47E-05	33.3	5	3A	
1ES0618-580	06 18 25	-58 02 05	0.33+0.10 -0.08	19/9	1.49E-10	48.9	5	3A	SAO	S:K2V	SAO 234448	0.2
1ES0620-666	06 20 13	-66 40 21	0.20+0.08 -0.08	9/8	4.87E-05	36.3	6	3A	
1ES0622-526	06 22 50	-52 40 19	0.13+0.04 -0.03	29/7	3.47E-07	150.4	6	3A	1642	0.3	x	BSC	S:F0II	HD 45348	0.2	
1ES0623+187	06 23 15	+18 47 57	0.23+0.06 -0.08	20/2	1.00E-10	76.5	5	3A	1646	0.7	SAO	S:K3V+	WLY 233AB	0.6	
1ES0625-536	06 25 16	-53 40 34	0.13+0.04 -0.04	29/9	4.06E-07	145.3	6	3E	1656	2.0	ABL	CG:0.053	A3391	1.7	
1ES0625-600	06 25 27	-60 01 12	0.19+0.08 -0.07	11/5	3.82E-05	45.9	6	3A	
1ES0626-544	06 26 31	-54 24 00	0.07+0.02 -0.02	46/6	6.78E-05	311.0	5	3E	ABL	CG:0.050	A3395	2.0	
1ES0627-018	06 27 17	-01 48 36	0.49+0.22 -0.18	7/5	1.32E-07	13.6	6	3A	
1ES0629+068	06 29 07	+06 49 03	0.16+0.06 -0.05	16/7	3.29E-05	71.2	4	3A	1678	0.6	SAO	S:G3IV	SAO 114005	0.5	
1ES0629+049	06 29 31	+04 57 17	0.09+0.03 -0.03	28/6	1.00E-05	199.6	6	3E	1684	1.7	2E	SNR	MON. NEBULA	1.5	
1ES0630-540	06 30 59	-54 03 30	0.15+0.04 -0.04	25/10	1.02E-07	119.1	6	3A	1695	1.0	2E	
1ES0630+178	06 30 59	+17 48 41	0.14+0.03 -0.03	40/8	1.00E-10	215.7	3	3A	1697	0.4	x	SBD	S	2CG 195+04	0.1	
1ES0635-747	06 35 08	-74 44 13	0.23+0.09 -0.08	13/6	1.15E-05	43.0	5	3A	1718	2.1	2E	
1ES0635-206	06 35 23	-20 39 27	0.14+0.06 -0.05	10/2	6.54E-05	57.1	6	3A	
1ES0635-698	06 35 30	-69 49 44	0.21+0.07 -0.07	18/11	7.73E-09	69.8	6	3A	SBD	S:G3V	HD 47875	2.2	
1ES0637-762	06 37 23	-75 14 09	0.16+0.06 -0.05	23/5	6.82E-06	95.0	5	3A	1720	0.6	x1H0633-752	0.5	VV	AGN:0.651	PKS	0.5		
1ES0637-614	06 37 26	-61 29 16	0.56+0.15 -0.13	19/9	1.00E-10	30.7	4	3A	BSC	S:G1-2V	HD48189	0.3	
1ES0638+039	06 38 12	+09 57 27	0.18+0.04 -0.04	29/4	1.00E-10	129.1	4	3A	1723	0.8	x	BSC	S:O7Ve	MON. STARS	0.9	
1ES0638+094	06 38 22	+09 29 07	0.11+0.03 -0.03	31/4	1.28E-07	191.5	5	3A	1724	1.3	x	SAO	S:B3	MON. STARS	2.0	
1ES0639-756	06 39 36	-75 36 11	0.14+0.06 -0.05	16/7	1.06E-04	75.3	7	2A	1725	0.4	2E	
1ES0640+059	06 40 47	+05 54 03	0.10+0.04 -0.03	18/4	1.05E-05	122.0	9	3A	1726	0.4	SAO	S:G5III	SAO 114321	0.1
1ES0642-166	06 42 56	-16 39 08	0.83+0.13 -0.12	50/3	1.00E-10	56.1	2	3A	1730	0.5	x	MCS	WD:DA2	α CMA B	0.3	
1ES0643-167	06 43 04	-16 47 50	0.21+0.08 -0.07	19/3	4.89E-05	59.0	8	3M	1731	0.6	x	2E	CV	HL CMA	0.6	
1ES0644-541	06 44 30	-54 10 18	0.27+0.09 -0.08	13/10	2.52E-08	42.7	5	3A	ABL	CG	A3404	1.3	
1ES0646-515	06 46 00	-51 32 09	0.32+0.10 -0.09	16/7	2.52E-09	43.2	5	3A	
1ES0647+260	06 47 40	+25 05 34	0.96+0.39 -0.32	8/2	1.59E-10	8.1	6	3A	

TABLE 6—Continued

Slew Design.	RA 1950	DEC 1950	IPC Rate (cts s ⁻¹)	NP/NS	P _{rand}	Exp. (s)	PI	QI	EOS #	Δ2E (<i>t</i>)	A3	Δ1H (<i>t</i>)	Cat.	Class: Type/z	Name	ΔC (<i>t</i>)	
1ES0655+542	06 55 30	+54 15 20	0.23 ^{+0.10} _{-0.08}	9/1	2.25E-06	35.0	5	3A	1750	1.1	x	...	VV	AGN:0.044	MRK 374	0.9	
1ES0657-558	06 57 28	-55 52 28	0.22 ^{+0.06} _{-0.03}	26/7	1.00E-10	96.6	6	3A	1759	0.2	2E	
1ES0702+646	07 02 27	+64 40 45	0.17 ^{+0.07} _{-0.06}	10/7	5.28E-05	46.6	4	3A	VV	AGN:0.079	VII Zw 118*	0.3	
1ES0702-241	07 02 56	-24 07 24	0.60 ^{+0.30} _{-0.23}	6/2	3.00E-06	9.4	10	3A	
1ES0712-363	07 12 23	-36 21 17	0.45 ^{+0.20} _{-0.17}	8/5	1.86E-05	15.5	7	3A	SAO	S:F6-7V	SAO 197732	1.3
1ES0715-810	07 15 44	-81 03 11	0.33 ^{+0.16} _{-0.13}	7/5	8.03E-06	19.1	11	3A	
1ES0715-703	07 15 45	-70 19 10	0.21 ^{+0.09} _{-0.08}	10/8	3.36E-05	38.6	4	3A	
1ES0715-259	07 15 56	-25 59 24	0.13 ^{+0.06} _{-0.05}	12/7	1.04E-04	66.9	7	2A	
1ES0716-248	07 16 38	-24 51 32	0.06 ^{+0.02} _{-0.02}	37/11	1.51E-06	373.3	6	3A	1804	0.1	SBD	S:091b	HD 57061*	0.2	
1ES0717+558	07 17 24	+55 52 47	0.31 ^{+0.05} _{-0.05}	53/2	1.00E-10	147.6	6	3A	1805	1.0	1H0712+558	2.8	ABL	CG:0.038	A576	2.9	
1ES0717-572	07 17 29	-57 14 55	0.48 ^{+0.16} _{-0.14}	14/9	9.27E-09	25.5	5	3A	SAO	S:G01V-V	SAO 235087	0.9	
1ES0718-313	07 18 29	-31 20 02	0.39 ^{+0.17} _{-0.14}	9/5	4.95E-06	19.8	2	3A	x	
1ES0730+074	07 30 06	+07 29 48	0.38 ^{+0.17} _{-0.14}	8/3	5.90E-06	18.8	9	3A	
1ES0731+319	07 31 27	+31 58 41	0.90 ^{+0.11} _{-0.10}	79/5	1.00E-10	82.3	5	3A	1827	0.4	x1H0729+316	0.2	A3	AC	YY GEM	0.2	
1ES0735+178	07 35 12	+17 48 54	0.04 ^{+0.01} _{-0.01}	44/14	6.70E-05	463.2	6	3A	1843	0.6	x	...	HB	BL:0.424	PKS	0.6	
1ES0736+053	07 36 35	+05 21 25	1.44 ^{+0.58} _{-0.48}	8/1	1.25E-10	5.4	2	3A	1849	1.4	x	...	WLY	S:F5IV	α CMIA	1.5	
1ES0737+395	07 37 08	+39 30 04	0.35 ^{+0.17} _{-0.14}	7/4	9.29E-06	17.8	9	3A	
1ES0737+746	07 37 46	+74 40 58	0.30 ^{+0.14} _{-0.11}	7/3	2.95E-06	21.2	7	3A	m1855	0.6	MS	BL:0.315	MS	0.6	
1ES0738+612	07 38 30	+61 15 37	0.86 ^{+0.33} _{-0.33}	9/2	1.00E-10	10.2	5	3A	SAO	S:K0	SAO 014296	1.1	
1ES0740+290	07 40 11	+29 00 15	2.09 ^{+0.15} _{-0.15}	197/5	1.00E-10	92.0	5	3A	1861	0.2	x1H0741+289	0.1	A3	AC	σ Gem	0.2	
1ES0740+228	07 40 38	+22 50 08	0.42 ^{+0.18} _{-0.15}	8/4	9.35E-06	16.7	6	3A	SAO	S:K0	SAO 079647	0.2	
1ES0742+036	07 42 03	+03 40 27	0.39 ^{+0.04} _{-0.04}	115/5	1.00E-10	261.5	4	3A	1871	0.1	x1H0743+037	0.1	A3	AC	YZ CMI	0.1	
1ES0752+393	07 52 06	+39 19 30	0.26 ^{+0.07} _{-0.06}	22/1	1.00E-10	71.0	5	3A	1888	0.4	x	...	VV	AGN:0.034	MRK 382	0.6	
1ES0758+574	07 58 29	+57 24 49	0.25 ^{+0.06} _{-0.06}	26/3	1.00E-10	85.8	5	3A	1900	0.3	BSC	AC:R8V	HD65626	0.5	
1ES0801-398	08 01 50	-39 52 06	0.34 ^{+0.08} _{-0.08}	21/4	1.31E-10	52.3	5	3A	1910	0.4	x	...	BSC	S:051af	HD66811	0.4	
1ES0801+242	08 01 51	+24 16 07	0.91 ^{+0.49} _{-0.37}	5/1	1.57E-06	5.3	9	3A	
1ES0804+761	08 04 50	+76 11 34	0.59 ^{+0.22} _{-0.18}	11/3	6.73E-09	16.9	5	3A	1919	0.7	x1H0758+762	0.9	A3	AGN:0.099	PG	0.9	
1ES0807-471	08 07 59	-47 11 03	0.18 ^{+0.05} _{-0.04}	26/5	1.00E-10	114.7	6	3A	1936	0.3	BS	S:WC8+07.5e	γ VEL	0.2	
1ES0808+627	08 08 06	+62 45 39	0.57 ^{+0.07} _{-0.06}	92/6	1.00E-10	151.6	5	3A	1938	0.4	x1H0811+625	0.3	A3	CV	SU UMA	0.3	
1ES0811-570	08 11 30	-57 04 44	0.39 ^{+0.13} _{-0.11}	15/5	5.44E-08	32.0	8	3A	1955	0.5	2E	
1ES0812-188	08 12 49	-18 53 36	2.78 ^{+0.40} _{-0.37}	56/4	1.00E-10	19.7	3	3A	1959	1.1	x	...	SHA	CV	VV PUP	0.9	
1ES0814-073	08 14 58	-07 21 47	0.64 ^{+0.05} _{-0.05}	215/12	1.00E-10	307.8	7	3E	1961	0.5	2E	CG:0.071	A644	0.5	
1ES0815-480	08 15 49	-48 03 22	0.23 ^{+0.10} _{-0.08}	9/4	1.07E-05	33.5	10	3A	

TABLE 6—Continued

Slew Desig.	RA 1950	DEC 1950	IPC Rate (cts s ⁻¹)	NP/NS	P _{rand}	Exp. (s)	PI	QI	EOS #	Δ2E (<i>i</i>)	A3 EXO	Δ1H (<i>i</i>)	Cat.	Class.: Type/ <i>z</i>	Name	ΔC (<i>i</i>)		
1ES0818+544	08 18 51	+54 28 16	0.16 ^{+0.07} -0.06	10/3	6.33E-05	48.9	4	3A	m1971	0.3	MS	AGN:0.086	MS	0.5		
1ES0821-426	08 21 26	-42 41 34	4.34 ^{+0.25} -0.25	1120/11	1.00E-10	135.0	5	2A		
1ES0824+662	08 24 10	+66 12 23	0.20 ^{+0.08} -0.08	12/2	2.31E-05	46.2	5	3A	1987	0.3	2E		
1ES0826-703	08 26 20	-70 21 37	0.28 ^{+0.10} -0.08	11/8	6.10E-05	37.5	5	3A		
1ES0826+660	08 26 34	+66 01 51	0.15 ^{+0.06} -0.05	12/1	9.17E-05	61.1	6	3A	1995	1.1	2E	CG:0.181	A665	1.2		
1ES0827-687	08 27 35	-68 43 09	0.15 ^{+0.07} -0.06	9/7	1.02E-04	48.5	8	3A		
1ES0829+237	08 29 11	+23 47 10	0.32 ^{+0.15} -0.12	8/1	9.54E-06	21.7	11	3A		
1ES0829+159	08 29 41	+15 59 17	0.56 ^{+0.25} -0.20	8/3	7.11E-06	12.7	6	3A	SAO 097895	2.4		
1ES0832-421	08 32 16	-42 10 50	0.36 ^{+0.12} -0.11	24/2	9.11E-06	43.5	3	3E		
1ES0833-450	08 33 38	-45 00 33	1.36 ^{+0.20} -0.18	91/7	1.00E-10	51.0	6	3A	2014	0.4	x	x	2E	P	HU VEL	0.5		
1ES0834+651	08 34 52	+65 11 10	0.35 ^{+0.16} -0.13	8/2	5.60E-06	20.1	3	3A	2018	0.8	x1H0333+654	0.8	A3	AC	π^1 UMA	0.8		
1ES0836-319	08 36 01	+31 57 35	0.14 ^{+0.06} -0.05	9/2	3.22E-05	52.3	7	3A	2022	0.8	SAO	ACK2III+K4I	RZ CNC	1.1	
1ES0836+710	08 36 20	+71 03 33	0.38 ^{+0.13} -0.11	9/6	1.80E-08	25.6	8	3A	VV	AGN:2.160	4C 71.07	0.8		
1ES0837-425	08 37 05	-42 31 35	0.48 ^{+0.17} -0.15	31/4	6.44E-05	35.4	3	3M		
1ES0837-430	08 37 12	-43 01 00	1.40 ^{+0.39} -0.34	35/4	8.64E-08	16.6	4	3M	2027	2.5	2E		
1ES0839-446	08 39 04	-44 39 13	0.46 ^{+0.12} -0.11	38/3	4.66E-08	53.5	4	3E		
1ES0839-445	08 39 19	-44 31 20	0.71 ^{+0.14} -0.13	50/4	1.00E-10	52.2	4	3A	HD	S:A0	HD74209	2.5		
1ES0840-420	08 40 03	-42 05 45	0.31 ^{+0.11} -0.10	19/2	1.20E-05	42.4	4	3A		
1ES0841-436	08 41 50	-43 39 23	0.21 ^{+0.07} -0.06	56/3	3.76E-05	119.5	3	1A		
1ES0842-425	08 42 21	-42 35 06	0.49 ^{+0.14} -0.14	32/2	1.40E-05	37.8	3	1A		
1ES0844+349	08 44 35	+34 56 17	0.13 ^{+0.06} -0.05	12/4	3.48E-05	69.9	5	3A	2048	0.3	x	x	VV	AGN:0.064	PG	0.3		
1ES0847+267	08 47 42	+26 44 00	0.19 ^{+0.09} -0.07	8/5	4.74E-05	36.0	6	3A		
1ES0849+080	08 49 34	+08 04 57	0.48 ^{+0.07} -0.07	58/3	1.00E-10	107.4	5	3A	m2060	0.3	x	x	VV	AGN:0.063	1E	0.7		
1ES0851+392	08 51 05	+39 17 20	0.55 ^{+0.18} -0.16	12/1	5.39E-09	20.6	3	3A		
1ES0851+203	08 51 57	+20 18 07	0.45 ^{+0.03} -0.03	243/17	1.00E-10	489.7	5	3A	2076	0.1	x	x	HB	BL:0.306	OJ 287	0.2		
1ES0853-445	08 53 20	-44 32 51	0.58 ^{+0.17} -0.15	28/1	1.07E-07	33.7	2	3E		
1ES0853-448	08 53 58	-44 52 30	0.69 ^{+0.21} -0.19	27/2	6.15E-07	26.4	3	3E	ABL	CG:0.053	A754	1.2
1ES0855+369	08 56 56	+36 58 04	0.11 ^{+0.04} -0.04	15/5	2.78E-05	97.2	4	3A	2084	0.7	S:FB	AGN:0.059	A773	0.9	
1ES0906-0944	09 06 20	-09 26 19	0.25 ^{+0.07} -0.07	27/3	9.38E-08	75.5	6	3M	2100	2.6	1H0906-095	1.4	ABL	CG:0.053	MRK 704	0.6		
1ES0906-0943	09 06 45	-09 28 30	0.49 ^{+0.09} -0.09	43/3	1.00E-10	73.9	7	3M	2103	1.2	x	x	2E	CG:0.053	SAO 61189	2.8		
1ES0914+519	09 14 28	+51 55 48	0.22 ^{+0.10} -0.08	8/6	3.54E-05	31.4	6	3A	ABL	CG:0.197	3C218	0.2
1ES0915+165	09 15 40	+16 30 26	0.47 ^{+0.08} -0.07	43/3	1.00E-10	85.3	7	3A	2116	0.6	VV	AGN:0.029	A754	1.0		
1ES0915-118	09 15 41	-11 53 15	0.81 ^{+0.21} -0.18	20/3	1.00E-10	23.3	6	3A	2117	0.4	x1H0917-121	0.2	A3	AGN:0.055	3C218	0.2		

TABLE 6—Continued

Slew Desig.	RA 1950	DEC 1950	IPC Rate (cts s ⁻¹)	NP/NS	P _{rand}	Exp. (s)	PI	QI	EOS #	Δ2E (<i>t</i>)	A3 EXO	Δ1H (<i>t</i>)	Cat.	Class.: Type/z	Name	ΔC (<i>i</i>)
1ES019-549	09 19 03	-54 59 23	4.33±1.87	7/1	1.00E-10	1.6	6	3A	x1H0918-548	1.1	A3	XRB	X0918-549	1.1
1ES019+404	09 19 15	+40 24 41	0.86±0.38	7/2	2.43E-08	7.8	6	3A	SAO	S:K2V	SAO 042826	1.0
1ES020-136	09 20 30	-13 36 51	0.63±0.31	6/1	7.71E-07	9.0	7	3A	SAO	S:K0IV	SAO 155136	0.6
1ES021+143	09 21 25	+14 22 29	0.13±0.05	16/2	1.19E-05	93.0	7	1A	2131	1.5	ABL	CG:0.136	A796	1.8
1ES021-630	09 21 28	-63 04 39	0.50±0.13	21/9	1.00E-10	38.7	6	3A	x1H0920-629	0.4	A3	XRB	2S	0.4
1ES021+525	09 21 44	+52 30 41	1.40±0.25	39/11	1.00E-10	26.5	6	3A	VV	AGN:0.036	MRK 110	0.6
1ES023+129	09 23 18	+12 56 32	0.34±0.15	8/1	1.85E-06	20.9	5	3A	2139	0.7	x1H0929+122	0.7	VV	AGN:0.028	MRK 705	0.7
1ES023-392	09 23 56	+39 15 09	0.12±0.04	22/3	1.05E-05	126.0	5	3A	2141	0.2	x	...	VV	AGN:0.098	4C 39.25	0.3
1ES027+500	09 27 11	+50 04 49	0.65±0.23	11/6	1.84E-09	15.6	5	3A	SBD	...	H 0927+50.1	2.6
1ES029+216	09 29 14	+21 41 48	0.10±0.03	19/4	1.66E-06	140.7	5	3A	2151	2.4	RNG	GAL:0.002	NGC 2003	1.1
1ES030+700	09 30 04	+70 03 18	0.82±0.09	88/5	1.00E-10	102.6	5	3A	2153	0.2	BSC	S:G4III-IV	DK UMA	0.3
1ES039+759	09 39 18	+75 57 37	0.37±0.18	6/4	4.13E-06	15.1	9	3A
1ES042+098	09 42 49	+09 50 03	0.24±0.06	21/4	1.00E-10	77.6	5	3A	m2182	0.4	1H0932+107	0.0	VV	AGN:0.013	VV	0.8
1ES043-140	09 43 17	-14 05 55	0.40±0.10	25/6	1.00E-10	54.4	8	3A	2183	0.3	x1H0946-144	0.3	VV	AGN:0.008	NGC 2992	0.2
1ES050+495	09 50 52	+49 30 09	0.23±0.08	15/7	5.10E-07	53.4	5	3A	m2193	0.6	MS	BL	MS	1.2
1ES051+693	09 51 24	+69 18 32	0.19±0.03	61/8	1.00E-10	260.6	6	3A	2195	0.4	x1H0950+696.B	0.5	VV	AGN:0.000	M81	0.5
1ES051+699	09 51 39	+69 54 29	0.41±0.06	74/10	1.00E-10	160.4	6	3A	2197	0.6	x1H0950+696.A	0.5	A3	GAL:0.001	M82	0.5
1ES053+693	09 53 53	+69 18 37	0.08±0.03	28/4	3.08E-05	203.4	6	3A	2199	0.4	x	...	SBD	GAL:0.175	UGC 5336*	2.6
1ES057+247	09 57 09	+24 47 35	0.97±0.30	14/3	1.00E-10	13.7	4	3A	SAO	ACK0VE+B:	DH LEO	1.3
1ES1002-559	10 02 09	-55 56 13	0.43±0.17	9/5	1.13E-07	19.2	6	3A	SAO	S:K1-III	SAO 237656	0.7
1ES1003+777	10 03 06	+67 46 59	0.12±0.05	15/4	1.95E-05	92.4	7	3A	2225	1.7	SHA	CV	CH UMA	0.5
1ES1007+491	10 07 09	+49 08 44	0.21±0.09	10/2	3.91E-05	37.4	5	3A
1ES1011+496	10 11 52	+49 41 07	0.63±0.18	12/2	1.00E-10	17.7	5	3A	2250	0.7	1H1013+498	0.6	HB	BL	GB 1011+498	0.6
1ES1016+201	10 16 49	+20 07 40	1.58±0.20	74/3	1.00E-10	45.3	4	3A	2259	1.0	x	...	WLY	S:M4EV	AD LEO	1.2
1ES1020+493	10 20 31	+49 20 17	0.25±0.10	11/4	3.36E-06	36.3	7	3A	SBD	S:F6	HD 88944	2.9
1ES1020+201	10 20 45	+20 07 31	0.42±0.05	82/7	1.00E-10	175.2	7	3A	2275	0.3	x1H1017+202	0.5	VV	AGN:0.004	NGC 3227	0.6
1ES1022+519	10 22 23	+51 57 09	0.42±0.17	10/4	1.27E-06	20.6	4	3A	2283	2.8	A3	CG:0.012	MRK 142	1.3
1ES1023+207	10 23 00	+20 46 25	0.15±0.06	10/5	3.62E-05	54.7	7	3A	ZCT	GAL:0.010	I2597*	2.7
1ES1028+511	10 28 14	+51 08 56	1.91±0.52	16/5	1.00E-10	8.3	4	3A	SAO	S:B	SAO 238418	1.7
1ES1034-272	10 34 18	-27 17 32	0.28±0.08	23/3	2.21E-08	62.8	7	3A	1H1033-273	2.4	A3	CG:0.012	A1060	2.4
1ES1035-268	10 35 30	-26 51 48	0.14±0.05	14/3	2.10E-05	75.1	7	3A	2300	0.3
1ES1039-630	10 39 23	-63 00 21	0.23±0.10	9/8	7.45E-06	33.4	7	3A
1ES1042-594	10 42 28	-59 27 41	0.20±0.06	27/10	1.03E-04	77.1	6	3M	2313	1.6	SAO	S:B	SAO 238418	1.7

TABLE 6—Continued

Slew Design	RA 1950	DEC 1950	IPC Rate (cts s ⁻¹)	NP/NS	P _{rand}	Exp. (s)	PI	QI	EOS # EMSS	Δ2E (<i>t</i>)	A ₃ EXO	Δ1H (<i>t</i>)	Cat.	Class: Type/z	Name	ΔC (<i>t</i>)	
1ES1043-594	10 43 16	-59 25 16	0.32±0.09	33/9	4.36E-08	69.8	7	3M	2318	1.1	x1H1045-597	1.1	A3	SPEC	η CAR	1.2	
1ES1044-491	10 44 33	-49 07 58	0.65±0.31	6/5	9.65E-09	9.0	5	3A	2326	1.7			BSC	S:G5III+G2V	ν VEL	1.4	
1ES1044+549	10 44 37	+54 54 35	0.64±0.34	5/2	1.46E-06	7.5	5	3A	
1ES1047+070	10 47 46	+07 00 38	0.17±0.07	9/1	6.42E-05	42.3	8	3A	
1ES1048-596	10 48 04	-59 37 21	0.16±0.05	15/6	8.42E-06	69.6	9	3A	2336	0.5		x	...	2E	P	2E	
1ES1052+607	10 52 33	+60 44 09	0.57±0.10	43/4	1.00E-10	69.2	5	3A	x1H1051+607	0.4	A3	AC	DM UMA	0.4	
1ES1053+072	10 53 58	+07 17 16	0.17±0.07	10/2	8.64E-05	46.8	6	3A	2358	0.8		...	GCV	S:M6.5VE	CN LBO	2.8	
1ES1055+605	10 55 29	+60 31 47	0.20±0.09	9/4	1.86E-05	37.8	3	3A	x	...	HB	AGN:0.149	E1055+605	1.8
1ES1055-521	10 55 51	-52 11 24	0.10±0.02	67/10	1.00E-10	477.5	3	3A	2365	0.8	x	...	2E	P	2E	0.7	
1ES1100+772	11 00 17	+77 15 01	0.18±0.04	36/5	1.00E-10	161.2	5	3A	2389	0.7	HB	AGN:0.311	3C249.1	0.6	
1ES1101-606	11 01 03	-60 39 02	0.21±0.04	57/10	1.00E-10	218.3	7	3E	SAO	S:M0	SAO 251235	0.4	
1ES1101-232	11 01 10	-23 12 08	1.90±0.56	14/3	1.00E-10	7.2	6	3A	x1H1100-230	1.2	VV	BL	4U 1057-21	2.3	
1ES1101+384	11 01 42	+38 28 26	3.36±0.22	236/4	1.00E-10	69.2	4	3A	2393	0.4	x1H1104+382	0.4	VV	BL:0.031	MRK 421*	0.4	
1ES1103+728	11 03 28	+72 50 03	0.17±0.03	45/5	1.00E-10	208.7	7	3A	2395	0.3	x	...	VV	AGN:0.009	NGC 3516	0.5	
1ES1105+853	11 05 20	+83 21 54	0.47±0.22	7/3	1.69E-06	13.6	3	3A	SAO	S:K0	SAO 001824	1.0	
1ES1111-374	11 11 38	-37 24 30	0.26±0.05	39/4	1.00E-10	126.5	5	3A	2424	0.2	2E	CV	V 436 CEN	0.1	
1ES1113+432	11 13 01	+43 15 12	10.12±1.32	64/2	1.00E-10	6.3	3	3A		
1ES1113-369	11 13 06	-36 58 13	0.11±0.05	12/3	9.79E-05	79.7	6	3A		
1ES1115+318	11 15 28	+31 48 49	2.58±0.55	26/4	1.00E-10	9.8	6	3A	2440	0.6	x1H1121+309B	0.7	A3	AC	ζ UMA	0.7	
1ES1116+686	11 16 21	+68 41 31	0.39±0.17	8/6	6.34E-07	19.0	5	3A		
1ES1118+424	11 18 01	+42 28 51	1.16±0.30	18/5	1.00E-10	15.0	4	3A	x1H1118-602	0.2	A3	XRB	CEN X-3	0.2	
1ES1119-603	11 19 02	-60 21 12	8.32±0.45	332/8	1.00E-10	41.8	7	3A	2450	0.4	x1H1121+309B	0.7	A3	AC	Z 1121.0-0117	2.2	
1ES1121-012	11 21 02	-01 14 51	0.32±0.21	5/3	3.43E-09	9.5	6	3A	SBD	GAL	MSH 11-54	1.1	
1ES1122-589	11 22 15	-58 59 09	5.82±0.31	371/20	1.00E-10	62.9	6	3A	2460	1.3	x1H1121-591	1.1	A3	SNR	HD 306536	0.4	
1ES1126-610	11 26 48	-61 00 17	0.37±0.17	8/5	1.75E-05	18.5	7	2A	SBD	S:A	MRK 180	0.7	
1ES1133+704	11 33 24	+70 26 14	1.72±0.21	79/9	1.00E-10	44.0	4	3A	2487	0.9	x1H1137+699	0.8	VV	AGN:0.009	NGC 3783	0.3	
1ES1136-374	11 36 34	-37 27 54	0.84±0.07	151/6	1.00E-10	171.1	6	3A	2501	0.2	x1H1135-372	0.3	VV	AGN:0.033	VV	0.5	
1ES1136+842	11 36 34	+34 12 42	0.35±0.15	9/2	4.28E-07	22.9	5	3A	m2499	0.6		
1ES1137-651	11 37 06	-65 07 18	1.29±0.39	14/4	1.00E-10	10.5	6	3A	1H1137-649	0.4	A3	AC	HD101379	0.4	
1ES1137+660	11 37 06	+66 03 55	0.14±0.03	41/6	1.00E-10	217.8	5	3A	2603	0.7	x	...	HB	AGN:0.646	3C 263	0.6	
1ES1138+522	11 38 05	+52 16 38	0.17±0.07	15/5	1.73E-05	63.0	6	3A	2507	0.2	GCV	AC:F9+K1IV	RW UMA	0.1	
1ES1140+719	11 40 48	+71 58 10	0.40±0.08	38/9	1.00E-10	82.4	6	3A	m2515	0.3	1H1140+719	0.2	A3	CV	YY DRA	0.2	
1ES1141+799	11 41 56	+79 57 50	0.47±0.22	7/5	3.87E-06	13.6	6	3A	UGC	GAL	UO6728	1.5	

TABLE 6—Continued

Slew Design:	RA 1950	DEC 1950	IPC Rate (cts s ⁻¹)	NP/NS	P _{rand}	Exp. (s)	PI	QI	EOS #	Δ2E (<i>i</i>)	A ₃ EXO	Δ1H (<i>i</i>)	Cat.	Class.: Type/z	Name	ΔC (<i>i</i>)
1ES1142+198	11 142 28	+19 52 42	0.15 ^{+0.03} _{-0.03}	65/3	1.13E-10	266.5	6	3E	2521	0.7	x	...	VV	AGN:0.021	NGC 3862	0.5
1ES1143-550	11 43 20	-55 04 04	0.20 ^{+0.10} _{-0.08}	8/5	4.24E-05	33.2	4	3A
1ES1145+204	11 45 27	+20 29 37	0.41 ^{+0.10} _{-0.09}	23/3	1.00E-10	50.6	5	3A	2584	0.6	SAO	AC:AT7+G5II	SAO 081998	0.3
1ES1145-619	11 45 35	-61 54 25	0.38 ^{+0.14} _{-0.12}	13/7	1.05E-07	29.1	6	3A	2535	1.2	x1H1144-617.B	1.3	2E	P	V801 CEN	1.3
1ES1147-625	11 47 36	-62 30 24	0.31 ^{+0.08} _{-0.07}	30/6	1.09E-10	74.4	5	3E	2541	0.4	x	...	SBD	S:B9V	HD 103867	1.9
1ES1148-624	11 48 56	-62 24 34	0.20 ^{+0.07} _{-0.06}	21/3	2.57E-05	68.2	5	3E	SBD	S:B8	HD 303207	2.7
1ES1148-620	11 48 57	-62 01 35	0.29 ^{+0.10} _{-0.09}	17/7	1.36E-06	44.6	5	3A	2550	1.1	x	...	2E
1ES1149-110	11 49 33	-11 05 21	0.63 ^{+0.25} _{-0.20}	9/6	5.08E-09	13.5	4	3A	VV	AGN:0.049	PG	0.6
1ES1155+557	11 55 25	+55 43 51	0.44 ^{+0.10} _{-0.09}	26/2	1.00E-10	51.7	5	3A	2561	0.3	x	...	VV	AGN:0.003	NGC 3998	0.6
1ES1159+583	11 59 37	+58 19 14	0.09 ^{+0.03} _{-0.03}	19/4	9.26E-05	140.0	5	3E	2574	0.4	2E	CG:0.103	A1446	1.0
1ES1200+448	12 00 35	+44 48 36	0.94 ^{+0.08} _{-0.08}	164/8	1.00E-10	166.2	4	3A	2578	0.3	x1H1205+440	0.2	VV	AGN:0.002	NGC 4051	0.2
1ES1201+021	12 01 54	+02 09 44	0.47 ^{+0.21} _{-0.17}	8/4	1.20E-05	15.0	5	3A	2583	0.7	2E	CG:0.020	MKW 4	0.8
1ES1202+281	12 02 09	+28 10 35	0.23 ^{+0.07} _{-0.07}	17/2	3.71E-08	60.0	6	3A	2584	0.5	HB	AGN:0.165	GQ COM	0.3
1ES1204-526	12 04 29	-52 36 04	0.08 ^{+0.03} _{-0.03}	28/14	2.83E-05	198.6	6	3A
1ES1207-521	12 07 24	-52 09 45	0.07 ^{+0.02} _{-0.02}	44/13	8.12E-05	311.6	6	3A	2599	0.2	2E	SNR	PKS	0.2
1ES1208+396	12 08 02	+39 41 04	0.31 ^{+0.03} _{-0.03}	158/15	1.00E-10	438.9	6	3A	2603	0.2	x1H1210+393	0.1	VV	AGN:0.003	NGC 4151	0.2
1ES1209-524	12 09 00	-52 26 43	0.08 ^{+0.03} _{-0.02}	67/11	3.63E-05	344.1	4	3E
1ES1210-646	12 10 36	-64 36 06	0.55 ^{+0.10} _{-0.09}	42/12	1.00E-10	69.5	7	3A
1ES1211+143	12 11 45	+14 20 02	1.38 ^{+0.17} _{-0.16}	75/2	1.00E-10	52.7	5	3A	2620	0.4	x	...	VV	AGN:0.085	PG	0.2
1ES1212-652	12 12 04	-65 15 40	0.25 ^{+0.11} _{-0.09}	11/8	8.67E-05	33.1	7	3E	SBD	S:GD/G1V:	HD 106392	1.7
1ES1212-651	12 12 30	-65 09 31	0.42 ^{+0.13} _{-0.11}	16/9	7.51E-10	33.1	5	3E
1ES1212+384	12 12 33	+33 28 08	0.17 ^{+0.05} _{-0.05}	19/4	1.23E-07	88.4	7	3A	2626	0.6	UGC	GAL:0.004	NGC 4203	0.6
1ES1212+078	12 12 36	+07 48 53	0.25 ^{+0.11} _{-0.09}	10/7	3.38E-05	32.4	7	3A	SAO	S:K0	SAO 119284	0.9
1ES1213+728	12 13 26	+72 49 32	0.58 ^{+0.08} _{-0.08}	62/9	1.00E-10	99.1	5	3A	2631	0.3	1H1213+718.A	0.4	A3	AC	DK DRA	0.4
1ES1214+328	12 14 32	+32 48 14	0.15 ^{+0.08} _{-0.05}	11/3	2.36E-05	59.6	9	3A
1ES1215+039	12 15 03	+03 54 51	0.34 ^{+0.13} _{-0.11}	11/4	1.64E-06	27.7	7	3A	SBD	GAL:0.075	4C +04.41*	1.6
1ES1215+303	12 15 20	+30 22 34	0.22 ^{+0.06} _{-0.06}	21/4	2.92E-10	78.3	4	3A	2644	1.2	x	...	HB	BL	ON 325	1.1
1ES1215+300	12 15 55	+30 05 24	0.95 ^{+0.14} _{-0.13}	59/5	1.00E-10	58.8	4	3A	m2648	0.4	x1H1219+301.B	0.2	VV	AGN:0.012	MRK 766	0.2
1ES1216+426	12 16 21	+42 39 16	0.23 ^{+0.10} _{-0.09}	8/4	2.01E-05	30.3	8	3A
1ES1217+023	12 17 40	+02 19 30	0.26 ^{+0.05} _{-0.04}	47/10	1.00E-10	147.3	6	3A	2661	1.1	x	...	HB	AGN:0.240	ON 029	0.9
1ES1218+637	12 18 05	+63 43 44	0.39 ^{+0.19} _{-0.15}	7/2	2.21E-05	16.0	9	3A
1ES1218-637	12 18 45	-63 47 07	0.13 ^{+0.04} _{-0.04}	18/9	1.67E-06	106.3	5	3A	2671	0.4	2E	SNR*	1218-63.7	0.1
1ES1218+304	12 18 50	+30 27 12	2.25 ^{+0.76} _{-0.63}	11/2	1.00E-10	4.8	5	3A	x1H1219+301.A	0.4	VV	BL	3A 1218+303	0.3

TABLE 6—Continued

Slew Desig.	RA 1950	DEC 1950	IPC Rate (cts s ⁻¹)	NP/NS	P_{rand}	Exp. (s)	PI	QI	EOS #	$\Delta 2E$	A ₃	$\Delta 1H$	Cat.	Class.: Type/z	Name	ΔC (ℓ)
1ES1218+285	12 18 57	+28 30 39	0.28 ^{+0.07} -0.06	19/2	6.13E-09	66.3	7	3A	2673	1.1	VV	BL:102	ON 231	0.9
1ES1219+755	12 19 31	+75 35 29	0.47 ^{+0.04} -0.04	147/13	1.00E-10	281.9	5	3A	m2677	0.2	x1H1211+762	0.3	HB	AGN:0.070	MRK 205	0.3
1ES1219+044	12 19 48	+04 29 32	0.13 ^{+0.03} -0.03	43/6	5.72E-10	220.7	6	3A	2679	0.6	HB	AGN:0.965	PKS	0.5
1ES1228+132	12 23 37	+13 14 48	0.30 ^{+0.08} -0.07	26/3	2.43E-10	68.1	5	3A	2707	2.2	UGC	GAL:-0.001	N4406	1.5
1ES1223-628	12 23 57	-62 48 58	0.16 ^{+0.28} -0.24	21/9	1.00E-10	17.7	4	3A	x1H1226+022	0.1	x	S:B1V+B0.5V	α^2 CRU	1.0
1ES1226+023	12 26 34	+02 19 44	3.20 ^{+0.12} -0.12	712/8	1.00E-10	218.5	5	3A	2729	0.2	x1H1226+022	0.1	VV	AGN:0.158	3C 273.0	0.2
1ES1227+082	12 27 15	+08 16 18	0.25 ^{+0.04} -0.04	79/9	1.00E-10	225.3	6	3A	2735	0.2	1H1228+081	0.2	A3	GAL:0.003	N4472	0.3
1ES1228-465	12 28 08	-46 30 24	0.45 ^{+0.20} -0.16	7/4	4.68E-07	14.7	7	3A	SAO	S:F5V	SAO 223481	0.8
1ES1228+126	12 28 17	+12 39 01	2.50 ^{+0.51} -0.46	37/4	1.00E-10	12.6	6	3E	2744	1.0	x1H1226+128	1.0	A3	CG:0.004	VIRGO CL.	1.0
1ES1229+710	12 29 30	+71 00 35	0.20 ^{+0.07} -0.06	18/10	6.35E-08	70.5	5	3A
1ES1230+176	12 30 13	+17 39 55	0.21 ^{+0.10} -0.08	9/5	4.94E-05	35.4	9	3A
1ES1231+100	12 31 49	+10 05 13	0.17 ^{+0.07} -0.06	15/8	9.38E-06	64.9	6	3A
1ES1233-634	12 33 45	-63 27 54	0.48 ^{+0.14} -0.12	15/3	2.36E-09	29.2	6	3A
1ES1234+223	12 34 01	+22 18 56	0.16 ^{+0.06} -0.05	14/4	4.28E-06	67.7	6	3A
1ES1234+459	12 34 26	+45 55 22	0.32 ^{+0.13} -0.11	10/4	2.78E-06	26.6	6	3A	SBD	GAL	Z 1234.5+4556	0.9
1ES1235+120	12 35 10	+12 05 16	0.23 ^{+0.04} -0.04	47/9	1.00E-10	161.7	6	3A	2801	0.6	VV	AGN:0.005	NGC 4579	0.6
1ES1235-399	12 35 42	-39 55 37	0.10 ^{+0.04} -0.03	24/5	6.33E-05	150.5	6	3A
1ES1238-332	12 38 07	-33 17 59	0.38 ^{+0.18} -0.14	7/4	1.56E-05	16.6	7	3A	SBD	GAL	ESO 381-7	0.4
1ES1239-011	12 39 04	-01 10 45	0.86 ^{+0.42} -0.33	6/1	2.07E-07	6.7	4	3A	WLY	S:F0V	WLY 482A	0.8
1ES1239+069	12 39 23	+06 54 56	0.25 ^{+0.11} -0.09	10/6	2.43E-05	32.4	7	3A
1ES1239-627	12 39 50	-62 46 38	0.26 ^{+0.08} -0.07	17/3	3.89E-09	55.9	7	3A	2828	0.3	1H1249-637	0.6	BSC	S:B2pe	HD 110432	0.6
1ES1240+029	12 40 17	+02 57 38	0.36 ^{+0.07} -0.06	46/7	1.00E-10	107.2	5	3A	2829	0.2	UGC	GAL:0.003	N4636	0.4
1ES1241+275	12 41 06	+27 33 10	0.32 ^{+0.15} -0.12	7/4	6.85E-06	19.7	4	3A	ABL	CG:0.241	A1602	1.6
1ES1241+723	12 41 24	+72 18 18	0.24 ^{+0.11} -0.09	8/5	6.08E-05	28.3	7	3A
1ES1244+026	12 44 02	+02 38 32	0.39 ^{+0.07} -0.06	52/7	1.00E-10	116.3	5	3A	2854	0.4	VV	AGN:0.048	PG	0.0
1ES1246-410	12 46 00	-41 01 34	1.04 ^{+0.09} -0.09	16/17	1.00E-10	135.7	6	3A	2862	1.0	x1H1244-409	0.7	ABL	CG:0.011	A3526	1.2
1ES1246+085	12 46 03	+08 35 43	0.08 ^{+0.03} -0.03	25/4	1.64E-05	186.8	6	3A	2861	0.7	2E
1ES1246+605	12 46 30	+60 35 50	0.19 ^{+0.05} -0.04	26/2	1.00E-10	111.6	6	3A	2865	0.3	1H1241+626.B	0.3	A3	AC	HD111456	0.3
1ES1246-588	12 46 39	-58 48 40	1.91 ^{+0.40} -0.36	27/7	1.00E-10	13.7	7	3A	x1H1244-588	0.5	A3	XRB	X1246-588	0.5
1ES1248-296	12 48 55	-29 39 45	0.41 ^{+0.18} -0.14	8/4	8.54E-07	17.8	8	3E
1ES1249-296	12 49 06	-29 37 03	0.35 ^{+0.17} -0.14	7/6	1.43E-05	17.6	6	3A
1ES1249+174	12 49 13	+17 28 11	0.20 ^{+0.10} -0.08	8/4	9.53E-05	32.6	9	3A
1ES1249+278	12 49 17	+27 48 03	0.48 ^{+0.17} -0.14	12/3	4.00E-10	22.8	4	3A	2874	0.9	x	...	BS	S:G0IIIp	HD111812	0.8

TABLE 6—Continued

Slew Desig.	RA 1950	DEC 1950	IPC Rate (cts s ⁻¹)	NP/NS	P _{rand}	Exp. (s)	PI	QI	EOS #	Δ2E (<i>t</i>)	A3 EXO	Δ1H (<i>t</i>)	Cat.	Class.: Type/z	Name	ΔC (<i>t</i>)
1ES1249-131	12 49 36	-13 07 52	0.45 ^{+0.20} _{-0.16}	8/2	2.76E-06	15.9	6	3A	x	...	VV	AGN:0.014	IRAS 1249-13	0.8
1ES1249-289	12 49 43	-28 58 41	4.08 ^{+0.22} _{-0.22}	354/5	1.00E-10	85.6	6	3A	2876	0.2	x1H1251-291	0.0	A3	CV	EX HYA	0.1
1ES1252-060	12 52 20	-06 03 36	0.12 ^{+0.05} _{-0.04}	16/3	6.42E-05	88.6	7	3A	WLY	SK8V	WLY 9424	0.6
1ES1253+275	12 53 14	+27 31 15	0.23 ^{+0.09} _{-0.07}	15/4	7.19E-06	49.3	5	3A	2896	0.6	SBD	GAL:0.024	Z 1253.3+2731	1.4
1ES1253-055	12 53 38	-05 31 13	0.19 ^{+0.04} _{-0.04}	31/4	1.00E-10	132.6	6	3A	2900	0.5	HB	AGN:0.538	3C 279	0.5
1ES1254-690	12 54 27	-69 00 21	6.97 ^{+2.04} _{-1.73}	14/2	1.00E-10	2.0	8	3A	2908	0.8	x1H1254-690	0.9	A3	XRB	X1254-690	1.0
1ES1254-171	12 54 31	-17 08 59	0.24 ^{+0.06} _{-0.05}	32/2	1.00E-10	105.9	6	3A	2909	0.6	SBD	CG:0.048	A1644	0.8
1ES1254+223	12 54 36	+22 18 06	0.53 ^{+0.06} _{-0.06}	136/12	1.00E-10	200.9	2	3A	2912	0.6	MCS	WD:DA	EG 187	0.3
1ES1254-172	12 54 51	-17 12 21	0.12 ^{+0.04} _{-0.04}	21/2	6.21E-06	110.2	7	2A	EXC	GAL:0.046	GAL 1254-1710*	1.7
1ES1255+244	12 55 06	+24 28 54	0.36 ^{+0.12} _{-0.10}	14/8	1.18E-09	34.2	7	3A
1ES1255+354	12 55 20	+35 29 16	0.17 ^{+0.03} _{-0.03}	53/6	1.00E-10	243.9	4	3A	m3920	0.7	WLY	SM0EV	BF CVN	0.6
1ES1256-014	12 56 08	-01 28 58	0.58 ^{+0.09} _{-0.09}	53/3	1.00E-10	82.6	6	3A	2925	0.5	ABL	CG:0.084	A1650	1.0
1ES1256-039	12 56 45	-03 54 22	0.51 ^{+0.20} _{-0.17}	10/2	3.89E-07	17.3	6	3A	ABL	CG:0.083	A1651	1.0
1ES1257+282	12 57 10	+28 13 02	0.71 ^{+0.07} _{-0.07}	244/4	1.00E-10	235.6	6	3A	2931	0.6	2E	CG:0.023	COMA CL.	0.6
1ES1257+286	12 57 59	+28 40 41	0.14 ^{+0.03} _{-0.03}	62/4	1.00E-10	268.7	5	3A	2935	0.7	HB	AGN:0.092	X COM	0.5
1ES1258+126	12 58 19	+12 37 54	0.33 ^{+0.10} _{-0.08}	18/2	1.46E-10	47.8	3	3A	2940	0.7	WLY	SM2EV	DT VIR.	0.8
1ES1259+289	12 59 07	+28 54 05	0.12 ^{+0.04} _{-0.03}	28/5	8.16E-07	149.8	5	3A	2946	0.7	GCV	S:G2II	UX COM*	0.3
1ES1259+337	12 59 20	+33 46 07	0.12 ^{+0.04} _{-0.03}	19/5	9.39E-07	122.0	5	3A
1ES1301-239	13 01 01	-23 57 41	0.20 ^{+0.07} _{-0.06}	15/5	5.83E-07	61.3	7	3A	ABL	CG	A1664*	0.7
1ES1301-411	13 01 45	-41 08 10	0.39 ^{+0.13} _{-0.11}	8/5	3.31E-06	24.3	6	3A	SBD	SK0	CD-40 7656	2.7
1ES1303+182	13 03 16	+18 17 28	0.39 ^{+0.10} _{-0.09}	20/6	1.00E-10	46.5	6	3A	2967	0.2	2E	CV	GP COM	0.5
1ES1304-650	13 04 48	-65 02 09	0.14 ^{+0.04} _{-0.04}	30/7	5.71E-08	146.3	7	3A	2972	0.5	BSC	S:Bo1s+WC5;	θ MUS	0.5
1ES1306-013	13 06 51	-01 23 19	0.09 ^{+0.03} _{-0.03}	19/5	1.96E-05	140.5	8	2A	m2975	2.2	2E
1ES1307+086	13 07 19	+08 36 14	0.35 ^{+0.09} _{-0.08}	22/1	1.00E-10	55.7	6	3A	2978	0.8	HB	AGN:0.155	PG	0.8
1ES1308+326	13 08 07	+32 36 46	0.16 ^{+0.04} _{-0.03}	40/8	1.00E-10	181.7	5	3A	2979	0.5	HB	BL:0.049	OP 313	0.2
1ES1308+361	13 08 17	+36 11 58	0.38 ^{+0.07} _{-0.07}	39/7	1.00E-10	90.5	4	3A	2980	0.2	WLY	AC:FAV	RS CVN	0.2
1ES1308-010	13 08 55	-01 04 51	0.42 ^{+0.07} _{-0.07}	47/3	1.00E-10	101.7	6	3A	2986	0.3	ABL	CG:0.181	A1689	1.7
1ES1309+281	13 09 32	+28 08 12	0.16 ^{+0.05} _{-0.12}	20/2	2.86E-08	97.0	4	3A	2990	0.4	WLY	S:GOV	WLY 502	0.3
1ES1309+355	13 09 58	+35 31 53	0.09 ^{+0.03} _{-0.03}	20/5	1.38E-05	146.8	6	3A	HB	AGN:0.184	TON 1565	0.6
1ES1310-327	13 10 29	-32 42 39	1.78 ^{+0.42} _{-0.37}	23/2	1.00E-10	12.3	3	3A	ABL	CG	S724	1.7
1ES1312+347	13 12 02	+34 46 08	0.31 ^{+0.09} _{-0.08}	17/6	2.19E-10	48.0	4	3A
1ES1312-423	13 12 08	-42 20 33	0.50 ^{+0.14} _{-0.12}	19/8	1.00E-10	33.7	6	3A	m3002	0.4	MS	BL:0.108	MS	0.6
1ES1314+293	13 14 04	+29 22 09	5.51 ^{+0.77} _{-0.71}	57/7	1.00E-10	10.2	3	3A	3009	0.8	MCS	WD:DA1	HZ 43A	0.9

TABLE 6—Continued

Slew Desig.	RA 1950	DEC 1950	IPC (cts s ⁻¹)	Rate NP/NS	P _{rand}	Exp. (s)	PI	QI	EOS #	Δ2E (<i>i</i>)	A3 EXO	Δ1H (<i>i</i>)	Cat.	Class.: Type/ <i>z</i>	Name	ΔC (<i>i</i>)
1ES1314+096	13 14 19	+09 41 16	0.31 ^{+0.09} _{-0.08}	17/3	1.11E-10	48.1	5	3A	3010	0.2	x	...	SAO	S:GOV	SAO 119847	0.2
1ES1314+172	13 14 26	+17 16 34	0.33 ^{+0.12} _{-0.10}	11/6	9.96E-07	30.0	6	3A	WLY	S:K2V+M2V	WLY 505AB	1.0
1ES1316-424	13 16 40	-42 29 50	0.19 ^{+0.07} _{-0.06}	14/3	5.99E-07	59.8	4	3A	m3018	0.2	MS	S:M1.5E	MS	0.8
1ES1318+274	13 18 07	+27 27 53	0.30 ^{+0.15} _{-0.12}	6/4	3.73E-06	18.9	4	3A	SBD	GAL	G 149-80	1.3
1ES1318-632	13 18 14	-63 17 50	0.49 ^{+0.19} _{-0.16}	10/6	3.64E-07	18.2	6	3A	SBD	S:B	LS 3039	2.1
1ES1319+429	13 19 59	+42 55 32	0.13 ^{+0.05} _{-0.04}	17/4	6.42E-06	89.5	8	3A
1ES1320+701	13 20 20	+70 09 09	0.11 ^{+0.04} _{-0.04}	32/7	9.34E-05	147.6	6	3A
1ES1320+984	13 20 23	+08 25 34	1.44 ^{+0.68} _{-0.54}	6/2	9.69E-10	4.1	6	3A	VV	AGN:0.050	MRK 1347	0.5
1ES1322-108	13 22 32	-10 53 38	0.25 ^{+0.05} _{-0.05}	33/6	1.00E-10	112.8	3	3A	3039	0.3	BSC	S:BIII-IV+B	α VIR	0.5
1ES1322-427	13 22 33	-42 45 41	1.01 ^{+0.09} _{-0.09}	130/6	1.00E-10	120.9	10	3A	3038	0.1	1H1323-428	0.3	A3	AGN:0.002	CEN A	0.3
1ES1322-297	13 22 48	-29 46 20	0.16 ^{+0.07} _{-0.06}	11/2	7.64E-05	52.7	8	3A
1ES1323+717	13 23 32	+71 47 26	0.22 ^{+0.11} _{-0.09}	13/2	2.50E-05	36.6	5	3A	EXC	GAL 1323+7145	2.8	
1ES1324-269	13 24 04	-26 54 37	0.15 ^{+0.04} _{-0.04}	29/4	8.91E-07	129.5	7	3P	SBD	GAL:0.046	ESO 509-9	1.7
1ES1324-268	13 24 48	-26 53 10	0.15 ^{+0.05} _{-0.04}	29/4	8.83E-07	127.2	8	3P	SBD	GAL	ESO 509-14	1.8
1ES1325-261	13 25 07	-26 06 35	0.17 ^{+0.08} _{-0.08}	9/2	6.23E-05	43.5	7	3A	SBD	S:K5II	HD 117033	2.7
1ES1325-312	13 25 14	-31 17 14	0.69 ^{+0.30} _{-0.24}	8/4	1.11E-06	10.5	6	3A	SAO	S:F5V	SAO 204500	2.7
1ES1326+789	13 26 34	+78 54 04	0.38 ^{+0.16} _{-0.13}	9/7	6.43E-07	21.1	6	3A	BSC	S:G2.5IIb	HD 117566	0.1
1ES1327-313	13 27 12	-31 19 54	0.11 ^{+0.07} _{-0.06}	13/3	7.27E-06	57.8	6	3A	SAO	S:K1III	SAO 204527	2.6
1ES1328-547	13 28 08	-54 43 35	0.20 ^{+0.06} _{-0.05}	18/2	3.45E-09	73.5	6	3A	3071	0.8	SHA	CV	BV CEN	0.6
1ES1328+244	13 28 25	+24 29 31	0.23 ^{+0.05} _{-0.05}	27/4	1.00E-10	104.7	5	3A	3074	0.1	SAO	S:G5	FK COM	0.4
1ES1330+022	13 30 22	+02 15 15	0.19 ^{+0.05} _{-0.05}	23/4	1.00E-10	98.8	5	3A	3081	0.9	VV	AGN:0.215	3C287.1	1.0
1ES1330-313	13 30 45	-31 23 58	0.23 ^{+0.06} _{-0.06}	31/7	1.00E-10	96.0	6	3A	3083	0.7	x	...	ABL	CG:0.050	A3562	1.2
1ES1332-080	13 32 05	-08 05 16	0.16 ^{+0.05} _{-0.04}	20/3	2.70E-09	99.6	4	3A	3091	0.6	x	...	WLY	S:K5EV	EQ VIR	0.5
1ES1332+374	13 32 34	+37 25 35	1.20 ^{+0.32} _{-0.28}	19/4	1.00E-10	14.7	4	3A	3098	0.8	1H1332+372	0.7	A3	AC	SAO 063623	0.7
1ES1332-295	13 32 40	-29 35 22	0.16 ^{+0.04} _{-0.03}	35/7	1.00E-10	168.7	7	3A	m3100	0.3	2E
1ES1333-340	13 33 03	-34 02 33	1.75 ^{+0.17} _{-0.17}	113/10	1.00E-10	62.3	6	3A	3102	0.4	x1H1334-340	0.3	VV	AGN:0.008	MCG-6-30-15	0.3
1ES1333+412	13 33 05	+41 14 57	0.23 ^{+0.06} _{-0.05}	22/5	5.21E-09	84.1	7	3A	3103	1.0	ABL	CG:0.228	A1763	2.0
1ES1334-296	13 34 19	-29 36 30	0.10 ^{+0.02} _{-0.02}	41/5	5.33E-10	287.9	6	3A	3112	1.2	x	...	RNG	GAL:0.002	NGC 5236	0.4
1ES1336+280	13 36 13	+28 00 36	0.19 ^{+0.08} _{-0.07}	11/5	5.01E-05	44.0	12	3A	SBD	GAL:0.036	Z 1336.4+2800	2.3
1ES1339-688	13 39 20	-68 52 06	0.80 ^{+0.42} _{-0.33}	5/2	6.51E-07	6.1	3	3A	SAO	S:G2IV-V	SAO 252423	0.7
1ES1340-611	13 40 35	-61 07 02	0.68 ^{+0.11} _{-0.10}	50/3	1.00E-10	69.4	5	3A	3127	0.2	1H1338-604.B	0.1	A3	AC	SAO 0252429	0.1
1ES1344-326	13 44 43	-32 37 09	1.15 ^{+0.51} _{-0.41}	8/3	1.34E-06	6.2	6	3A	1H1344-326	1.7	ABL	CG:0.040	A3571	1.5
1ES1346-300	13 46 26	-30 03 45	1.68 ^{+0.23} _{-0.21}	64/2	1.00E-10	36.5	7	3A	3141	0.8	x1H1345-300	0.4	VV	AGN:0.014	IC 4329A	0.4

TABLE 6—Continued

Slew Desig.	RA 1950	DEC 1950	IPC Rate (cts s ⁻¹)	NP/NS	P _{rand}	Exp. (s)	PI	QI	EOS # EMSS	Δ2E (<i>t</i>)	A ₃ EXO	Δ1H (<i>t</i>)	Cat.	Class: Type/z	Name	ΔC (<i>t</i>)	
1ES1346+268	13 46 34	+26 50 07	1.24 ^{+0.12} _{-0.12}	118/3	1.00E-10	90.2	5	3A	3142	0.5	x1H1348+267	0.3	ABL	CG:0.062	A1795	1.8	
1ES1351+400	13 51 38	+40 05 24	0.07 ^{+0.03} _{-0.02}	30/5	6.15E-05	232.5	5	3A	m3146	0.5	MS	AGN:0.062	MS	0.8	
1ES1351+695	13 51 57	+69 33 24	1.36 ^{+0.17} _{-0.16}	80/7	1.00E-10	55.4	5	3A	3147	0.2	x1H1350+696	0.5	VV	AGN:0.031	MRK 279*	0.2	
1ES1354-314	13 54 42	-31 24 22	0.65 ^{+0.31} _{-0.25}	7/2	5.80E-06	9.7	6	3A	SAO	S:KOV	SAO 205032	0.3	
1ES1402+242	14 02 16	+04 16 26	0.08 ^{+0.03} _{-0.02}	24/7	6.90E-06	200.3	5	3A	m3177	0.9	HB	BL	2E	0.9	
1ES1404-267	14 04 36	-26 46 33	0.55 ^{+0.19} _{-0.16}	13/4	4.85E-09	21.1	5	3A	1H1409-267	0.5	ABL	CG:0.021	A3551	0.4	
1ES1405-450	14 05 51	-45 03 01	0.43 ^{+0.16} _{-0.13}	11/3	7.59E-08	22.7	5	3A	3194	1.4	x1H1404-450	1.3	A3	CV	1E1405-451	1.3	
1ES1410-029	14 10 38	-02 58 28	0.31 ^{+0.03} _{-0.03}	112/8	1.00E-10	309.1	8	3A	3205	0.1	x1H1408-031	0.2	VV	AGN:0.006	NGC 5506	0.3	
1ES1410+683	14 10 58	+68 19 20	0.33 ^{+0.16} _{-0.13}	8/5	7.68E-05	20.0	4	3A	
1ES1414+203	14 14 13	+20 21 27	0.28 ^{+0.13} _{-0.11}	8/3	3.50E-05	24.4	3	3A	BSC	S:F8V	HD 125540	0.2	
1ES1414-197	14 14 42	-19 43 34	0.26 ^{+0.10} _{-0.09}	11/3	4.11E-06	35.6	5	3A	SAO	S:A5IV	SAO 158468	0.5	
1ES1415+451	14 15 03	+45 10 34	0.27 ^{+0.13} _{-0.11}	8/6	1.04E-04	24.5	3	3A	HB	AGN:0.114	PG	0.7	
1ES1415-209	14 15 29	-20 57 23	0.21 ^{+0.09} _{-0.08}	9/5	2.40E-05	36.2	8	3A	
1ES1416-129	14 16 23	-12 57 03	0.21 ^{+0.04} _{-0.04}	37/7	1.00E-10	145.4	6	3A	m3238	0.4	HB	AGN:0.129	PG	0.4	
1ES1417-192	14 17 00	-19 14 09	0.15 ^{+0.05} _{-0.04}	17/2	4.77E-07	88.1	5	3A	3244	0.5	AGN:0.119	PKS	0.8	
1ES1421+582	14 21 09	+58 15 09	0.46 ^{+0.18} _{-0.15}	10/6	5.87E-08	19.9	5	3A	
1ES1423+520	14 23 29	+52 04 34	0.38 ^{+0.08} _{-0.07}	33/3	1.00E-10	76.2	5	3A	3265	0.2	WLY	S:F6V	WLY 549A	0.4
1ES1426-624	14 26 04	-62 27 53	0.33 ^{+0.04} _{-0.04}	78/4	1.00E-10	210.4	4	3A	3278	0.4	SBD	S:MVE	PM14263-6228	1.7	
1ES1426+515	14 26 33	+01 30 31	0.34 ^{+0.08} _{-0.07}	28/6	1.00E-10	69.7	5	3A	m3280	0.5	x1H1427+013	0.3	VV	AGN:0.086	MRK 1383	0.2	
1ES1426+528	14 26 38	+02 53 41	2.55 ^{+0.67} _{-0.58}	17/3	1.00E-10	6.6	4	3A	x1H1430+423	0.3	A3	BL	H1426+427	0.4	
1ES1435-067	14 35 37	-06 45 18	0.22 ^{+0.08} _{-0.07}	14/2	3.30E-06	50.6	5	3A	3305	0.2	HB	AGN:0.129	PG	0.1	
1ES1435-606	14 35 48	-60 37 09	0.76 ^{+0.16} _{-0.14}	29/2	1.00E-10	36.5	2	3A	3308	1.3	SBD	S:G2V	α CEN AB	2.9	
1ES1436-624	14 36 38	-62 26 07	1.49 ^{+0.34} _{-0.30}	28/1	1.00E-10	16.7	5	2A	SAO	S:A0	SAO 255841	1.6	
1ES1437-252	14 37 52	-25 17 43	0.82 ^{+0.44} _{-0.34}	5/3	1.14E-06	5.9	10	3A	SBD	S:F0/F2V	HD 129009	2.9	
1ES1440+122	14 40 22	+12 13 16	0.52 ^{+0.19} _{-0.16}	11/6	1.28E-08	19.1	5	3A	
1ES1449+193	14 49 07	+19 18 17	0.79 ^{+0.12} _{-0.11}	54/5	1.00E-10	63.9	4	3A	3337	0.3	1H1450+190.B	0.5	SAO	S:G8V+K4V	HD131156AB	0.2	
1ES1450+679	14 50 07	+67 56 10	0.10 ^{+0.04} _{-0.03}	16/4	3.02E-05	114.6	8	3A	3340	3.0	2E	
1ES1452+188	14 52 14	+18 50 24	0.29 ^{+0.06} _{-0.05}	45/7	1.00E-10	130.2	5	3A	3350	0.3	1H1450+190.A	0.9	ABL	CG:0.059	A1991	0.6	
1ES1454+225	14 54 58	+22 32 09	0.32 ^{+0.12} _{-0.10}	11/4	1.78E-07	30.5	6	3A	m3356	0.6	MS	CG:0.259	MS	0.6	
1ES1456+448	14 56 02	+64 51 52	0.24 ^{+0.12} _{-0.09}	7/4	2.73E-05	25.4	8	3A	
1ES1456-400	14 56 32	-40 01 14	0.75 ^{+0.37} _{-0.30}	6/1	4.56E-06	7.5	9	3A	SBD	S:F7/F8V	HD 132349	2.3	
1ES1457+033	14 57 17	+03 18 23	0.40 ^{+0.20} _{-0.16}	6/3	3.61E-06	13.9	6	3A	
1ES1458+215	14 58 02	+21 33 12	0.24 ^{+0.07} _{-0.07}	19/2	9.75E-09	63.0	8	3E	3363	0.7	1H1457+214.	1.3	ABL	CG:0.153	A2009	0.9	

TABLE 6—Continued

Slew Desig.	RA 1950	DEC 1950	IPC Rate (cts s ⁻¹)	NP/NS	P _{rand}	Exp. (s)	P _I	Q _I	EOS #	Δ2E (<i>i</i>)	A ₃ EXO	Δ1H (<i>i</i>)	Cat.	Class.: Type/ <i>z</i>	Name	ΔC (<i>i</i>)	
1ES1500-415	15 00 17	-41 35 59	0.49 ^{+0.06} _{-0.06}	136/1	1.00E-10	204.3	5	3E	WD	WD1501+664	0.3
1ES1501+163	15 01 25	+66 23 56	2.03 ^{+0.27} _{-0.25}	65/13	1.00E-10	30.8	3	3A	x	MCS	AGN:0.036	MRK 841	0.4
1ES1501+106	15 01 35	+10 38 06	0.57 ^{+0.10} _{-0.10}	39/2	1.00E-10	63.1	5	3A	3372	0.5	x	...	VV	AGN:0.036	ZZ BOO	0.2	
1ES1502+478	15 02 07	+47 50 55	2.23 ^{+0.51} _{-0.45}	23/7	1.00E-10	10.0	4	3A	3373	0.2	x1H1504+473	0.2	A3	AC	RNG	NGC 5546*	0.4
1ES1503+017	15 03 57	+01 47 59	0.14 ^{+0.04} _{-0.04}	21/3	1.81E-06	109.8	5	3A	3380	0.2	ABL	CG:0.151	A2034	1.3
1ES1508+337	15 08 06	+33 42 30	0.49 ^{+0.16} _{-0.14}	9/5	1.32E-07	20.4	6	3A	1H1510+335	1.9
1ES1508+059	15 08 26	+05 55 55	1.54 ^{+0.27} _{-0.25}	39/3	1.00E-10	24.3	6	3A	3385	0.4	1H1508+060	1.6	ABL	CG:0.077	A2029	1.5	
1ES1509+763	15 09 01	+76 22 44	0.44 ^{+0.19} _{-0.18}	8/3	1.91E-06	16.4	5	3A	SAO	S:G5	SAO 008175	1.1
1ES1509-589	15 09 48	-58 56 14	0.89 ^{+0.19} _{-0.17}	31/1	1.00E-10	30.4	8	3A	3389	1.6	x	...	2E	P	MSH 11-52	MSH 11-52	1.6
1ES1509-588	15 09 49	-58 49 42	0.43 ^{+0.15} _{-0.13}	17/1	2.76E-06	29.7	6	3M	3388	0.6	x	...	2E	SNR	MSH 15-52	MSH 15-52	2.0
1ES1513+002	15 13 47	+00 16 17	0.15 ^{+0.05} _{-0.04}	24/4	8.18E-07	112.6	8	3A	3404	0.8	ABL	CG:0.118	A2050	0.8	
1ES1514+072	15 14 18	+07 12 15	0.94 ^{+0.15} _{-0.14}	46/2	1.00E-10	46.1	6	3A	3407	0.2	x1H1514+072	0.7	ABL	CG:0.035	A2052	1.3	
1ES1517+656	15 17 07	+65 36 26	0.91 ^{+0.29} _{-0.24}	13/7	1.00E-10	13.7	5	3A	1H1515+660	0.2	A3	BL	...	H1517+656	0.2
1ES1518-071	15 18 13	-07 10 36	0.23 ^{+0.11} _{-0.09}	8/1	2.03E-05	29.3	9	2A	VV	AGN:0.079
1ES1518+593	15 18 13	+59 18 51	0.36 ^{+0.14} _{-0.12}	11/7	1.72E-06	26.0	3	2A
1ES1519+078	15 19 22	+07 52 48	0.41 ^{+0.13} _{-0.11}	15/7	1.59E-09	31.7	6	3A	3419	1.1	2E	CG:0.045
1ES1520+278	15 20 20	+27 53 12	0.33 ^{+0.07} _{-0.07}	29/3	1.00E-10	76.1	7	3E	3426	0.7	2E	CG:0.072	A2065	0.8	
1ES1520+067	15 20 36	+08 47 08	0.61 ^{+0.10} _{-0.09}	51/6	1.00E-10	74.2	8	3A	3427	0.7	1H1521+083	2.3	ABL	CG:0.034	A2063	1.9	
1ES1522+300	15 22 13	+30 00 54	0.18 ^{+0.06} _{-0.05}	17/3	5.43E-07	71.7	5	3A	m3432	3.0	2E	CG:0.115	A2069	2.8	
1ES1527+714	15 27 21	+71 24 15	0.13 ^{+0.05} _{-0.04}	14/5	8.60E-05	79.2	5	2A
1ES1533+335	15 33 36	+53 30 00	0.49 ^{+0.18} _{-0.15}	11/6	1.18E-09	20.7	6	3A
1ES1536+515	15 36 48	+51 34 02	0.32 ^{+0.15} _{-0.12}	7/3	1.74E-05	19.4	5	3A
1ES1539+187	15 39 57	+18 44 48	0.24 ^{+0.11} _{-0.09}	9/6	1.84E-05	31.7	8	3A
1ES1543+362	15 43 12	+36 13 11	0.12 ^{+0.05} _{-0.04}	16/5	2.53E-05	94.9	6	3E	1H1544+360	1.6	ABL	CG:0.065	A2124	1.2	
1ES1544+320	15 44 08	+82 04 32	0.53 ^{+0.14} _{-0.12}	19/12	1.00E-10	33.1	5	3A
1ES1545+210	15 45 32	+21 01 17	0.19 ^{+0.02} _{-0.02}	112/11	1.00E-10	474.4	6	3A	3500	0.3	VV	AGN:0.264	3C 323.1	0.2	
1ES1546+104	15 46 40	+10 25 38	0.25 ^{+0.11} _{-0.09}	8/5	4.58E-06	28.8	9	3A
1ES1547+262	15 47 31	+26 13 14	0.20 ^{+0.07} _{-0.06}	14/7	2.56E-07	58.3	4	3A	3507	0.1	BSC	SG3.5III-IV	HD 141714	0.2	
1ES1548+114	15 48 21	+11 29 11	0.09 ^{+0.03} _{-0.03}	21/6	6.88E-06	152.1	7	3A	3508	0.6	HB	AGN:0.436	MC	0.6	
1ES1549+203	15 49 50	+20 22 27	0.10 ^{+0.03} _{-0.03}	25/5	1.67E-07	179.4	5	3A	m3513	0.4	VV	AGN:0.250	LB 906*	0.5	
1ES1550+191	15 50 31	+19 06 01	1.21 ^{+0.30} _{-0.27}	20/2	1.00E-10	15.8	3	3A	...	x	SHA	CV	MR SER	0.9	
1ES1552+203	15 52 14	+20 20 22	0.21 ^{+0.06} _{-0.05}	24/4	1.47E-10	93.1	7	3A	m3523	0.6	2E
1ES1553+113	15 53 19	+11 20 20	1.61 ^{+0.18} _{-0.17}	94/3	1.00E-10	56.1	4	3A	3529	0.3	HB	BL0.360	PG	0.5	

TABLE 6—Continued

Slew Desig.	RA 1950	DEC 1950	IPC Rate (cts s ⁻¹)	NP/NS	<i>P_{r and}</i>	Exp. (s)	PI	QI	EOS #	Δ2E (<i>t</i>)	A3 EXO	Δ1H (<i>t</i>)	Cat.	Class: Type/ <i>n</i>	Name	ΔC (<i>t</i>)
1ES1556+273	15 56 15	+27 22 33	1.01 ^{+0.12} _{-0.11}	87/8	1.00E-10	81.8	6	3A	3541	0.3	x1H1556+273	0.3	ABL	CG:0.090	A2142	0.9
1ES1556+257	15 56 38	+25 42 23	0.30 ^{+0.15} _{-0.12}	7/3	2.75E-05	20.4	6	3A	3543	0.3	SAO	S:K2V	SAO 084114	0.7
1ES1559+161	15 59 58	+16 08 16	0.11 ^{+0.03} _{-0.03}	53/6	2.54E-06	249.6	6	3E	3565	2.0	2E	CG:0.035	A2147	2.0
1ES1601+160	16 01 24	+16 02 11	0.16 ^{+0.06} _{-0.05}	22/7	2.88E-05	90.3	6	3A	3572	0.6	ZCT	GAL:0.100	1601+1602	1.5
1ES1601+669	16 01 36	+66 57 09	0.17 ^{+0.04} _{-0.04}	42/10	1.00E-10	179.2	3	3A	3573	1.5	SBD	S:K0	AG DRA	1.5
1ES1602+178	16 02 23	+17 51 57	0.18 ^{+0.03} _{-0.03}	78/17	1.00E-10	322.2	5	3A	3577	0.5	UGC	GAL:0.042	U10170*	1.5
1ES1602+240	16 02 42	+24 03 52	0.14 ^{+0.05} _{-0.04}	19/7	4.99E-07	101.1	7	3A	3581	1.6	2E	CG:0.042	AWM 4	1.6
1ES1604+218	16 06 54	+21 53 30	0.16 ^{+0.07} _{-0.06}	10/6	7.16E-05	50.4	8	3A	SBD	S:K2	AG+21 1576	2.7
1ES1607+621	16 07 31	+62 06 10	0.18 ^{+0.08} _{-0.07}	10/6	1.12E-04	42.3	10	2A	XRB
1ES1609-522	16 09 01	-52 17 31	7.35 ^{+1.75} _{-1.54}	21/1	1.00E-10	2.8	8	3A	x1H1608-522	1.4	A3	QX NOR	QX NOR	1.4
1ES1610+669	16 10 08	+66 59 45	0.15 ^{+0.05} _{-0.05}	23/5	2.82E-05	96.7	5	3A
1ES1612+261	16 12 09	+26 11 52	0.27 ^{+0.07} _{-0.06}	22/9	1.00E-10	69.9	6	3A	3617	0.1	HB	AGN:0.131	TON 256	0.1
1ES1612+339	16 12 47	+33 59 14	2.27 ^{+0.20} _{-0.21}	129/12	1.00E-10	55.2	5	3A	3618	0.2	WLY	AC:F6V+G1V	WLY 9550AB	0.3
1ES1613+658	16 13 34	+65 50 53	0.20 ^{+0.04} _{-0.04}	35/10	1.00E-10	140.9	4	3A	3624	0.5	x1H1615+655	0.4	VV	AGN:0.129	MRK 876	0.3
1ES1613-509	16 13 58	-50 57 19	4.43 ^{+0.31} _{-0.32}	209/2	1.00E-10	46.1	6	3A	3626	0.6	SNR	RCW 103	RCW 103	0.8
1ES1614+446	16 14 08	+44 40 38	0.36 ^{+0.10} _{-0.09}	18/12	1.00E-10	44.8	6	3A	SAO	S:G0	SAO 045997	0.4
1ES1615+061	16 15 19	+06 11 11	0.27 ^{+0.07} _{-0.06}	27/5	2.10E-10	77.6	7	3A	3634	0.2	VV	AGN:0.038	H 1613+06	0.2
1ES1615+553	16 15 57	+55 22 47	0.24 ^{+0.05} _{-0.04}	37/8	1.00E-10	127.9	4	3A	3641	0.9	WLY	S:M1EV	WLY 9552	1.1
1ES1616+436	16 16 53	+43 36 54	0.28 ^{+0.14} _{-0.11}	8/6	1.08E-04	23.4	8	2A
1ES1618+411	16 18 11	+41 06 09	0.14 ^{+0.04} _{-0.04}	25/2	3.33E-08	131.1	5	3A	3650	0.1	2E
1ES1621+274	16 21 35	+27 26 56	0.14 ^{+0.06} _{-0.05}	12/5	2.31E-05	66.2	8	2A	3658	2.6	2E
1ES1622+261	16 22 06	+26 11 41	0.09 ^{+0.03} _{-0.03}	19/6	6.61E-05	144.0	7	3A	EHG	AGN	EXO	0.8
1ES1625+261	16 25 01	+26 08 59	0.10 ^{+0.04} _{-0.03}	22/7	3.39E-05	137.0	8	2A
1ES1626+279	16 26 33	+27 58 54	0.35 ^{+0.16} _{-0.13}	8/6	2.09E-05	19.5	9	3A
1ES1626+396	16 26 54	+39 39 54	1.63 ^{+0.09} _{-0.09}	346/8	1.00E-10	199.5	6	3A	3705	0.4	x1H1631+394	1.7	ABL	CG:0.030	A2199	1.9
1ES1626+554	16 26 54	+55 29 53	0.38 ^{+0.12} _{-0.10}	12/6	1.02E-07	31.4	4	3A	VV	AGN:0.132	PG	0.9
1ES1627+402	16 27 22	+40 13 05	0.19 ^{+0.06} _{-0.05}	23/7	3.80E-09	93.1	4	3A	EHG	AGN	EXO	1.0
1ES1631+781	16 31 31	+78 11 18	0.61 ^{+0.17} _{-0.15}	17/10	1.00E-10	26.0	2	3A	WFC	WD:DA	RE1629+781	1.0
1ES1634-104	16 34 22	-10 27 43	0.10 ^{+0.04} _{-0.04}	14/3	1.00E-04	95.1	5	3A	3732	1.0	BSC	S:O9.5Vn	ζ OPH	0.6
1ES1635+663	16 35 39	+66 18 55	0.16 ^{+0.04} _{-0.04}	28/11	2.84E-09	130.6	8	3A	3739	0.1	ABL	CG:0.171	A2218	0.3
1ES1638+608	16 38 23	+60 48 15	0.35 ^{+0.09} _{-0.08}	24/16	1.00E-10	57.7	6	3A	3742	0.5	SAO	S:G0V	WW DRA	0.3
1ES1638+634	16 38 45	+63 29 33	0.14 ^{+0.06} _{-0.05}	13/10	2.66E-05	72.4	9	3A
1ES1641+399	16 41 18	+39 54 01	0.23 ^{+0.04} _{-0.04}	59/8	1.00E-10	200.5	5	3A	3752	0.3	VV	AGN:0.594	3C345.0	0.2

TABLE 6—Continued

Slew Design:	RA 1950	DEC 1950	IPC Rate (cts s ⁻¹)	NP/NS	P _{rand}	Exp. (s)	P1	Q1	EOS # EMSS	Δ2E (<i>t</i>)	A ₃ EXO	Δ1H (<i>t</i>)	Cat.	Class.: Type/z	Name	ΔC (<i>t</i>)
1ES1649-403	16 49 07	-40 20 24	0.18+0.08 -0.07	9/2	3.42E-05	40.6	7	3A
1ES1649+758	16 49 34	+75 49 13	0.18+0.08 -0.07	10/9	4.90E-05	43.5	7	3A
1ES1650-417	16 50 22	-41 47 30	0.12+0.04 -0.04	20/2	2.95E-05	114.9	8	3A	SAO	S:B	SAO 227370	1.1
1ES1652+398	16 52 12	+39 50 25	3.24+0.13 -0.13	616/11	1.00E-10	186.8	5	3A	3780	0.1	x1H1651+398	0.3	VV	BL:0.034	MRK 501	0.1
1ES1652-082	16 52 49	-08 15 17	0.55+0.10 -0.10	39/1	1.00E-10	63.2	4	3A	3783	0.5	x1H1653-083	0.6	A3	AC	V1054 OPH	0.6
1ES1653+795	16 53 08	+79 35 09	0.18+0.07 -0.06	13/8	2.21E-06	58.2	6	3A
1ES1656+354	16 56 02	+35 25 12	0.48+0.07 -0.06	70/6	1.00E-10	131.2	5	3A	3791	0.1	x1H1656+354	0.2	A3	XRB	HER X-1	0.1
1ES1659+341	16 59 12	+34 07 20	0.16+0.07 -0.06	12/4	3.56E-05	57.5	7	3A	3895	1.2	2E
1ES1659+572	16 59 50	+57 17 07	0.20+0.10 -0.08	8/8	8.22E-05	32.6	8	2A
1ES1700+341	17 00 52	+34 08 27	0.49+0.16 -0.14	15/5	7.29E-10	26.8	6	3A	3809	0.8	1H1702+336	0.8	ABL	CG:0.097	A2244	1.5
1ES1701-369	17 01 38	-36 59 40	0.14+0.04 -0.04	25/2	1.30E-06	121.8	8	2M
1ES1702+457	17 02 02	+45 44 26	0.30+0.14 -0.11	9/5	2.53E-05	24.6	5	3A	SAO	S:F8	SAO 046462*	1.3
1ES1702-369	17 02 23	-36 58 24	0.22+0.07 -0.07	19/2	3.31E-06	62.8	7	2A	SBD	...	IRAS 17023-3659	1.4
1ES1702+482	17 02 58	+48 12 50	0.22+0.10 -0.08	8/5	8.63E-05	30.7	5	2A
1ES1704+545	17 04 10	+54 32 33	0.18+0.07 -0.06	13/6	1.49E-05	54.5	4	3A	m3830	1.1	WLY	SP6V	WLY 9584*	1.1
1ES1704+607	17 04 13	+60 47 56	0.04+0.01 -0.01	67/22	5.66E-05	704.3	6	3A	3828	1.2	1H1704+605	1.3	HB	AGN:0.371	3C351	1.3
1ES1704+736	17 04 16	+73 36 28	0.17+0.07 -0.06	12/9	1.75E-05	54.2	10	3A
1ES1704+240	17 04 31	+24 02 14	0.08+0.09 -0.08	73/3	1.00E-10	100.3	7	3A	3831	0.4	x1H1706+241	0.2	SAO	S:M0	SAO 084844	0.3
1ES1706+787	17 06 58	+78 43 49	0.38+0.04 -0.04	126/20	1.00E-10	280.5	7	3A	3842	0.8	UGC	GAL	U10726*	1.8
1ES1711-547	17 11 29	-54 47 08	0.40+0.16 -0.13	10/1	2.57E-07	22.2	8	3A	SAO	S:F0IV-V	SAO 244557	1.4
1ES1711+657	17 11 48	+65 45 50	0.16+0.07 -0.06	13/9	4.10E-05	59.4	9	3A
1ES1712+641	17 12 25	+64 06 28	0.25+0.04 -0.04	54/14	1.00E-10	172.2	7	3A	3866	1.3	2E	CG:0.081	A2255	1.2
1ES1714+574	17 14 27	+57 27 19	0.27+0.08 -0.07	17/10	6.09E-10	54.7	7	3A	RNG	GAL:0.028	NGC 6338*	1.3
1ES1716+551	17 16 16	+55 08 14	0.21+0.09 -0.08	10/7	7.11E-05	37.9	9	3A	SAO	S:K0	SAO 030326	2.8
1ES1717+265	17 17 57	+26 32 18	0.19+0.07 -0.06	14/1	1.06E-05	56.1	4	3A	m3884	0.6	MS	S:MAV+M5V	WLY 669AB	0.9
1ES1718+266	17 18 12	+26 40 44	0.28+0.08 -0.07	21/2	1.00E-10	63.6	6	3A	3885	0.4	1H1720+269B	0.6	2E	CG:0.164	2E	0.3
1ES1718+650	17 18 12	+65 01 48	0.13+0.05 -0.04	15/5	6.83E-05	83.8	6	3A
1ES1720+309	17 20 46	+30 55 30	0.35+0.08 -0.07	25/2	1.00E-10	63.3	5	3A	3893	0.2	x1H1727+308	0.1	VV	AGN:0.043	MRK 506	0.2
1ES1721+343	17 21 32	+34 20 34	0.57+0.07 -0.07	33/7	1.00E-10	134.9	5	3A	3896	0.3	HB	AGN:0.206	KEPLER	1.0
1ES1727+502	17 27 05	+50 15 14	0.77+0.03 -0.03	571/21	1.00E-10	701.9	5	3A	3909	0.5	x1H1730+500	0.3	VV	BL:0.055	I ZW 187	0.3
1ES1727-214	17 27 40	-21 27 52	2.99+0.32 -0.30	100/2	1.00E-10	32.6	5	3A	3911	1.4	x1H1728-213	1.0	A3	SNR	4C 34.47	0.1
1ES1727+530	17 27 52	+59 04 13	0.45+0.19 -0.15	8/6	1.74E-07	16.7	5	3A	SAO	S:G0	SAO 030416	0.9
1ES1728-169	17 28 49	-16 55 25	67.92+3.52 -3.54	376/1	1.00E-10	5.5	6	3A	x1H1728-169	0.4	A3	XRB	GX9+9	0.3

TABLE 6—Continued

Slew Design.	RA 1950	DEC 1950	IPC Rate (cts s ⁻¹)	NP/NS	P _{rand}	Exp. (s)	PI	QI	EOS #	Δ2E (<i>t</i>)	A ₃ EXO	ΔIH (<i>t</i>)	Cat.	Class.: Type/z	Name	ΔC (<i>t</i>)
1ES1731-325	17 31 26	-32 32 53	0.18 ^{+0.06} _{-0.05}	20/2	1.03E-08	86.5	6	3A	3920	0.1	x	...	2E	XRB	TERZ 1*	0.6
1ES1734+742	17 34 10	+74 15 50	0.80 ^{+0.12} _{-0.11}	57/24	1.00E-10	65.8	5	3A	1H1739+744	0.5	A3	AC	SAO 008842	0.5
1ES1734+686	17 34 25	+68 40 36	0.24 ^{+0.10} _{-0.08}	9/6	2.85E-06	32.8	8	3A
1ES1735-269	17 35 09	-26 57 40	0.91 ^{+0.23} _{-0.21}	22/1	1.00E-10	21.7	7	3A	SBD	S	IRAS 17345-2656	1.0
1ES1735-444	17 35 19	-44 25 09	39 02 ^{+0.78} _{-1.79}	483/5	1.00E-10	12.3	7	3A	x1H1735-444	0.2	A3	XRB	V926 SCO	0.2
1ES1737+612	17 37 58	+61 16 44	0.23 ^{+0.10} _{-0.08}	9/6	4.48E-06	33.9	5	3A	SBD	S.M.	HD 160934	2.0
1ES1739+518	17 39 19	+51 51 44	0.15 ^{+0.06} _{-0.05}	15/7	9.30E-05	67.1	5	3A	3934	0.7	VV	AGN-0.061	E 1739+518	0.6
1ES1741+196	17 41 46	+19 36 16	0.54 ^{+0.23} _{-0.19}	9/4	1.72E-06	14.8	7	3A
1ES1742-294	17 42 55	-29 29 56	1.88 ^{+0.25} _{-0.23}	65/2	1.00E-10	33.4	9	3A	3943	1.8	x1H1744-293	0.3	A3	XRB	X1742-294	0.3
1ES1743+480	17 43 48	+48 03 41	0.31 ^{+0.14} _{-0.12}	8/5	9.19E-06	22.5	7	3A
1ES1745+720	17 45 10	+72 04 24	0.17 ^{+0.06} _{-0.05}	17/13	7.99E-07	79.3	7	3A
1ES1749+504	17 45 13	+50 29 16	0.24 ^{+0.11} _{-0.09}	9/5	5.61E-05	30.1	6	3A
1ES1746+748	17 46 29	+74 53 38	0.19 ^{+0.07} _{-0.06}	12/9	5.88E-06	51.4	4	3A	SAO	S.K0	SAO 008910	0.2
1ES1746-370	17 46 47	-37 02 11	8.65 ^{+2.45} _{-2.14}	15/1	1.00E-10	1.7	8	3A	x1H1746-370	0.4	A3	XRB	NGC 6441	0.3
1ES1750+707	17 50 59	+70 47 52	0.17 ^{+0.07} _{-0.06}	16/9	3.00E-05	66.7	7	3A	m3969	1.3	x	...	2E	S	2E	1.6
1ES1755-338	17 55 07	-33 49 47	5.18 ^{+2.11} _{-1.72}	8/1	1.50E-10	1.5	10	3A	BMC	XRB	4U1755-338	3.0
1ES1757-233	17 57 29	-23 20 25	0.31 ^{+0.10} _{-0.09}	23/2	3.59E-07	53.4	7	2E
1ES1758-250	17 58 02	-25 04 40	56.86 ^{+1.98} _{-1.98}	837/2	1.00E-10	14.6	9	3A	x1H1758-250	0.2	A3	XRB	GX5-1	0.3
1ES1758-257	17 58 06	-25 44 04	2.64 ^{+0.50} _{-0.45}	34/3	1.00E-10	12.4	8	3A	x
1ES1802+025	18 02 52	+02 30 28	0.35 ^{+0.09} _{-0.08}	25/1	1.00E-10	62.0	4	3A	4004	1.2	WLY	S:K0V+K5V	WLY 702AB	1.0
1ES1805-118	18 05 09	-11 53 00	0.79 ^{+0.33} _{-0.27}	8/2	7.98E-09	9.6	8	3A
1ES1807+698	18 07 11	+69 48 47	0.08 ^{+0.02} _{-0.02}	51/14	1.96E-08	394.2	6	3A	4023	0.9	x1H1803+696	0.7	VV	BL-0.051	3C 371.0	0.7
1ES1808-579	18 08 18	-57 57 43	0.81 ^{+0.39} _{-0.31}	6/2	7.57E-08	7.2	6	3A
1ES1810+696	18 10 23	+69 40 53	0.06 ^{+0.02} _{-0.01}	52/14	1.37E-06	482.2	5	2A	m4039	0.6	x	...	SAO	S.K2	SAO 017800	0.8
1ES1811-171	18 11 34	-17 10 26	18.99 ^{+2.68} _{-2.50}	56/1	1.00E-10	2.9	8	3A	x1H1811-171	0.7	A3	XRB	GX13+1	0.8
1ES1814+782	18 14 38	+78 12 34	0.13 ^{+0.05} _{-0.04}	15/7	7.11E-05	81.1	5	3A
1ES1814+498	18 14 58	+49 50 29	0.63 ^{+0.09} _{-0.08}	69/7	1.00E-10	102.5	3	3A	4051	0.5	x1H1814+498	0.5	A3	CV	AM HER	0.5
1ES1817+537	18 17 10	+53 42 59	0.55 ^{+0.19} _{-0.16}	11/5	1.87E-10	18.9	4	3A
1ES1820-303	18 20 29	-30 23 23	99.31 ^{+1.66} _{-1.69}	309/1	1.00E-10	3.1	7	3A	x1H1820-303	0.2	A3	XRB	NGC 6624	0.3
1ES1821+643	18 21 43	+64 19 13	1.08 ^{+0.23} _{-0.21}	28/10	1.00E-10	24.3	6	3A	4066	0.3	x1H1820+643	0.3	HB	AGN-0.297	KUV 1821+64*	0.3
1ES1824+151	18 24 38	+15 07 03	1.18 ^{+0.37} _{-0.39}	8/1	1.00E-10	6.7	7	3A	SAO	S.K0	SAO 103722	1.2
1ES1827+206	18 27 48	+20 41 56	0.14 ^{+0.06} _{-0.05}	10/1	7.03E-05	58.3	8	2A
1ES1832+516	18 32 43	+51 40 04	1.02 ^{+0.30} _{-0.26}	15/5	1.00E-10	14.0	5	3A	4094	0.9	x	...	WLY	AC:MoEV	BY DRA	1.0

TABLE 6—Continued

Slew Desig.	RA 1950	DEC 1950	IPC Rate (cts s ⁻¹)	NP/NS	P _{rand}	Exp. (s)	PI	QI	EOS #	Δ2E (<i>i</i>)	A3	Δ1H (<i>i</i>)	Cat.	Class:	Name	ΔC (<i>i</i>)
1ES1833+326	18 33 11	+32 33 41	0.49 ^{+0.10} _{-0.09}	35/3	1.00E-10	65.4	7	3A	4097	0.7	x1H1835+326	0.6	VV	AGN:0.059	3C382.0	0.7
1ES1833+169	18 33 40	+16 56 41	0.17 ^{+0.06} _{-0.05}	18/5	7.53E-07	78.6	5	3A	BSC	SG2V+G2V	HD 171746	0.6		
1ES1841-044	18 41 55	-04 27 10	0.42 ^{+0.20} _{-0.16}	7/2	2.22E-05	14.9	3	3A	GCV	S	FT SGT	1.6		
1ES1845+797	18 45 41	+79 43 04	0.20 ^{+0.02} _{-0.02}	156/24	1.00E-10	61.8	7	3A	4136	0.2	x1H1858+797	0.2	VV	AGN:0.057	3C 380.3	0.2
1ES1846+005	18 46 22	+00 31 37	0.22 ^{+0.06} _{-0.07}	12/2	7.32E-08	48.3	6	3A	4138	0.2	SHA	CV	V603 AQL	0.2
1ES1846-238	18 46 45	-23 53 05	0.43 ^{+0.13} _{-0.11}	17/2	1.00E-10	35.4	3	3A	4140	0.6	WLY	SM4EV	WLY 729	0.4
1ES1846-009	18 46 56	-00 59 03	0.24 ^{+0.11} _{-0.09}	8/1	1.03E-05	29.6	8	3A
1ES1850+005	18 50 04	+00 34 51	0.23 ^{+0.06} _{-0.05}	26/3	1.00E-10	93.7	6	3A	4150	1.5	SBD	SNR	4C 70	2.9
1ES1850-087	18 50 20	-08 45 53	4.21 ^{+0.26} _{-0.27}	260/3	1.00E-10	60.9	7	3A	4151	0.2	x1H1850-087	0.3	A3	XRB	NGC6712	0.3
1ES1851-312	18 51 51	-31 13 27	0.94 ^{+0.27} _{-0.23}	16/3	1.00E-10	16.1	7	3A	x1H1853-312	0.5	A3	CV	V1223 SGR	0.5
1ES1853-379	18 53 13	-37 58 25	0.86 ^{+0.31} _{-0.28}	10/5	1.00E-10	11.2	3	3A
1ES1853+012	18 53 23	+01 16 13	0.78 ^{+0.29} _{-0.25}	11/2	1.76E-07	12.4	7	3A	1H1852+015	2.5	A3	SNR	G34:7.0	2.5
1ES1853+671	18 53 56	+67 09 44	0.15 ^{+0.06} _{-0.05}	12/8	5.48E-05	59.6	6	3A
1ES1900+699	19 00 52	+69 54 36	0.15 ^{+0.05} _{-0.04}	18/5	1.12E-06	92.1	7	3A	ABL	CG:0.094	A2315	2.3		
1ES1902-524	19 02 22	-52 25 05	1.12 ^{+0.60} _{-0.46}	5/2	8.97E-07	4.3	7	3A	BSC	S:FTV	ρ TEL	0.2		
1ES1905+070	19 05 08	+07 04 27	0.45 ^{+0.21} _{-0.17}	7/3	1.63E-05	14.0	6	2A	SBD	...	HSNH 111	0.7
1ES1905+000	19 05 51	+00 05 23	3.85 ^{+0.67} _{-0.61}	38/4	1.00E-10	9.7	8	3A	x1H1905+000	0.7	A3	XRB	X1905+000	0.8
1ES1907+523	19 07 14	+52 20 45	0.81 ^{+0.26} _{-0.22}	13/5	1.00E-10	15.1	4	3A	4195	0.2	BSC	AC:KIV	HD179094	0.3
1ES1907+097	19 07 15	+09 44 48	0.53 ^{+0.10} _{-0.09}	38/6	1.00E-10	67.0	9	3A	x1H1909+096	0.1	A3	XRB-Be	X1907+097	0.1
1ES1908+090	19 08 44	+09 02 12	0.25 ^{+0.08} _{-0.07}	15/5	2.38E-08	50.1	7	3A	4203	0.7	2E	SNR	W49B	0.8
1ES1908+005	19 08 45	+00 30 30	3.42 ^{+0.61} _{-0.55}	39/2	1.00E-10	10.8	8	3A	BMC	XRB	AQL X-1	0.6
1ES1909+048	19 09 21	+04 53 45	0.87 ^{+0.04} _{-0.04}	437/21	1.00E-10	476.6	7	3A	4204	0.2	x1H1908+047	0.2	A3	SNR	SS433	0.2
1ES1914+092	19 14 38	+09 15 09	0.14 ^{+0.05} _{-0.04}	18/2	4.16E-06	93.6	6	2A	SAO	S:KII	SAO 124465*	1.2
1ES1916-053	19 16 07	-05 19 54	7.13 ^{+0.37} _{-0.37}	382/6	1.00E-10	53.0	7	3A	4222	0.1	x1H1916-053	0.3	SHA	CV	V1336 AQL	1.5
1ES1916+195	19 16 39	+19 30 53	0.28 ^{+0.12} _{-0.10}	8/5	5.69E-06	25.3	8	3A	4225	0.6	SAO	S:B8II+K	U SGE	0.3
1ES1920+233	19 20 44	+22 23 02	0.53 ^{+0.28} _{-0.22}	5/4	1.99E-06	9.1	7	3A	SBD	SA2	HD 344230	1.9
1ES1921-233	19 21 45	-29 20 31	0.07 ^{+0.03} _{-0.02}	29/4	3.57E-05	222.2	7	3A	4245	0.6	HB	AGN:0.352	OV 236	0.6
1ES1927+654	19 27 00	+65 28 02	0.93 ^{+0.17} _{-0.15}	37/17	1.00E-10	37.9	5	3A
1ES1928+738	19 28 56	+73 51 28	0.34 ^{+0.13} _{-0.11}	11/7	2.39E-07	28.3	7	2A	x1H1922+746	0.5	VV	AGN:0.302	4C 73.1.8	0.5
1ES1932+695	19 32 28	+69 33 36	0.11 ^{+0.04} _{-0.04}	13/6	4.62E-05	88.8	5	3A	4267	0.4	WLY	SK0V	WLY 764	1.0
1ES1934-063	19 34 53	-06 19 38	1.48 ^{+0.46} _{-0.39}	13/3	1.00E-10	8.6	7	3A	1H1934-063.A	0.3	A3	AGN:0.011	SS 442	0.3
1ES1935+501	19 35 09	+50 07 07	0.12 ^{+0.04} _{-0.03}	24/7	3.86E-08	144.1	3	3A	4269	0.5	SAO	S:F4V	SAO 031815	0.7
1ES1948+087	19 48 23	+08 44 20	0.07 ^{+0.02} _{-0.02}	25/5	1.86E-05	228.1	5	3A	4294	0.4	x	...	SAO	S:A7V	SAO 125122	0.3

TABLE 6—Continued

Slew Desig.	RA 1950	DEC 1950	IPC Rate (cts s ⁻¹)	NP/NS	P _{rand}	Exp. (s)	P1	Q1	EOS # EMSS	Δ2E (<i>t</i>)	A3 EXO	Δ1H (<i>t</i>)	Cat.	Class.: Type/z	Name	ΔC (<i>t</i>)	
1ES1948+085	19 48 47	+08 34 35	0.08 ^{+0.03} _{-0.03}	25/6	2.14E-05	189.7	4	3A	4295	0.6	x	...	2E	S	AG+08 2640	0.3	
1ES1957+405	19 57 47	+40 35 54	0.40 ^{+0.11} _{-0.10}	23/1	8.66E-10	46.3	8	3E	4309	0.3	1H1958+406	0.5	A3	AGN:0.058	CYG A*	0.6	
1ES1959+650	19 59 35	+65 00 14	1.59 ^{+0.28} _{-0.26}	38/10	1.00E-10	23.1	6	3A	
1ES2001+068	20 01 41	+06 51 03	1.19 ^{+0.58} _{-0.46}	7/1	2.02E-05	5.2	4	2A	SBD	S:K2	HD 190342	2.4	
1ES2005+175	20 05 20	+17 33 30	0.20 ^{+0.04} _{-0.04}	32/3	1.00E-10	132.0	5	3A	4322	0.2	x	...	SHA	CW	WZ SGE	0.1	
1ES2005-489	20 05 47	-48 58 45	1.44 ^{+0.70} _{-0.55}	6/4	1.50E-07	4.0	6	3A	x	...	VV	BL:0.071	PKS	0.1	
1ES2008-570	20 08 23	-57 01 20	0.45 ^{+0.21} _{-0.17}	9/6	9.99E-05	15.9	6	2A	4331	2.6	SBD	GAL:0.055	ESO 186-11	2.8	
1ES2010+463	20 10 33	+46 20 06	0.38 ^{+0.07} _{-0.06}	43/12	1.00E-10	99.0	7	3A	4336	0.3	2E	S	31 CYG	0.4	
1ES2013+448	20 13 12	+44 52 37	0.17 ^{+0.07} _{-0.06}	11/7	7.43E-06	52.9	6	3A	SAO	SK0	SAO 049357	0.4	
1ES2018+436	20 18 49	+43 41 30	0.36 ^{+0.12} _{-0.10}	14/7	1.37E-08	33.9	6	3A	x1H2018+439	0.4	SAO	S:WC7P+05	SAO 049491	0.4	
1ES2025+573	20 25 19	+57 22 34	0.24 ^{+0.12} _{-0.09}	7/5	1.95E-05	26.1	8	3A	
1ES2028+513	20 28 10	+51 19 47	0.24 ^{+0.13} _{-0.10}	5/5	5.10E-08	20.3	4	3A	
1ES2030+407	20 30 39	+40 47 13	14.21 ^{+0.10} _{-0.10}	19909/26	1.00E-10	1384.8	8	3A	4376	0.4	x1H2030+407	0.2	A3	XRB	CYG X-3	0.3	
1ES2031+411	20 31 28	+41 08 43	0.11 ^{+0.01} _{-0.01}	250/18	1.00E-10	1059.0	7	3A	4382	0.2	SAO	S:O61b	SAO 049781*	0.2	
1ES2033+110	20 33 05	+11 00 18	0.13 ^{+0.06} _{-0.05}	12/2	6.88E-05	69.8	8	3A	
1ES2037-010	20 37 35	-01 03 02	0.16 ^{+0.07} _{-0.06}	12/2	4.12E-05	56.8	4	3A	4404	0.3	x	...	SHA	CW	AE AQR	0.2	
1ES2037+521	20 37 57	+52 09 42	0.10 ^{+0.04} _{-0.03}	16/7	6.99E-05	111.1	6	3A	4405	0.6	2E	
1ES2038-007	20 38 18	-00 46 43	0.10 ^{+0.04} _{-0.03}	18/4	7.81E-06	123.6	6	3A	m4408	0.6	SAO	S:F8	SAO 144692	1.2	
1ES2039+758	20 39 42	+75 51 07	0.24 ^{+0.12} _{-0.09}	7/5	1.44E-05	25.9	9	2A	
1ES2042+335	20 42 49	+33 31 51	0.10 ^{+0.04} _{-0.03}	19/11	3.12E-05	127.8	6	3A	SAO	S:G5	SAO 070451	2.2	
1ES2048+314	20 48 50	+31 25 17	0.26 ^{+0.08} _{-0.08}	185/11	1.00E-10	181.6	4	3A	SAO	S:K0	SAO 070569	0.9	
1ES2052+441	20 52 08	+44 11 40	1.00 ^{+0.21} _{-0.19}	29/10	1.00E-10	27.3	5	3A	SAO	S:G2V	SAO 050198	0.5	
1ES2055+298	20 55 55	+29 51 05	0.25 ^{+0.12} _{-0.10}	9/4	8.50E-05	29.2	7	3A	
1ES2055+443	20 55 57	+44 20 43	0.28 ^{+0.14} _{-0.11}	8/4	9.27E-05	23.4	6	2A	
1ES2056+504	20 56 53	+50 29 55	0.20 ^{+0.08} _{-0.07}	11/3	3.05E-06	45.6	7	2A	
1ES2058+398	20 58 08	+39 52 07	0.41 ^{+0.13} _{-0.11}	14/7	1.00E-10	30.7	4	3A	WLY	AC:M3EV+M3EV	WLY 815AB	0.6
1ES2129-026	21 29 31	-02 37 12	0.22 ^{+0.10} _{-0.08}	69/8	1.00E-10	111.8	5	3A	4438	0.1	x	...	SAO	S:GOV+GSV	ER VUL	0.4	
1ES2129+470	21 29 36	+47 04 11	1.25 ^{+0.16} _{-0.15}	70/2	1.00E-10	52.8	8	3A	4435	0.2	1H2131+473	0.1	A3	XRB	M15	0.3	
1ES2127+119	21 27 34	+11 56 56	4.28 ^{+0.66} _{-0.61}	47/5	1.00E-10	10.8	7	3A	SBD	S:K8	BD+22 4409	6.7	
1ES2128+231	21 28 47	+23 06 50	0.46 ^{+0.18} _{-0.15}	9/3	3.11E-10	18.8	5	3A	
1ES2129-147	21 35 01	-14 46 16	0.14 ^{+0.04} _{-0.04}	24/4	4.51E-08	132.1	7	3A	4497	0.1	x	...	VV	AGN:0.200	PHL 1657	0.2	

TABLE 6—Continued

Slew Desig.	RA 1950	DEC 1950	IPC Rate (cts s ⁻¹)	NP/NS	P _{rand}	Exp. (s)	PI	QI	EOS # EMSS	Δ2E (<i>t</i>)	A3 EXO	Δ1H (<i>t</i>)	Cat.	Class: Type/z	Name	ΔC (<i>t</i>)	
1ES2135+011	21 35 02	+01 10 38	0.20+0.09 -0.07	11/8	7.33E-05	43.0	8	2A	SBD	S:K0	AG+01 2623	2.4	
1ES2137+204	21 37 00	+20 26 22	0.21+0.10 -0.08	8/7	8.51E-05	32.2	7	2A	
1ES2137+241	21 37 26	+24 10 25	0.75+0.37 -0.29	6/3	4.71E-07	7.6	5	3A	
1ES2143+751	21 43 03	+75 10 25	0.29+0.11 -0.09	11/5	1.37E-08	34.0	5	3A	
1ES2149+054	21 49 40	+05 24 21	0.19+0.06 -0.05	19/2	1.89E-08	82.2	5	3A	4536	0.5	2E	
1ES2152-548	21 52 53	-54 52 47	0.68+0.24 -0.20	12/3	8.52E-10	16.1	4	3A	
1ES2153+441	21 53 14	+44 10 17	0.59+0.13 -0.12	25/8	1.00E-10	40.1	6	3A	SAO	S:K0	SAO 051437	1.0
1ES2155-081	21 55 14	-08 08 32	0.13+0.05 -0.04	14/3	9.44E-05	78.8	5	3A	SBD	S	BD-08 5773	0.7
1ES2155-304	21 55 58	-30 27 48	5.08+0.16 -0.16	1043/5	1.00E-10	202.1	4	3A	4544	0.1	x1H2156-304	0.1	VV	BL:0.117	PKS	0.1	
1ES2156+032	21 56 20	+03 15 35	0.08+0.03 -0.03	19/1	8.10E-05	163.9	12	2A	
1ES2159+436	21 59 29	+43 38 56	0.12+0.02 -0.02	59/8	1.00E-10	360.0	6	3A	4550	0.1	SAO	S:G5	SAO 051563	0.5
1ES2200+826	22 00 09	+82 37 38	0.59+0.27 -0.22	7/5	4.78E-07	11.0	7	3A	BSC	S:F6IV-V	HD 203942	0.2
1ES2200+420	22 00 40	+42 01 47	0.27+0.07 -0.06	22/4	1.00E-10	72.2	7	3A	4558	0.5	VV	BL:0.070	BL LAC	0.4	
1ES2201+315	22 01 02	+31 31 13	0.22+0.08 -0.08	8/1	1.69E-05	31.2	6	3A	4561	0.3	HB	AGN:0.297	4C 31.63	0.2	
1ES2202+469	22 02 56	+46 59 06	0.30+0.11 -0.10	12/2	1.94E-07	33.9	4	3A	4567	0.4	1H2213+484	0.4	A3	AC	HK LAC	0.4	
1ES2206+445	22 06 25	+44 30 34	0.11+0.04 -0.04	17/2	6.45E-06	111.0	6	3A	
1ES2206+455	22 06 40	+45 30 02	1.86+0.08 -0.08	576/6	1.00E-10	302.0	5	3A	4573	0.2	x1H2207+455	0.3	A3	AC	AR LAC	0.3	
1ES2207+643	22 07 06	+64 20 20	0.14+0.06 -0.05	12/5	8.06E-05	62.8	7	3A	
1ES2207-124	22 07 37	-12 25 27	0.29+0.05 -0.04	55/5	1.00E-10	168.3	6	3A	4575	1.3	ABL	CG:0.084	A2420	1.3
1ES2216+845	22 16 16	+84 30 24	0.28+0.13 -0.10	8/6	6.32E-06	25.0	5	3A	SAO	S:K2	SAO 003717	0.5
1ES2216+565	22 16 58	+56 35 39	0.22+0.09 -0.08	11/6	4.15E-05	39.1	5	3A	
1ES2221-018	22 21 22	-01 50 48	0.18+0.06 -0.05	18/3	8.21E-08	81.1	8	3A	4597	1.6	1H2221-017A	1.3	ABL	CG:0.090	A2440	1.0	
1ES2223-051	22 23 09	-05 11 51	0.17+0.03 -0.03	42/6	1.00E-10	200.4	7	3A	4603	0.5	VV	AGN:1.404	3C 446	0.7	
1ES2236-208	22 36 04	-20 52 31	0.66+0.08 -0.08	70/4	1.00E-10	99.4	4	3A	4632	0.4	SAO	AC:M2V+M4V	WLY 867AB	0.4	
1ES2240+294	22 40 18	+29 28 17	1.88+0.35 -0.32	33/7	1.00E-10	17.2	5	3A	1H2239+294	0.5	VV	AGN:0.025	AKN 564	0.5	
1ES2244-019	22 44 48	-01 54 11	0.15+0.05 -0.05	16/4	1.09E-06	82.4	13	2A	
1ES2246-646	22 46 36	-64 41 41	0.44+0.18 -0.15	9/6	7.94E-07	18.1	6	2E	1H2245-646	2.8	ABL	CG	A3921	2.8	
1ES2247+106	22 47 53	+10 37 37	0.76+0.33 -0.27	8/2	3.90E-07	9.7	6	3A	ABL	CG:0.077	A2495*	0.5	
1ES2251+376	22 51 23	+37 40 29	0.16+0.05 -0.04	20/2	9.67E-08	93.7	4	3A	4644	0.0	SAO	S:K0V	SW LAC	0.6
1ES2251-178	22 51 26	-17 50 20	0.45+0.10 -0.09	31/2	1.00E-10	61.4	8	3A	4645	0.6	x1H2251-179	0.6	HB	AGN:0.068	MR 2251-178	0.6	
1ES2254-371	22 54 62	-37 11 34	0.28+0.07 -0.06	25/4	1.00E-10	76.2	4	3A	m4664	0.7	MS	AGN:0.039	MS	0.6	
1ES2257-340	22 57 38	-34 01 28	0.45+0.21 -0.17	7/4	1.53E-06	14.3	4	3A	SAO	S:G5VP	SAO 214237	1.7	
1ES2257+620	22 57 39	+62 04 26	0.15+0.06 -0.05	13/8	1.31E-05	68.5	7	3A	

TABLE 6—Continued

Slew Desig.	RA 1950	DEC 1950	IPC Rate (cts s ⁻¹)	NP/NS	P _{rand}	Exp. (s)	PI	QI	EOS # EMSS	$\Delta 2E$ (ℓ)	A ₃ EXO	$\Delta 1H$ (ℓ)	Cat.	Class.: Type/z	Name	ΔC (ℓ)
1ES2255+586	22 59 06	+58 36 31	0.93 ^{+0.10} _{-0.10}	128/10	1.00E-10	116.9	7	3A	4673	0.3	x1H2255+585	0.4	A3	SNR	G109.1-1.0	0.4
1ES2304+042	23 04 29	+04 16 40	1.11 ^{+0.43} _{-0.36}	9/2	2.43E-09	7.7	7	3A	x1H2303+039	0.3	VV	AGN;0.042	PG	0.3
1ES2304+252	23 04 38	+25 12 19	0.11 ^{+0.04} _{-0.04}	13/4	1.28E-05	92.0	7	3A	4682	0.9	1H2315+257	0.7	A3	AC	56 PEG B	0.7
1ES2307+476	23 07 33	+47 41 36	0.54 ^{+0.15} _{-0.13}	19/7	1.00E-10	32.0	4	3A	4687	1.2	SAO	AC;G5	KZ AND	1.6
1ES2310-219	23 10 20	-21 54 55	0.20 ^{+0.04} _{-0.04}	41/4	1.00E-10	160.5	7	3A	4695	0.7	1H2307-222A	0.9	ABL	CG;0.086	A2556	1.3
1ES2311-430	23 11 13	-43 00 13	1.03 ^{+0.13} _{-0.12}	78/7	1.00E-10	71.6	6	3A	m4659	0.4	2E	CG;0.056	S1101*	0.8
1ES2316-423	23 16 22	-42 22 24	0.12 ^{+0.03} _{-0.03}	42/10	1.00E-10	240.1	6	3A	m4709	0.6	MS	CG;0.045	S1111	0.4
1ES2319-421	23 19 00	-42 10 15	0.15 ^{+0.04} _{-0.04}	26/9	3.04E-08	122.7	7	3A	m4721	2.0	ABL	CG	A3998	1.1
1ES2321+585	23 21 06	+58 33 08	28.63 ^{+1.17} _{-1.17}	612/12	1.00E-10	21.2	7	3A	4724	0.6	x1H2321+585	0.8	A3	SNR	CAS A	0.8
1ES2321+419	23 21 23	+41 54 59	0.12 ^{+0.05} _{-0.04}	12/4	3.04E-05	78.3	8	1A	4725	1.2	1H2318+417	1.1	A3	BL	H2321+419	1.0
1ES2321+143	23 21 47	+14 22 26	0.14 ^{+0.04} _{-0.04}	23/3	1.39E-07	123.0	8	2E	1H2320+146	2.6	A3	CG;0.041	A2593	2.7
1ES2322-409	23 22 02	-40 56 46	0.70 ^{+0.29} _{-0.23}	8/4	1.33E-09	11.0	6	3A	ABL	CG;0.085	A2597	1.7
1ES2322-124	23 22 46	-12 24 27	0.55 ^{+0.16} _{-0.14}	17/2	1.00E-10	28.0	8	3A	4728	0.8	SBD	S.M2	G 190-28	0.4
1ES2326+411	23 26 59	+41 11 16	0.38 ^{+0.16} _{-0.13}	8/4	5.83E-07	19.4	2	3A	WLY	S.M+E+M6	WLY 896AB	0.0
1ES2329+196	23 29 20	+19 39 44	0.54 ^{+0.07} _{-0.06}	88/6	1.00E-10	151.1	4	3A	4733	0.2	SAO	S:G0	SAO 128282	0.8
1ES2334+063	23 34 07	+06 18 05	0.32 ^{+0.14} _{-0.11}	9/3	7.38E-06	24.5	8	3A	ABL	CG;0.085	A2597	1.7
1ES2335+461	23 35 06	+46 11 20	2.85 ^{+0.18} _{-0.18}	251/8	1.00E-10	86.6	5	3A	4740	0.2	x1H2336+462	0.2	A3	AC	λ AND	0.1
1ES2340-152	23 40 53	-15 12 37	0.17 ^{+0.07} _{-0.06}	11/1	3.46E-05	50.8	3	3A	m4755	0.6	ZCT	GAL:0.137	MS	0.8
1ES2342+089	23 42 25	+08 55 11	0.38 ^{+0.06} _{-0.05}	65/8	1.00E-10	150.4	6	3A	4758	0.5	1H2343+090	2.9	A3	CG;0.040	A2657	2.9
1ES2343-151	23 43 02	-15 06 15	0.23 ^{+0.10} _{-0.08}	9/2	1.15E-05	34.1	5	3A	4760	0.4	SBD	...	068.16-70.38	0.6
1ES2344+514	23 44 37	+51 25 50	0.43 ^{+0.16} _{-0.14}	10/7	1.22E-08	21.6	7	3A	ABL	CG	S1158	1.4
1ES2347+485	23 47 58	+48 31 57	0.40 ^{+0.19} _{-0.15}	7/3	9.62E-06	15.9	4	3A
1ES2349-561	23 49 31	-56 11 39	0.88 ^{+0.42} _{-0.33}	6/4	7.55E-08	6.6	6	3A	ABL	CG	S1158	1.4
1ES2352-208	23 52 03	-20 51 58	1.07 ^{+0.64} _{-0.48}	4/1	3.69E-07	3.7	3	3A
1ES2352+283	23 52 32	+28 21 49	2.98 ^{+0.57} _{-0.52}	31/6	1.00E-10	10.2	4	3A	4789	0.5	x1H2354+285	0.9	HD	S:K0V	HD 224085	0.8
1ES2352+600	23 52 54	+60 03 32	0.32 ^{+0.15} _{-0.12}	6/4	3.66E-07	18.0	7	3A
1ES2352+512	23 52 59	+51 15 33	0.76 ^{+0.41} _{-0.31}	5/3	4.34E-07	6.4	4	3A

Column (8).—*Mean pulse height bin.* The average of the “pulse-invariant” (PI; Harnden et al. 1984) channel numbers (1–15) for each photon, which coarsely indicates the source spectrum.

Column (9).—*Quality control index (Q)* and *image code (I).* The Q (1, 2, or 3; 3 being highest quality) value is a visual estimate of the reliability of the source. The *image code* highlights cases where Prob1/Prob2 (defined in § 4.3) is large ($>10^3$), and which a visual inspection shows to be extended, or to have multiple sources within 15' (see § 4.5). The *image code* has the following values:

- A, generally acceptable Prob1/Prob2;
- E, extended source ($>15'$);
- M, multiple sources within 15';
- P, part of source (extended source existing in more than one field).

Columns (10) and (11).—*EOSCAT number, Einstein Medium Survey membership* (noted by *m*), and *offset from EOSCAT position ($\Delta 2E$)*. For sources with counterparts in the 2E Catalog (Harris et al. 1991), we provide the EOSCAT number and the difference between the Slew Survey and catalog positions, in arc minutes. In addition, Medium Survey (Gioia et al. 1990; Stocke et al. 1991) sources are noted with a letter *m* preceding the EOSCAT number.

Columns (12) and (13).—*HEAO 1 A-3 counterpart, EXOSAT detections* (noted by *x*), and *offset from HEAO A-3 position ($\Delta 1H$)*. For sources with counterparts in the HEAO 1 A-3 catalog (Remillard et al. 1991), we provide the “1H” name and the difference between the Slew Survey and catalog positions, in arcminutes. In addition, EXOSAT sources are noted with a letter *x* preceding the 1H name.

Columns (14)–(17).—*Optical catalog (Cat.), object classification (Class.), counterpart name (Name), and offset from catalog position (ΔC)*. For sources with counterparts in (mainly) optical catalogs searched to date (see below for catalog list and references), we provide the name of the catalog, the classification (e.g., AGN), the counterpart name, and the difference between the Slew Survey and catalog positions, in arcminutes. If the redshift or stellar spectral type is known, it is listed after the object classification in column (15).

Composite spectral types in Table 6 indicate a binary (or other multiple star system). In general, we have tried to use the most common names of objects. For cases in which two objects (most commonly an SAO star and an extragalactic object) were found in the same error box, we compared their f_x/f_o ratios with those for the Medium Survey sources (Maccacaro et al. 1988). In most cases, only one of the objects was a plausible counterpart given these ratios. Cases in which more than one object is a likely counterpart are indicated with asterisks and noted below (§ 7.3).

If the counterpart name is the same as the Slew name in column (1) and the catalog is well known, only the catalog designator is listed in column (16) (e.g., PG, EXO, 2E). Woolley names with letters A, B, . . . indicate multistar systems (e.g., WLY 127AB). For each of the newly discovered X-ray sources, we list all the names known to us in Table 7.

Abbreviations for names of catalogs are as follows:

- 2E, Second *Einstein* IPC Catalog (‘EOSCAT’; Harris et al. 1991);
- A3, *HEAO A-3 Catalog* (Remillard et al. 1991);
- ABL, Abell Catalog (1958; Struble & Rood 1987) and

Southern Abell Catalog (Abell, Corwin, & Olowin 1989);

BMC, Bradt & McClintock (1983);

BSC, Bright Star Catalog (Hoffleit & Jaschek 1982); EHG, *EXOSAT* High Galactic Latitude Survey (Giommi et al. 1991);

EXC, *EXOSAT* data base of optical and other astronomical catalogs;

GCV, General Catalog of Variable Stars (Kholopov et al. 1985–1988);

HB, Hewitt & Burbidge (1987);

HD, Henry Draper Catalog (Cannon & Pickering 1918–1924);

MCS, McCook & Sion (1987);

MS, *Einstein* Extended Medium-Sensitivity Survey (Gioia et al. 1990);

RNG, Revised NGC Catalog (Sulentic & Tifft 1973);

SAO, SAO Catalog (SAO Staff 1966);

SBD, SIMBAD data base;

SHA, Shara (1990);

UGC, Uppsala General Catalogue of Galaxies (Nilsson 1973);

VV, Véron-Cetty & Véron (1987);

WFC, ROSAT Wide-Field Camera (Cooke et al. 1991);

WLY, Woolley Catalog (Woolley et al. 1970);² and ZCT, CfA Redshift Catalog; Huchra (1990).

Abbreviations for object classification are as follows:

AC, active star;

AGN, active galactic nucleus;

BL, BL Lacertae object;

CG, cluster of galaxies;

CV, cataclysmic variable;

GAL, normal galaxy;

P, pulsar;

S, normal star;

SNR, supernova remnant;

WD, white dwarf;

XRB, X-ray binary; and

(XRB-Be), X-ray binary (with Be star secondary).

6.2. Notes on Individual Objects

1ES 0013+195.—The error box also contains G32–7 (S:M4.5), but at $V = 14$ (cf. 13 for G32–6), it is an unlikely counterpart based on f_x/f_o (Maccacaro et al. 1988).

1ES 0100+405.—The stars G132–51B and G132–51C are in the error box and have acceptable f_x/f_o ratios, although both (at $V = 13.01$) are 2.2 mag fainter than G132–51A.

1ES 0120+004.—Besides the star, the error box contains MCG +00-04-103, a 16th mag galaxy which may be an AGN.

1ES 0122+084A and B.—Besides the cluster, the error box also includes the galaxy UGC 977, which may be a previously unknown AGN.

1ES 0237–531.—The error box also contains SAO 232842 (S:K5), which at $V = 8.3$ is 0.9 mag fainter than HD 16699.

1ES 0255+128.—Besides the cluster, the error box also contains the galaxy UGC 2438, another possible AGN.

1ES 0305–284.—The error box also contains LTT 1477 (S:M3), but this source has $V = 14.0$, and can be ruled out by f_x/f_o arguments.

² This is an extended version of the Gleise catalog, using the same numbering scheme as Gleise.

1ES 0316+413.—Besides the cluster, the error box also contains the AGN NGC 1275, a known X-ray source (Branduardi-Raymont et al. 1981).

1ES 0429+130.—The error box also contains HD 286839 (S:K0).

1ES 0538–019.—The Slew Survey error box contains part of the Orion star-forming region, based on an HRI detection.

1ES 0702+646.—Other than the AGN, the error box contains SAO 14073 (S: G0).

1ES 0716–248.—The error box contains a substantial portion of the globular cluster N2362, of which HD 57061 is the brightest star (at $V = 4.32$). There are more than 30 other possible counterparts, ranging from $V = 8.12$ to $V = 13$, with known spectral types B2–A0.

1ES 0953+693.—The error box also contains 0953+6917, a $B = 13.7$ galaxy which may have an active nucleus.

1ES 1035–268.—Error box contains the compact group HCG 048, which includes the galaxy counterpart.

1ES 1101+384.—The error box contains two identifications based on the 2E catalog: Mrk 421 (BL), and 51 UMA (S: A3), but the latter is 2.1' from the 1ES position. Mrk 421 is a well-known source at high energies (Wood et al. 1984) and is clearly the preferred identification based on an HRI position (from *einline*).

1ES 1215+039.—The counterpart is a double galaxy.

1ES 1218–637.—The optical counterpart is a young SNR candidate, based on HRI data in *einline*.

1ES 1254–172.—The error box also contains 1254–1711 (GAL:0.049), a possible AGN.

1ES 1259+289.—The error box also contains 1259+2857 (GAL:0.030), a possible AGN.

1ES 1301–239.—Error box also contains A3541 (CG).

1ES 1351+695.—Error box also includes MCG +12-13-024 (AGN: 0.031). With $V = 17$ MCG +12-13-024 is a marginally acceptable candidate based on f_x/f_o (Maccacaro et al. 1984). Mrk 279 is the preferred identification based on an HRI position (in *einline*).

1ES 1503+017.—The counterpart, N5486, is part of a galaxy pair with the fainter N5486A (GAL: 0.007).

1ES 1549+203.—There are two acceptable identifications: LB 906 (AGN), and SAO 084044 (S: G0), but the latter is 1.6' from the 1ES position.

1ES 1602+178.—The UGC counterpart is a galaxy pair. In addition, the error box contains an NGC pair at $z \sim 0.035$ and a Zwicky triple at $z = 0.038$.

1ES 1702+457.—The error box also contains two galaxies—1702+4544A (GAL:0.061) and 1701+4544B (GAL:0.007).

1ES 1704+545.—Triple system (with WLY 9584B, F6V; WLY 9584C).

1ES 1706+787.—The error box also contains a Zwicky triple (1706+7842), and another Zwicky galaxy.

1ES 1714+574.—Error box also includes NGC 6345 (GAL), 2.7' from the 1ES position.

1ES 1731–325.—Error box also includes HD 159176 (S:O6 V+O6 V), possibly a member of the globular cluster.

1ES 1821+643.—Error box also includes K1-16 (WD: D0Z1), which had an *EXOSAT* detection, (1.2' from the 1ES position). However, the PI bin value (=6) suggests that the AGN is the correct identification, since white dwarfs typically have a mean PI bin of 2 (Schachter et al. 1991).

1ES 1914+092.—Error box also includes SAO 124466 (S: F0).

1ES 1957+405.—Both the cluster and the radio galaxy are possible counterparts.

1ES 2031+411.—The Slew Survey field contains part of the OB association VI Cygni. The SAO star identification is based on IPC and HRI data in Harnden et al. (1979). There are two or more HRI sources present within a 0.3 radius (also see Fig. 9).

1ES 2247+106.—Other than the cluster, the error box also contains MCG +02-58-021, a 16th mag galaxy which is possibly an AGN.

1ES 2311–430.—The error box also contains 2311–4300 (GAL:0.056), with the same redshift as the cluster, a possible AGN.

7. IDENTIFICATIONS

Identifications of Slew Survey sources with known X-ray sources have played an important role in producing this catalog (as detailed in § 3). Identifications with other, primarily optical, catalogs are also useful in providing a final check on the reality of the sources and the accuracy of the derived positions. All the identifications with counterparts presented here come from searching 3' fields centered on the Slew Survey positions, slightly more conservative than the 95% confidence radius estimated in Figure 7d. A total of 313 (38%) of the Slew Survey sources are new as X-ray sources, and 637 (78%) have been identified with optical catalog sources, including 133 (16%) of the new X-ray sources. Few of these are likely to be chance coincidences since a 3' radius search circle gives $\sim 5 \times 10^6$ independent bins on the sky. Thus, assuming that all the objects are randomly distributed, for the ~ 1000 Slew Survey sources, only about one in 5000 objects will accidentally associated with a catalog object. Most catalogs contain fewer sources than this, so one chance coincidence or less per catalog is expected. The SAO catalog (with $\sim 100,000$ entries) is an exception. A detailed examination of the identifications and their reliability will be presented in a forthcoming paper (Schachter et al. 1991).

In the case of extended objects, especially supernova remnants and clusters of galaxies, this technique may fail to identify some objects. A solution to this problem is to increase the search radius systematically while also checking for any duplicate counterpart identifications. A preliminary analysis suggests that increasing the radius to $\sim 5'$ – $15'$ gives ~ 20 %– 30 % more supernova remnant and cluster candidates.

We are presently extending the identification program to handle the extended sources in more detail and also to include the *IRAS* survey (including both the Point Source Catalog and the Faint Source Catalog), the HST Guide Star Selection System catalog, and the radio 87GB and UT 327 MHz surveys. Optical magnitudes for candidate identifications in all fields are being obtained from digitizations of the Palomar and UK Schmidt surveys. An on-line data base of identifications will be maintained at CfA, accessible remotely through the *einline* system. To allow for detailed follow-up, we will make available an on-line ascii version of the source identification list, which will be updated periodically. We welcome contributions to this identification list, which will be referenced in the data base.

TABLE 7
NEW IDENTIFIED X-RAY SOURCES

Name (1)	Type/z (2)	Counterpart Name (3)	Other Counterpart Names (4)
AGNs			
1ES 0702+646	0.079	VII Zw 118*	
1ES 0836+710	2.160	4C 71.07	S5 0836+710 ...
1ES 0921+525	0.036	Mrk 110	PG
1ES 1149-110	0.049	PG	...
1ES 1309+355	0.184	TON 1565	PG
1ES 1320+084	0.050	Mrk 1347	...
1ES 1415+451	0.114	PG	...
1ES 1518+593	0.079	SBS 1518+593	...
1ES 1626+554	0.132	PG	...
Galaxies ^a			
1ES 0257+442	U02468	...
1ES 0403-373	0.055	ESO 359-19	...
1ES 0412-382	0.050	ESO(B)303R	...
1ES 0543-555	0.015	NGC 2087	ESO 159-26
1ES 0559-399	GAL 0559-3959	...
1ES 1121-012	Z1121.0-0117	...
1ES 1141+799	UO6728	...
1ES 1215+039	0.075	4C+04.41*	PKS 1214+038
1ES 1234+459	Z1234.5+4556	...
1ES 1238-332	ESO 381-7	...
1ES 1254-172	0.046	GAL 1254-1710*	...
1ES 1318+274	G149-80	...
1ES 1323+717	0.072	GAL 1323+7145	...
1ES 1324-269	0.046	ESO 509-9	...
1ES 1324-268	ESO 509-14	...
1ES 1336+280	0.036	Z1336.4+2800	...
1ES 1714+574	0.028	NGC 6338*	U10784
Clusters of Galaxies			
1ES 0122+084A	0.045	A193*	...
1ES 0122+084B	0.045	A193*	...
1ES 0644-541	A3404	...
1ES 0914+519	0.197	A773	...
1ES 1241+275	0.241	A1602	...
1ES 1256-039	0.083	A1651	...
1ES 1301-239	A1664*	...
1ES 1310-327	S724	...
1ES 2247+106	0.077	A2495*	...
1ES 2349-561	S1158	...
White Dwarfs			
1ES 1631+781	DA	RE 1629+781	...
Stars: Known to Be Active			
1ES 0957+247	K0VE+B	DH Leo	SAO 081134
1ES 2058+398	M3EV+M3EV	WLY 815AB	...
Stars: Binaries			
1ES 0154-518	G5 IV+	WLY 81AB	SAO 23273, χ Eri, HD 11937
1ES 0309-291	F8 IV+	WLY 127AB	SAO 168373, α For, HD 20010
1ES 1314+172	K2 V+M2 V	WLY 505AB	SAO 100491
1ES 1833+169	G2 V+G2 V	HD 171746	SAO 103886
Stars: Early-Type			
1ES 0157+706	A3 IV	SAO 4554	48 Cas, HD 12111
1ES 0324+095	B9 Vn	HD 21364	214 Tau, SAO 168373
1ES 0426-131	B1 Vne	DU Eri	HD 28497, SAO 149674
1ES 0510-119	B8 V	SAO 150223	309 Lep, HD 33802
1ES 0839-445	A0	HD 74209	...
1ES 1126-610	A	HD 306536	...

TABLE 7—Continued

Name (1)	Type/z (2)	Counterpart Name (3)	Other Counterpart Names (4)
1ES 1148–624	B8	HD 309207	...
1ES 1318–632	B	LS 3039	...
1ES 1348–588	B9 IV	SAO 241229	...
1ES 1414–197	A5 IV	SAO 158468	...
1ES 1650–417	B	SAO 227370	...
1ES 1920+223	A2	HD 344230	...
Stars: Late-Type ^b			
1ES 0013+195	M4	G32–6*	...
1ES 0120+004	G0	HD 8358*	...
1ES 0143–253	F1 V	ε Scl	HD 10830, SAO 167275
1ES 0226–615	F8	SAO 248569	...
1ES 0238+057	M	BD +05 378	...
1ES 0305–284	K7 V	CD –28 1030*	...
1ES 0357–400	K0	HD 25300	...
1ES 0415+231	K0	HD 284303	...
1ES 0419+148	F8	HD 285758	...
1ES 0423+146	G7 III	SAO 093935	7316 Tau, HD 28100
1ES 0444–704	K7	HD 270712	...
1ES 0447+068	F6 V	SAO 112106	WLY 178, 116 ³ Ori, HD 30652
1ES 0504–575	F8 V	WLY 189	Zeta Dor, HD 33262, SAO 233822
1ES 0603–484	G5	SAO 217708	HD 41824
1ES 0614+227	K2	HD 254475	...
1ES 0618–580	K2V	SAO 234448	...
1ES 0635–698	G3V	HD 47875	...
1ES 0637–614	G1–2 V	HD 48189	SAO 249604
1ES 0712–363	F6–7 V	SAO 197732	...
1ES 0717–572	G0 IV–V	SAO 235087	...
1ES 0738+612	K0	SAO 014296	...
1ES 0740+228	K0	SAO 079647	...
1ES 0919+404	K2 V	SAO 042826	...
1ES 0920–136	K0 IV	SAO 155136	...
1ES 0923–530	F7 V	SAO 236956	...
1ES 1002–559	K1–2 III	SAO 237656	...
1ES 1020+493	F5	HD 89944	...
1ES 1101–606	M0	SAO 251235	...
1ES 1105+833	K0	SAO 001824	...
1ES 1212–652	G0/G1 V	HD 106392	...
1ES 1212+078	K0	SAO 119284	...
1ES 1228–465	F5 V	SAO 223481	...
1ES 1239–011	F0 V	WLY 482A	SAO 138917, HD 110379, HD 110380
1ES 1252–060	K8 V	WLY 9424	...
1ES 1301–411	K0	CD –40 7655	...
1ES 1325–261	K5 III	HD 117033	...
1ES 1325–312	F5 V	SAO 204500	...
1ES 1326+789	G2.5 IIIb	HD 117566	SAO 007821
1ES 1327–313	K1 III	SAO 204527	...
1ES 1339–688	G2 IV–V	SAO 252423	...
1ES 1354–314	K0 V	SAO 205032	...
1ES 1414+203	F8 V	HD 125040	SAO 083259
1ES 1437–252	F0/F2 V	HD 129009	...
1ES 1456–400	F7/F8 V	HD 132349	...
1ES 1509+763	G5	SAO 008175	...
1ES 1606+218	K2	AG +21 1576	...
1ES 1614+446	G0	SAO 045997	...
1ES 1702+457	F8	SAO 046462*	...
1ES 1711–547	F0I V–V	SAO 244557	...
1ES 1716+551	K0	SAO 030326	...
1ES 1727+590	G0	SAO 030416	...
1ES 1737+612	M	HD 160934	...
1ES 1746+748	K0	SAO 008910	...
1ES 1824+151	K0	SAO 103722	...
1ES 1902–524	F7 V	ρ Tel	HD 177171
1ES 1914+092	K2 II	SAO 124465*	...
1ES 2001+068	K2	HD 190342	...
1ES 2013+448	K0	SAO 049357	...
1ES 2042+335	G5	SAO 070451	...
1ES 2048+314	K0	SAO 070569	...
1ES 2052+441	G2 V	SAO 050198	...

TABLE 7—Continued

Name (1)	Type/z (2)	Counterpart Name (3)	Other Counterpart Names (4)
1ES 2128+231	K8	BD +22 4409	...
1ES 2135+011	K0	AG+01 2623	...
1ES 2153+441	K0	SAO 051437	...
1ES 2216+845	K2	SAO 003717	...
1ES 2257–340	G5 VP	SAO 214237	...
1ES 2326+411	M2	G190–28	...
1ES 2334+063	G0	SAO 128282	...
Stars: Type Unknown			
1ES 0437–046	BF Eri	...
1ES 0437+444	OU Per	...
1ES 0829+159	SAO 097895	...
1ES 1735–269	IRAS 17345–2656	...
1ES 1841–044	FT Sct	...
1ES 2129–026	PHL 26	...
1ES 2155–081	BD –08 5773	...

^a These galaxies, although cataloged as normal, may possess active nuclei.

^b Many of the late-type stars may be previously unknown active stars.

7.1. New Identified X-Ray Sources

Table 7 contains a list of the 133 new X-ray sources with optical identifications by object class. By a new X-ray source, we mean a Slew Survey source undetected in the *EXOSAT*, pointed IPC (Harris et al. 1991), or *HEAO A-3* (Remillard et al. 1991) catalogs within 3' of the Slew position. Some sources may not be in these catalogs, yet be detected in other X-ray missions (e.g., *HEAO A-2*, *Uhuru*, *Ariel V*). Therefore, we inspected other comprehensive X-ray source compilations (e.g., Bradt & McClintock 1983; Kowalski et al. 1984). Three ($\sim 3\%$) of the candidate new identified X-ray sources were eliminated in this manner: the X-ray binaries 4U 1755–338 and Aql X-1 (4U 1908+005), and the cluster A2315 (a *HEAO A-2* source).

The entries in Table 7 are grouped by object type—AGN, galaxies, clusters, white dwarfs, and stars—while the stars are further subdivided as in Table 5 [active, binaries, early type (OBA), late type ($\geq F$), unknown type)]. The first column gives the 1ES (First *Einstein* Slew Survey) name of the object. If the redshift or stellar spectral type is known, it is indicated in column (2). We list in column (3) the common name of each object, including only a catalog designator such as PG for common catalogs, if the coordinate name is the same as in the 1ES name. An asterisk following the object name signifies an ambiguous identification (see § 6.2). Column (4) lists alternate names of the object, if any.

Based on their f_x/f_o ratios in comparison with the values given for Medium Survey sources by Maccacaro et al., we expect that the new “galaxies” are previously unknown active galaxies, primarily Seyfert galaxies.

8. PROPERTIES OF THE SLEW SURVEY

The Slew Survey contains 819 sources, which are concentrated toward the ecliptic poles (Fig. 17). Half of these sources are newly discovered as X-ray sources.

The range of source fluxes complements well that of the Medium Survey (Gioia et al. 1990, Fig. 1): there are similar numbers of sources in each survey; they each cover about a decade of flux with excellent statistics; and the Slew Survey sources are on average 10 times brighter. The uniform selection of the Slew Survey sources by soft X-ray emission will allow the formation of well-defined samples of most classes of X-ray emitter: stars, CVs, AGNs, clusters of galaxies, and BL Lacertae objects.

Some regions of the sky have especially favorable coverage. The Cygnus Loop has ~ 150 s exposure, which produces an image with over 100,000 photons (Fig. 18). Of more general interest is the north ecliptic pole region (Fig. 19) which has between 30 and 100 s exposure. In the region within 10° of the ecliptic pole, 21 sources can be seen, illustrating the ability of the Slew Survey to detect new “serendipitous” sources.

Two examples of the uses of the Slew Survey samples are given below, one for quasars and the other for BL Lacertae objects.

1. The steep luminosity function of AGN, means that low-luminosity AGNs (i.e., Seyfert galaxies) are likely to make up a major part of the AGN contribution to the diffuse X-ray background. Yet most optical studies cannot treat these AGNs because the host galaxy leads to fuzzy images and dilutes the AGN colors, both of which effects produce uncertain levels of incompleteness in the samples. Thus Schmidt & Green (1983), for example, could not extend their luminosity function fainter than $M_V = -23$. The Slew Survey will give a bright AGN survey, similar to the Palomar Bright Quasar Survey (BQS, ‘PG’, Schmidt & Green 1983), but with the advantage that it is free from the problem of galaxy starlight contamination. AGNs will be seen down to $M_V \sim -20$ with redshifts as high as $z \sim 0.1$, complementing the Medium Survey which reaches a similar absolute magnitude but has few AGNs at $z < 0.1$. The Slew Survey may also be a good means of finding high-luminosity quasars of moderate redshift since, being rare,

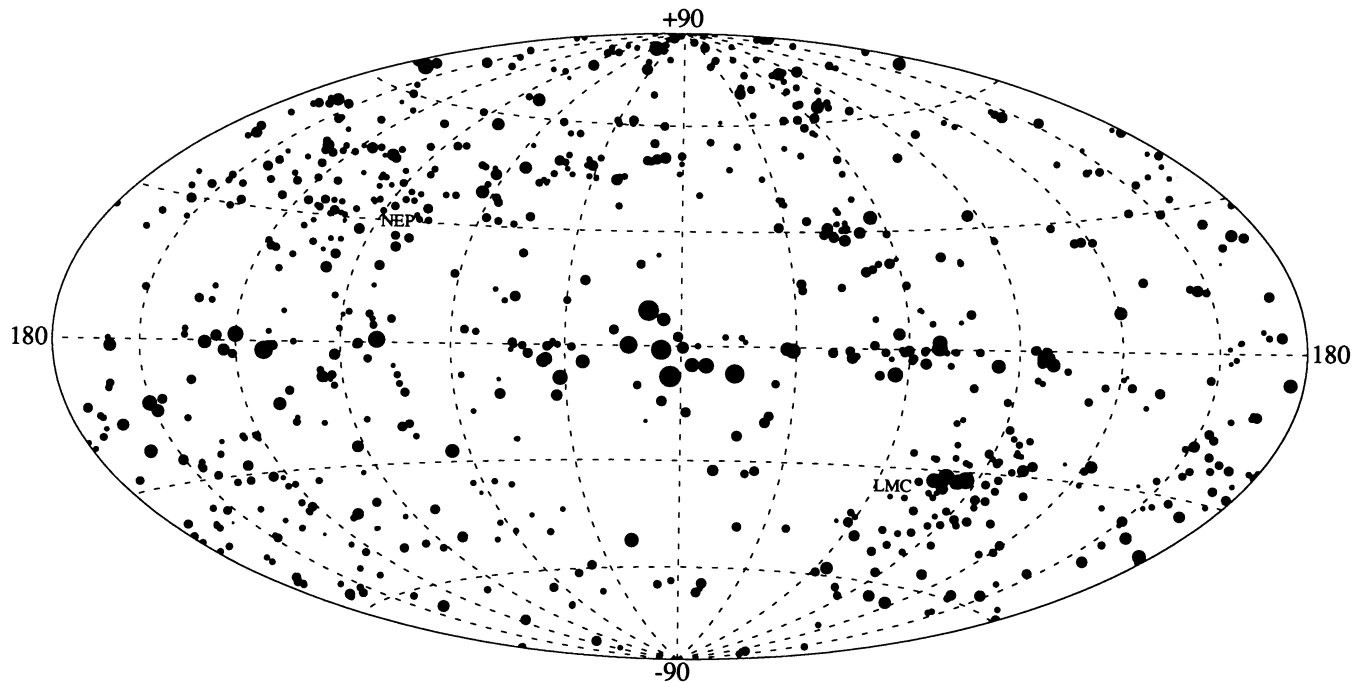


FIG. 17.—Distribution of Slew Survey sources in Galactic coordinates. The concentration of sources at the ecliptic poles (“NEP” and “LMC”), where the Slew Survey exposure time is greatest, is clear.

they require large sky coverage to be detected. Another problem, the dependence of AGN evolution on the unknown spectrum of the sources (Elvis et al. 1986; Tananbaum et al. 1986), can be removed empirically by using the Slew/A-2 flux ratios.

2. There is a peculiar break in the X-ray log N -log S for BL Lacertae objects, which may be related to relativistic beaming in these sources (Giommi et al. 1989) or to cosmological evolution (Wolter et al. 1991; Morris et al. 1991). The flux region of the break is not presently well sampled. This is the range covered by the Slew Survey. Recent X-ray surveys (Stocke et al. 1989) have clearly demonstrated that X-ray selection is currently the best method of discovering BL Lacertae objects. For the flux limit of the IPC Slew Survey, a uniform, X-ray-selected sample of ~ 80 objects will be detected (and identified through our ongoing program to identify all Slew Survey sources) in the high Galactic latitude sky. This compares with a total of 87 BL Lacertae objects, selected by all methods, in the Hewitt & Burbidge (1987) Catalog. There are about 40 known X-ray-selected BL Lacertae objects. All X-ray selected BL Lacertae objects are radio-loud (Stocke et al. 1989) and have well-defined and distinct X-ray/optical/radio flux ratios (Giommi et al. 1990). This tight α_{RO}/α_{OX} distribution implies that the BL Lacertae objects in the Slew Survey will have radio flux densities in the range 50–80 mJy. This, when combined with the correlation between radio and optical fluxes, gives an expected m_V in the range 18–19 for the faintest objects. The three fluxes alone are sufficient to select a large sample of BL Lacertae objects for further study.

Identification of the unidentified Slew Survey sources should be relatively easy since they are all bright. We can estimate their optical magnitudes using the nomogram constructed for Medium Survey sources (Maccacaro et al. 1988).

The typical AGN will be at $V \sim 16$ mag and the faintest M dwarfs will be at ~ 14 mag. This is 2–3 mag brighter than the Medium Survey identifications and our error circles have only ~ 5 times their area, so the typical number of possible optical candidates, and possible spurious counterparts, will be few.

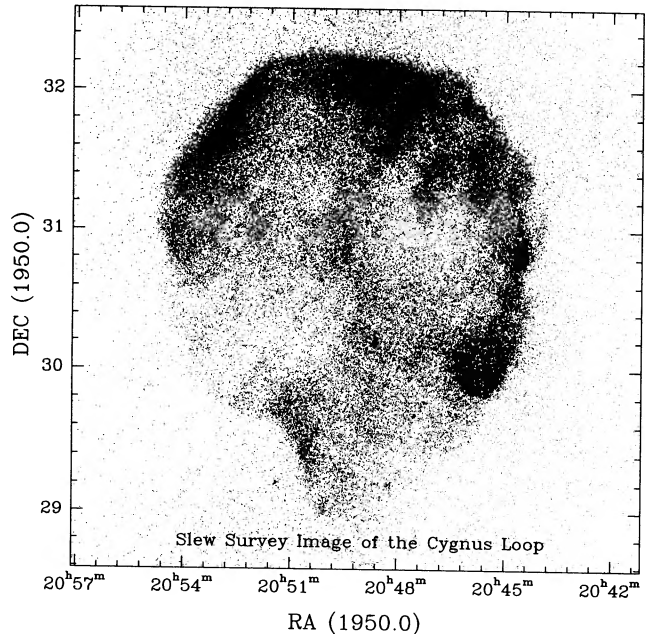


FIG. 18.—Slew Survey image of the Cygnus Loop. The mean exposure time in this image is ~ 150 s. A total of 108,000 photons are included in the image. The field shown is $4^\circ \times 4^\circ$.

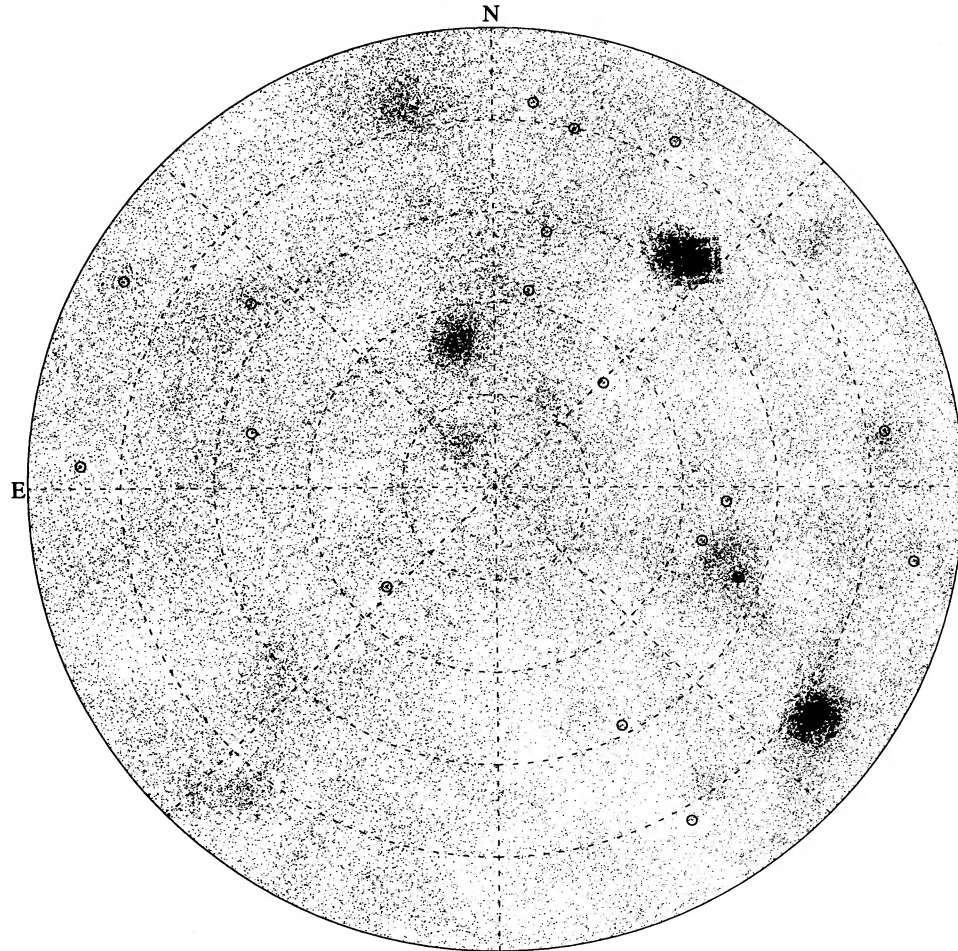


FIG. 19.—The region of the Slew Survey within 10° of the north ecliptic pole. The exposure time ranges from ~ 100 s (north) to ~ 30 s (south) which leads to the variations in photon density seen in the image. The image is not exposure corrected. The two darkest areas are short segments of data from the very beginning or end of slews when the spacecraft is virtually stationary. The 21 Slew Survey sources are circled. (One source is almost hidden in the heavily exposed region to the lower right.)

Many of the new sources will also show up in the IRAS Point Source Catalog, Version 2 1988 and the Green Bank (Gregory & Condon 1991) survey. We will use the Minnesota POSS (Humphreys 1991) and Edinburgh UK Schmidt digitizations to derive the bulk of our optical magnitudes. In this way relatively few new optical observations will be needed to make the remaining identifications.

We have not constructed a $\log N$ - $\log S$ for the Slew Survey in this paper. This obvious step is in practice quite difficult to do properly. The uncertainty on the count rates in the survey are mostly large, so that the “Eddington bias” is large. This is the effect by which sources below the formal flux threshold are detected while sources above the threshold are missed due to flux measurement errors. A simple flux threshold thus cannot be readily defined. Since the $\log N$ - $\log S$ is steep (Gioia et al. 1990), more sources will enter the survey than will drop out, systematically distorting and steepening the observed $\log N$ - $\log S$ at low fluxes. A proper treatment requires detailed simulations of the procedures used to produce the survey source list, and we defer this to a later paper.

9. CONCLUSIONS

We have presented a survey of the sky in soft (~ 0.1 – 3.5 keV) X-rays containing 819 sources. New, well-defined, samples of bright X-ray sources can be derived from this survey for many object types. The survey has a limiting flux a few times fainter than the largest previous all sky survey in X-rays (*HEAO A-1*, Wood et al. 1984) which took place in the ~ 2 – 10 keV band, and a factor ~ 10 brighter than the typical sensitivity of the *ROSAT* survey which covers the 0.1–2 keV band.

It is fair to ask what the value of the Slew Survey is in the context of the much larger and more sensitive *ROSAT* survey (Trümper 1991). This question has several answers: first, the Slew Survey makes available rapidly a large number of new bright X-ray sources suitable for follow-up study with *ROSAT* (and, in a few years, with *ASTRO-D*); second, virtually all of the existing faint source X-ray work has been carried out with IPC-selected sources as part of the *Einstein* Medium Survey (Maccacaro et al. 1988; Gioia et al. 1990) and the Deep Survey (Giacconi et al. 1979b; Primini et al. 1991), so that a compari-

son sample of bright identified sources selected with the same instrument can be put to use at once for source count and evolution work, without ambiguities due to different detector characteristics; third, a comparison of Slew Survey sources with *ROSAT* survey sources will allow the selection of unusual objects having extreme variability and/or extreme spectra; finally, the energy band of the *Einstein* IPC extends to significantly higher energies than that of the *ROSAT* survey, so that it will continue to be valuable (e.g., for the selection of hard X-ray sources) even when the *ROSAT* survey is published.

The large amplitude variations in exposure on a scale of a few arcminutes in the Slew Survey mean that it is not possible to derive upper limits for arbitrary positions on the sky from the present catalog. We are preparing two methods to allow this—an on-line service will be added to *einline* (the *Einstein* On-line Service; Harris et al. 1990); and the original, aspect-corrected, slew data is available on a CD-ROM as part of the SAO CD-ROM series of *Einstein* Data Products (Fabbiano 1990). This CD-ROM also allows timing, spectral, and structural information to be extracted from the Slew Survey via standard X-ray data reduction packages (e.g. IRAF/PROS, MIDAS).

The Slew Survey presently has only coarsely known completeness as a function of source flux. A program to derive accurate sky coverage and source detection efficiencies as a function of source flux and extent is being initiated. This will allow the derivation of statistical population properties such as luminosity functions from the Slew Survey.

We are pursuing a program of identifications for all Slew Survey sources. This is initially based on existing archival data and catalogs in an attempt to minimize the amount of optical observing needed. A first paper on these identifications is in preparation (Schachter et al. 1991). We shall maintain a data base of these identifications as part of the on-line *einline* system for general use. We welcome any contributions to these identifications. The on-line data base will include a reference

for the source of each identification. We ask that any publication using this information reference its source as listed in the on-line system.

We have received many requests for information on sources in the Slew Survey. As a result, we are forming working groups for astronomers interested in pursuing the active galaxies and quasars, and the BL Lacertae objects in the survey. The aim of these groups is to exchange information and prevent unnecessary duplication of effort, not to direct anyone's research. Any one interested in joining one of these groups or in forming another should send e-mail to the Slew Survey Project (slew@cfa.harvard.edu, cfa::slew). The *Einstein* Slew Survey data are part of the *Einstein* data bank. As such, they are part of the NASA Astrophysics Data Program and are available to all interested parties.

There exists some 50% more slew data in the *Einstein* data bank than was used for the present survey. These were originally rejected because of problems that would have complicated this first analysis, primarily long data dropouts that make the extrapolation of the gyro aspect solution less certain. Our experience now suggests that this problem can be overcome and we hope to include this data in constructing a second "definitive" Slew Survey, which should have roughly double the number of sources.

We thank John McSweeney and the *Einstein* data center team for assistance with data handling; Ron Remillard, Jonathan McDowell, Paolo Giommi, John Stocke, and Nick White for their assistance with the identifications; and John Stocke for a careful reading of the manuscript. This research has made use of the SIMBAD data base, operated at CDS, Strasbourg, France and also the NASA/IPAC Extragalactic Database (NED) which is operated by the Jet Propulsion Laboratory, California Institute of Technology, under contract with NASA. This work was supported by NASA contract NAS8-30751 (*HEAO* 2) and NASA grant NAG5-1201 (ADP).

REFERENCES

- Abell, G. 1958, ApJS, 3, 211
 Abell, G., Corwin, H., & Olowin, R. 1989, ApJS, 70, 1
 Bradt, H. V. D., & McClintock, J. E. 1983, ARA&A, 21, 13
 Branduardi-Raymont, G., Fabricant, D., Feigelson, E., Gorenstein, P., Grindlay, J., Soltan, A., & Zamorani, G. 1981, ApJ, 248, 55
 Cannon, A. J., & Pickering, E. C. 1918–1924, The Henry Draper Catalogue, Ann. Astron. Obs. Harvard College, 91–99
 Cooke, B. A., et al. 1991, Nature, submitted
 Elvis, M., Green, R. F., Bechtold, J., Schmidt, M., Neugebauer, G., Soifer, B. T., Matthews, K., & Fabbiano, G. 1986, ApJ, 310, 291
 Fabbiano, G. 1990, in Imaging X-Ray Astronomy, ed. M. Elvis (Cambridge: Cambridge Univ. Press), 155
 Giacconi, R., et al. 1979a, ApJ, 230, 540
 Giacconi, R., et al. 1979b, ApJ, 234, L1
 Gioia, I. M., Maccacaro, T., Schild, R. E., Stocke, J. T., Liebert, J. W., Danziger, I. J., Kunth, D., and Lub, J. 1984, ApJ, 283, 495
 Gioia, I. M., Maccacaro, T., Schild, R. E., Wolter, A., Stocke, J. T., Morris, S. L., and Henry, J. P. 1990, ApJS, 72, 567
 Giommi, P., et al. 1989, in Proc. Workshop on BL Lac objects, ed. L. Maraschi, T. Maccacaro, & M.-H. Ulrich (Berlin: Springer), 231
 Giommi, P., Barr, P., Garilli, B., Maccagni, D., & Pollock, A. M. T. 1990, ApJ, 356, 432
 Giommi, P., et al., 1991, ApJ, 378, 77
 Gorenstein, P., Harnden, R. F., & Fabricant, D. G. 1981, IEEE Trans. Nucl. Sci., NS-28, 869
 Gregory, P. C., & Condon, J. J. 1991, ApJS, 75, 1011
 Harnden, F. R., Branduardi, G., Elvis, M., Gorenstein, P., Grindlay, J., Pye, J. P., Rosner, R., Topka, R., & Vaiana, G. S. 1979, ApJ, 234, L51
 Harnden, R. F., Jr., Fabricant, D. G., Harris, D. E., & Schwarz, J. 1984, Smithsonian Astrophys. Obs. Spec. Rep. 393
 Harris, D. E. et al. 1991, *Einstein* IPC Source Catalog, NASA Publication, in press.
 Harris, D. E., Stern, C. P., & Biretta, J. A. 1990, in Imaging X-ray Astronomy, ed. M. Elvis (Cambridge: Cambridge Univ. Press), 299
 Hewitt, A., & Burbidge, G. 1987, ApJS, 63, 1
 Hoffleit, D., & Jaschek, C. 1982, The Bright Star Catalogue (4th rev. ed.; New Haven: Yale Univ. Obs.)
 Huchra, J. P. 1991, in preparation.
 Huchra, J. P., & Geller, M. J. 1984, ApJ, 257, 423
 Humphreys, R. 1991, private communication
IRAS Point Source Catalog, Version 2. 1988, Joint *IRAS* Science Working Group (Washington, DC: GPO)
 Kholopov, P. N., et al. 1985–1988, General Catalogue of Variable Stars (4th ed.; Moscow: Nauka)
 Koch, D., Hall, R., Tsao, H., Wollman, H., & Kilinski, R. 1978, IEEE Trans. Nucl. Sci., NS-25, 473
 Kowalski, M. P., Ulmer, M. P., Crudace, R. G., & Wood, K. S. 1984, ApJS, 56, 403
 Kraft, R., Burrows, D., & Nousek, J. 1991, ApJ, 374, 344
 Maccacaro, T., et al. 1988, ApJ, 326, 680

- McCook, G., & Sion, E. 1987, *ApJS*, 65, 603
- Morris, S., Stocke, J. T., Gioia, I. M., Schild, R. E., Wolter, A., Maccacaro, T., & Della Cecca, R. 1991, *ApJ*, 380, 49
- Nilsson, P. 1973, Uppsala General Catalogue of Galaxies, Uppsala Astron. Obs. Ann. 6
- Piccinotti, G., Mushotzky, R. F., Boldt, E. A., Holt, S. S., Marshall, F. E., Serlemitsos, P. J., & Shafer, R. A. 1982, *ApJ*, 253, 485
- Plummer, D., Schachter, J., Garcia, M., & Elvis, M. 1991, CD-ROM issued by Smithsonian Astrophysical Observatory
- Primini, F. A., Murray, S. S., Huchra, J., Schild, R., Burg, R., & Giacconi, R. 1991, *ApJ*, 374, 440
- Remillard, R., et al. 1991, in preparation
- SAO Staff. 1966, Star Catalog. Positions and Proper Motions of 258,997 Stars for the Epoch and Equinox of 1950.0 (Pub. 4652) (Washington: Smithsonian Institution)
- Schachter, J., et al. 1991, in preparation
- Schmidt, M. 1990, in Imaging X-Ray Astronomy, ed. M. Elvis (Cambridge: Cambridge Univ. Press), 201
- Schmidt, M., & Green, R. F. 1983, *ApJ*, 269, 352
- Shara, M. 1990, private communication
- Stocke, J. T., Morris, S. L., Gioia, I. M., Maccacaro, T., Schild, R. E., and Wolter, A. 1989, in BL Lac Objects, ed. L. Maraschi, T. Maccacaro, & M.-H. Ulrich (Berlin: Springer), 242
- Stocke, J. T., Morris, S. L., Gioia, I. M., Maccacaro, T., Schild, R., Wolter, A., Fleming, T. A., & Henry, J. P. 1991, *ApJS*, 76, 813
- Struble, M. V., & Rood, H. J. 1987, *ApJS*, 63, 543
- Sulentic, J. W., & Tifft, W. G. 1973, The Revised New General Catalogue of Nonstellar Astronomical Objects (Tucson: The University of Arizona Press)
- Tananbaum, H., Avni, Y., Green, R. F., Schmidt, M., & Zamorani, G. 1986, *ApJ*, 305, 57
- Trümper, J. et al. 1991, *Nature*, 349, 579
- Véron-Cetty, M.-P., & Véron, P. 1987, A Catalogue of Quasars and Active Nuclei (3d ed.; Saint-Michel, France: Observatoire de Haute Provence), 102
- Wolter, A., Gioia, I. M., Maccacaro, T., Morris, S. L., & Stocke, J. T. 1991, *ApJ*, 369, 314
- Wood, K. S., et al. 1984, *ApJS*, 56, 507
- Woolley, R., Epps, E. A., Penston, M. J., & Pocock, S. B. 1970, Catalogue of Stars within Twenty-Five parsecs of the Sun, R. Obs. Ann., 5